Profilin isoforms in the hippocampus in health and disease

Von der Fakultät für Lebenswissenschaften

der Technischen Universität Carolo-Wilhelmina zu Braunschweig

zur Erlangung des Grades

einer Doktorin der Naturwissenschaften (Dr. rer. nat.)

genehmigte

D i s s e r t a t i o n

von Sabine Zessin
aus Oldenburg

1. Referent: Prof. Dr. Martin Korte
2. Referent: Prof. Dr. Reinhard Köster
eingereicht am: 17.09.2014
mündliche Prüfung (Disputation) am: 02.12.2014

Druckjahr 2014

Vorveröffentlichungen der Dissertation

Teilergebnisse aus dieser Arbeit wurden mit Genehmigung der Fakultät für Lebenswissenschaften, vertreten durch den Mentor der Arbeit, in folgenden Beiträgen vorab veröffentlicht:

Tagungsbeiträge:

K. Michaelsen, K. Murk, M. Zagrebelsky, A. Dreznjak, **S. Zessin**, B.M. Jockusch, M. Rothkegel, M. Korte
'Specific role of Profilin2a as a mediator of structural plasticity in mature hippocampal neurons'
Society for Neuroscience Meeting, Chicago, 2009

S. Zessin, A. Remus, M. Rothkegel, M. Korte and K. Michaelsen-Preusse
'Isoform-specific functions of profilin1 and profilin2a in the mouse hippocampus'
10th Meeting of the German Neuroscience Society, Göttingen, March 2013

K. Michaelsen-Preusse, **S. Zessin**, A. Remus, M. Rothkegel, M. Korte
'Profilin isoforms in the mouse hippocampus and their role for spine plasticity'
9th FENS Forum of Neuroscience, Milan, July 2014

TABLE OF CONTENTS

Zusammenfassung

Neuronale Plastizität beruht auf aktivitätsabhängigen Veränderungen in der Morphologie von Neuronen und ihren Synapsen, die nicht nur während der Entwicklung, sondern auch im adulten Gehirn stattfinden. Da Aktin in dendritischen *spines* die vorrangige zytoskeletale Komponente bildet und ebenfalls für die Struktur und Stabilität von Dendriten essenziell ist, beeinflusst die Reorganisation des Aktinzytoskeletts die strukturelle Plastizität, Funktionalität sowie die Aufrechterhaltung der Zellform. Im Kontext von struktureller und funktioneller Plastizität spielen daher Aktin-bindende Proteine (ABP) eine entscheidende Rolle, da diese die Aktindynamik zeitlich und räumlich streng regulieren. Eines der wichtigsten ABP ist Profilin (PFN), welches die Aktinpolymerisation fördert und mit zahlreichen zytoskeletalen Proteinen interagiert. Im Gehirn von Säugetieren existieren zwei PFN Isoformen: das Gehirn-spezifische Profilin2a (PFN2a) und das ubiquitäre Profilin1 (PFN1). Die Tatsache, dass beide PFN im Säugergehirn zu finden sind, deutet auf Isoform-spezifische Funktionen hin.

In dieser Arbeit wurde die Rolle von PFN1 für die Morphologie und Funktion hippokampaler Pyramidenneurone sowie der Einfluss dieser Isoform auf aktivitätsabhängige strukturelle Plastizität untersucht. Mit Hilfe eines RNAi-vermittelten Knockdowns von PFN1 in sich entwickelnden und adulten Neuronen wurde der Einfluss des Proteins auf die dendritische Architektur sowie Stabilität von *spines* in verschiedenen Zelltypen des Hippokampus gezeigt. Während ein akuter *loss-of-function* Ansatz nur marginale Auswirkungen auf die dendritische Komplexität hatte, führte der akute Verlust von PFN1 zu einer global reduzierten Anzahl dendritischer *spines*. *Live imaging* Experimente mit PFN1 defizienten Neuronen zeigten, dass diese Isoform im Gegensatz zu PFN2a nicht essenziell für das aktivitätsinduzierte Wachstum von *spine*-Köpfen ist.

Plastizität an prä- und postsynaptischen Strukturen korreliert mit veränderter Funktion von exzitatorischen Synapsen und ist daher in neurologischen Entwicklungsstörungen, wie z.B. beim Fragilen X Syndrom (FXS), beeinträchtigt. Im zweiten Teil dieser Arbeit wurden wichtige ABP wie PFN1, PFN2a und Cofilin *in vitro* und *in vivo* im murinen FXS Modell analysiert. Die hier präsentierten Ergebnisse zeigen eine reduzierte PFN1 Proteinkonzentration in Hirnlysaten von *fmr1* KO Mäusen. Interessanterweise wurde der unreife *spine*-Phänotyp in *fmr1* KO Neuronen durch die Überexpression von sowohl PFN1 als auch PFN2a aufgehoben. Verhaltensexperimente zeigten Lerndefizite in *fmr1* KO Mäusen, deren anschließende Proteinanalysen eine Fehlregulierung von PFN1 und Cofilin (nicht aber PFN2a) ergaben. Somit scheinen beide PFN Isoform-spezifische Funktionen in Vorgängen von synaptischer Plastizität sowohl im gesunden als auch im kranken Gehirn zu erfüllen.

Abstract

Neurons are able to undergo morphological changes that require extensive reorganization of the underlying actin network not only during development, but also in adult neurons referred to as “structural plasticity”. Since actin is the predominant cytoskeletal component of postsynaptic structures such as dendritic spines and also important for dendritic architecture and stability, much work on structural plasticity has focused on actin-binding proteins (ABPs) in regulating actin dynamics, as those processes are tightly coordinated. Among the plethora of ABPs, both profilin (PFN) isoforms abundant in the brain are central regulators of actin polymerization – ubiquitous profilin1 (PFN1) and neuronal-specific profilin2a (PFN2a). Although it is known for a relatively long time that both are present in the mammalian brain, a clear understanding of the isoform-specific functions of the two PFNs is still missing.

In this study, I aimed at characterizing the role of PFN1 in shaping the structure and function of developing and mature hippocampal neurons, and to clarify its impact on activity-dependent plasticity processes. Therefore, a loss-of-function approach inducing RNAi-mediated knockdown of PFN1 (shPFN1) was used to investigate whether PFN1 modulates the dendritic architecture and spine stability of immature as well as mature pyramidal neurons. Interestingly, acute knockdown of PFN1 led to only mild alterations in dendritic complexity and arborization in a subregion- and age-dependent manner in contrast to a comparable approach using shPFN2a, but induced a strong global reduction in spine density and altered spine morphology. It has been shown before that PFN2a is crucially involved in activity-dependent structural plasticity, yet, live imaging experiments in PFN1 deficient hippocampal neurons could clearly show that this isoform is indeed dispensable for activity-dependent spine head growth.

Plasticity at pre- and postsynaptic elements is related to altered function of excitatory synapses, and therefore is involved in regulating normal brain function as well as in the pathology of a multitude of neurodevelopmental disorders such as the fragile X syndrome (FXS). Thus, in the second part of my work, I addressed the role of important actin-regulating proteins like PFN1, PFN2a and cofilin *in vitro* and *in vivo* in the mouse model of FXS. The data yielded by this study provide evidence that PFN1 levels were reduced in whole brain lysate of *fmr1* KO mice and the spine phenotype of *fmr1* KO hippocampal neurons could be rescued by overexpression of either PFN1 or PFN2a. Behavioral experiments demonstrated impairments of spatial learning in the *fmr1* KO mice. Subsequent analyses of relevant brain regions showed that indeed actin-regulating proteins (PFN1 and cofilin, but not PFN2a) were dysregulated in these animals. Thus, the results presented here indicate that both PFNs fulfill isoform-specific functions concerning synaptic plasticity in health and disease.

1 INTRODUCTION

Our brain is reputed to be the most complex living structure known in the universe. It allows perception, movement and interpretation of the world surrounding us. Beyond doubt, memory is one of the most important cognitive processes in our brains. Until today, the neuronal circuits involved in acquisition and consolidation of memory are still not completely understood and the exact localisation of memories in the central nervous system remains elusive, as memories are thought to be encoded along various pathways in the brain by cooperation of different circuits (Kandel et al., 2014). The mammalian brain is capable of learning new skills and integrating new experiences into long-lasting memory and, equally important, deleting information or erasing memories. Human memory that constitutes a major source for self-identity of the individual, as memories define to a great extent who we are, is not innate to humans, but has to be updated throughout lifetime. By definition, learning designates a process of acquiring new knowledge about the world encoded in neuronal networks, whereas memory is considered to be a process of retaining and reconstructing this knowledge over time (Kandel et al., 2014).

1.1 The hippocampal formation and its relation to memory

A plethora of studies identified the hippocampus as one of the main locations for transferring information into long-term memory. The hippocampus is one of the most studied neuronal systems in the brain and lays in the medial temporal lobe, surrounded by the entorhinal, parahippocampal and perirhinal cortices. Due to its relatively simple architecture, this cortical region became an excellent model for investigation. Receiving information from almost all cortical associated areas, these inputs are widely spread onto the different subpopulations of the hippocampus (Burwell et al., 1995). In contrast to the complex neocortical structure, the hippocampus consists of three layers with the middle layer containing the principal neurons – the pyramidal cells in the *cornu ammonis* and the granule cells in the dentate gyrus (cp. **Figure 1**). Strong evidence points to a pivotal role for the hippocampus in memory formation as indicated by studies of spared and impaired cognitive processes in patients with hippocampal damage, combined with results from

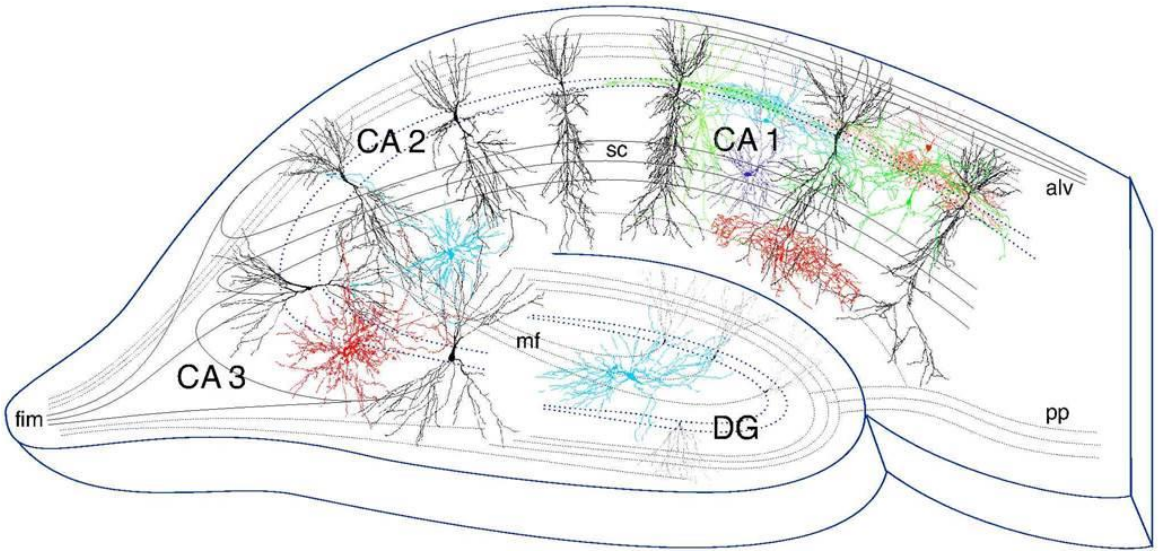

Figure 1 | The hippocampal formation in mammals

The hippocampus forms a principally unidirectional network with input from the axons of the entorhinal cortex connected to the granule cells of the dentate gyrus and CA3 neurons via the perforant path (lateral and medial; pp). Dendrites of CA3 neurons receive input from the DG via mossy fibers (mf) and project their axons to the CA1 region (Schaffer collateral pathway; sc) as well as to CA3 neurons of the contralateral hippocampus (associational commissural pathway). CA1 neurons receive direct input from the perforant path and project their axons to the subiculum, where output is sent back to the entorhinal cortex (Bruce MacIver lab, Stanford University).

animal models of amnesia (Eichenbaum, 2004). Studies using pharmacological inactivation of hippocampal function elegantly confirmed learning deficits or a loss of spatial memory formation (Morris et al., 1986). Henry M., probably the most famous neurological patient, displayed severe deficits in memory formation after the amygdala, the entorhinal and perirhinal cortices and about two-third of both hippocampi were removed by surgery (Scoville and Milner, 1957). He was no longer able to store new information regarding facts or events (episodic and semantic memory), while he could still learn new motor skills (procedural memory) and had memories of his life before surgery. This study pointed for the first time towards the fact that a certain type of memory such as daily experiences and personal history has to be processed in the hippocampus before getting stored as long-term memory in other brain regions, presumably in the neocortex (Squire et al., 2004; Milner, 2005; Moscovitch et al., 2006). More precisely, the hippocampus was suggested to mediate the transition from short- to long-term memory (Alvarez et al., 1994).

Various models exist trying to explain how the brain generates and stores memories over time. One model suggests that during an experience, sensory and associated neocortical regions are activated which then project to the hippocampus, leading to strengthening of synapses between neurons that respond to the neocortical inputs (Teyler and Rudy, 2007). As a result, the experience is represented as a set of reinforced synapses of the hippocampus associated with a subset of activated neurons in the neocortex. Subsequently, strengthened synapses are further stabilized by a process called consolidation, which is assumed to modify synaptic connections between different brain areas and depend on the synthesis of new proteins (Dudai, 2004; Frankland and Bontempi, 2005; Squire and Kandel, 2009).

Behavioural and electrophysiological studies examined the role of the entorhinal cortex for the memory network, as it is one of the cortical regions surrounding the hippocampus. Interestingly, it has reciprocal connections both with the hippocampus as well as with the neocortex. This connectivity could have an impact on memory consolidation and retrieval by initially interacting with the hippocampus but later with the medial prefrontal cortex or other cortical regions.

1.2 Synaptic plasticity in the hippocampus

For a long time neuroscientists assumed that the central nervous system of mammals becomes structurally stable soon after birth. This view has been dramatically revised as it could be shown extensively by now that indeed the brain remains structurally plastic throughout the entire lifespan of an organism. The hippocampus is a region showing high capacity for structural reorganization. These structural changes can occur upon damage, but also in the intact hippocampus. One of the most prominent structural changes is the addition of dendritic spines, also referred to as synaptogenesis. Dendritic spines are small protrusions emanating from the dendritic shaft of various types of neurons which receive inputs from excitatory axons forming the postsynaptic part of the synapse (Rochefort and Konnerth, 2012). All mature hippocampal cell types, namely granule cells and pyramidal neurons of areas CA3 and CA1, can undergo changes in dendritic trees or can be altered regarding the size, shape and density of dendritic spines. Importantly, structural remodeling can thereby occur in both directions - outgrowth/branching or retraction of

dendrites as well as addition/elimination of spines or changes in spine morphology are possible modifications.

Interestingly, changes in spine structure and number have been associated with long-term potentiation, a candidate cellular model for learning and memory (for review, see Carlisle & Kennedy 2005; Tada & Sheng 2006; Bourne & Harris 2008). Indeed, two forms of activity-dependent long-term changes in synaptic efficacy are believed to represent cellular correlates of learning and memory: long-term potentiation (LTP) and long-term depression (LTD), experimental phenomena which can be artificially induced by specific patterns of activity (Malenka, 1994). Simultaneous activation of a pre- and a postsynaptic neuron with a certain stimulus pattern leads to coincident depolarization and glutamate release from the presynaptic bouton. The resulting calcium influx through NMDARs activates intracellular signaling cascades that ultimately change the synaptic efficacy and in the long run strengthen the connection between two neurons (LTP). In contrast to this, LTD is induced by repeated activation of the presynaptic neurons at low frequencies (1 Hz) without postsynaptic activity and results in a long-term reduction in synaptic strength.

Processes of structural plasticity in the hippocampus, modified by environmental experiences, are assumed to play an important role in learning and memory formation in the hippocampus. A variety of studies utilizing learning tasks that depend on the hippocampus, e.g. long-delay eyeblink conditioning or spatial learning in the Morris water maze, suggested that learning and memory might require structural changes in the hippocampus (reviewed in (Nottebohm, 2002; Lamprecht and LeDoux, 2004). Supporting this, positive correlations between behavioural learning and structural plasticity such as gains and losses of dendritic spines have been demonstrated (reviewed in Caroni et al. 2012). Even without large-scale remodeling of dendritic and axonal arbors, changes in synaptic connectivity following *de novo* growth or elimination of spines and axonal boutons may promote functional rewiring (Holtmaat and Svoboda, 2009).

1.2.1 Structural plasticity on the level of single spines

Since their first description in 1888 by Santiago Ramón y Cajal, spines raise many open questions regarding their function and diverse morphologies. Found in all vertebrates and in some invertebrates, spines are localized on pyramidal neurons of the neocortex, medium spiny neurons of the striatum and Purkinje cells of the cerebellum. They are highly variable with respect to their density, size and shape, suggesting a high degree of functional diversity. Spine size varies between species and brain areas and even on the same stretch of dendrite spines are structurally highly heterogeneous. However, based on their morphology they are commonly classified into three types: thin (long, thin neck and small bulbous head), stubby (devoid of neck) and mushroom (large head). Filopodia are hair-like protrusions without a bulbous head and can be found mainly on immature, developing neurons (cp. **Figure** 2).

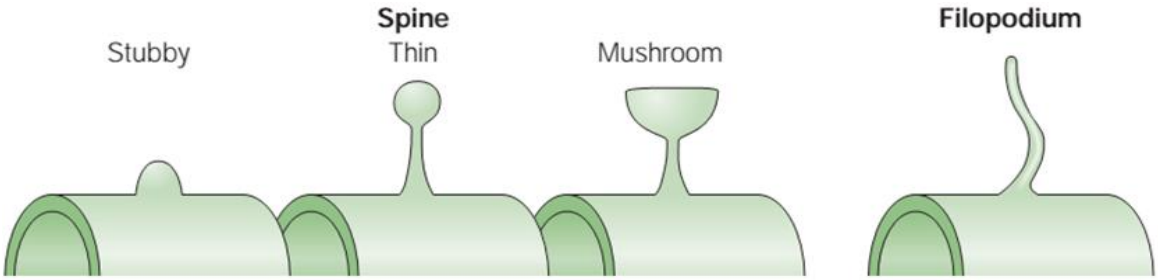

Figure 2 | Examples of different spine morphologies

Schematic drawing of diverse spine structures with categorization based on ratios between spine head, spine neck and spine length (Yuste and Bonhoeffer, 2004).

Strikingly, the morphology of a spine can change rapidly through activity-dependent and independent mechanisms (cp. **Figure 3**). Numerous studies were able to demonstrate that new spines grow in response to plasticity-inducing synaptic stimuli (Engert & Bonhoeffer 1999; Nägerl et al. 2004; Maletic-Savatic 1999; for a review see Segal 2005). Thus, morphological changes in spine structure are thought to be associated with functional changes in cortical circuits, as structural modifications are linked to an increase (LTP) or decrease (LTD) in synaptic strength (Zhou et al., 2004; Matsuzaki et al., 2004). Further studies described that the growth of new spines was associated with synapse formation, but the time course over which functional synapses form on individual new spines remains to be determined (Bresler et al., 2001; Trachtenberg et al., 2002; Matsuzaki et al., 2004b; Holtmaat et al., 2006).

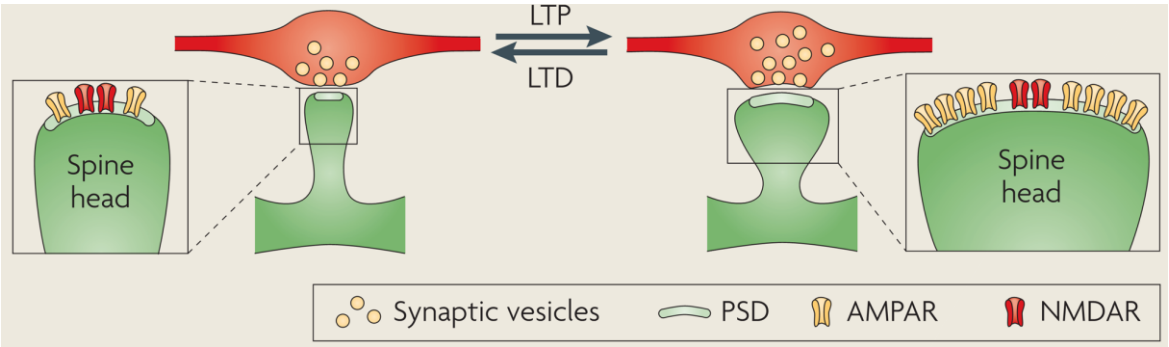

Figure 3| Plasticity in dendritic spines

Spine volumes increase after long-term potentiation (LTP) while long-term depression (LTD) causes spine head shrinkage. At the postsynaptic compartment AMPA and NMDA receptors are clustered in the PSD (adapted from Holtmaat & Svoboda 2009).

Thus, spines are highly dynamic structures which can respond to classical Hebbian plasticity as well as neuromodulatory signals, resulting in refinement of neural circuits and the processing and storage of information within the brain. Inside the spine, actin filaments are highly enriched providing the structural base for stability as well as changes in morphology and, according to this, alterations in spine morphology are tightly coupled to changes in filamentous actin present throughout the spine (Fifková and Delay, 1982; Matus et al., 1982; Matsuzaki et al., 2004b). In turn, the actin cytoskeleton is linked by a complex network of proteins to extracellular signals to tightly control spine morphology.

1.3 Function of the actin cytoskeleton in neurons and its regulation by profilins

A dynamic neuronal cytoskeleton provides an important substructure to allow for specialized functions in different compartments of the neuron. Actin structures are found throughout neurons and glia, but are most prominent in presynaptic terminals, growth cones and importantly, dendritic spines. Apparently, actin structures serve a variety of functions in the nervous system, such as maintaining the distribution of plasma membrane proteins, establishing cell morphologies and segregating axonal and dendritic proteins into their respective compartments. Actin is particularly concentrated in dendritic spines, representing highly specialized postsynaptic protrusions where synapses are biochemically and electrically compartmentalized. Hence, the actin cytoskeleton is thought to be the basis for both the formation of dendritic spines during development

and structural plasticity of mature synapses (Fischer et al., 1998; Matus, 2000). The filamentous form of actin (F-actin) supports processes as cell motility, cell division, cell polarity, protein trafficking and cell morphogenesis (Cingolani and Goda, 2008). Cell form and stability depend on organization of actin filaments und membrane connection.

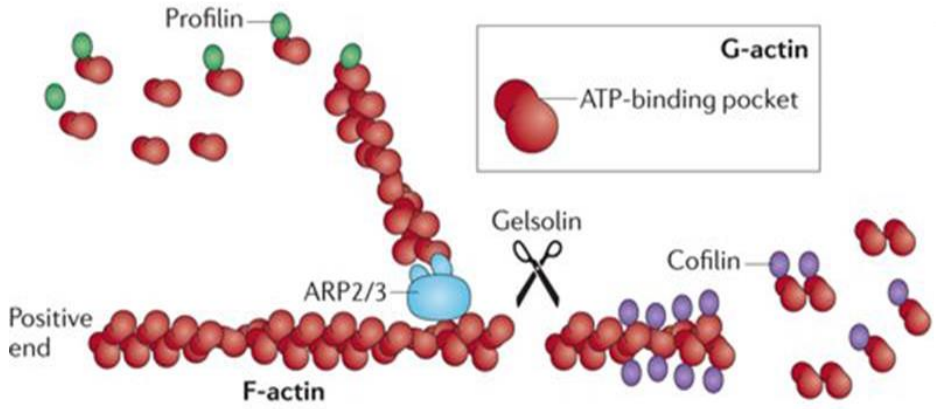

Figure 4 | Actin filaments are regulated by numerous proteins

Actin filaments are formed by two parallel strands of head–tail polymers of actin monomers. Actin polymerization is initiated by the Arp 2/3 complex and stimulated by cofactors such as profilin. Actin depolymerization can occur at either end of the filament. Cofilin interacts with actin dimers to promote disassembly, which can be initiated by the activity of gelsolin (Taylor et al., 2011).

Additionally, membrane protuberances as filopodia or lamellipodia are composed of F-actin. Each actin filament is made up of two helical intertwined actin polymers, which are generated via polymerization of free actin monomers (42 kDa) (cp. **Figure 4**). Hence, actin exists in two forms: a monomolecular, globule form (G-actin) and a polymer, filamentous form (F-actin). G-actin binds to Ca^{2+} and one adenosine triphosphate (ATP) molecule, consequently dimerization occurs under ATP hydrolysis; simplified, assembly of actin filament networks is based on the regulated transition between these two actin states. G-actin and F-actin reside in a dynamic equilibrium: one molecule of G-actin joins the barbed end of the actin filament while another G-actin dissociates from the pointed end (treadmilling). This simple steady state mechanism of assembly/disassembly does not explain the high degree of spatial and temporal regulation of actin dynamics in cells. Since spines can grow or shrink within minutes or hours, actin filaments have to be assembled or disassembled on a fast time scale. A remarkable variety of proteins has been found to tightly regulate these processes by interacting with either G-actin or F-actin.

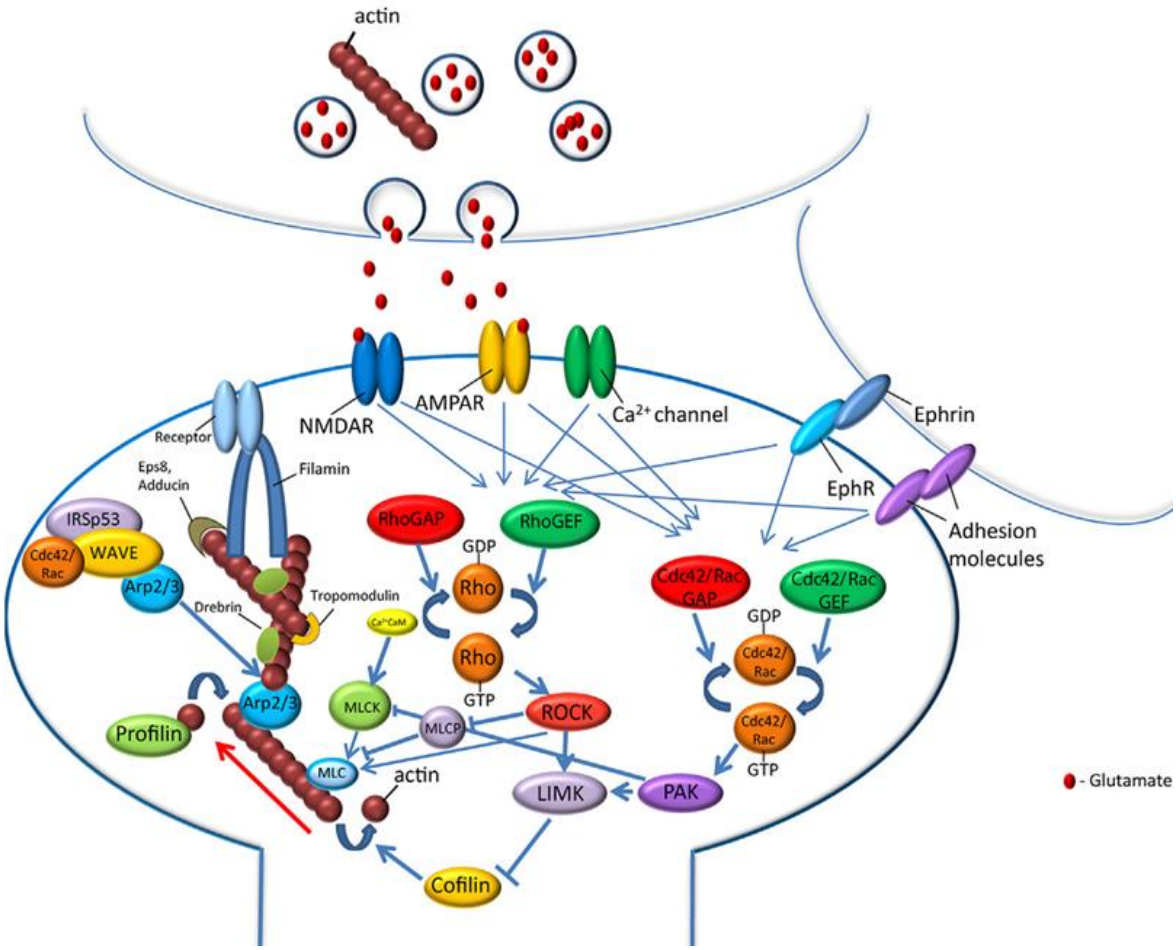

Figure 5 | Actin cytoskeleton and its regulatory proteins are involved in memory formation

Memory formation requires the activation of glutamate receptors, calcium channels, receptors tyrosine kinases and adhesion molecules which may activate intracellular signaling cascades that affect actin dynamics and structure. The most prominent proteins are the Rho, Rac, and Cdc42 GTPases and their effectors and actin-binding proteins such as profilin, cofilin, Arp2/3, drebrin, Filamin and Tropomodulin shown to regulate actin polymerization, branching, elongation and the timing and location of actin polymerization and therefore influence the structure of actin networks (Lamprecht, 2014).

The list of proteins discovered to bind actin is ever increasing, fulfilling a plethora of functions ranging from sequestering monomers to elongating filaments or severing filaments into shorter ones, cross-linking, bundling, capping and anchoring actin filaments (Dominguez, 2009). Another group of proteins is able to add branching points to pre-existing filaments thereby increasing the complexity of the actin network. In general, these proteins control the timing and location of actin polymerization and therefore influence the structure of actin networks (dos Remedios et al., 2003).

1.3.1 Actin in the maintenance of spines

Most dendritic spines can be maintained for hours, weeks and possibly even for years in humans. The spine is filled with a mixture of linear and (long or short) branched actin networks, ranging from the base of the spine to the postsynaptic density (PSD) (Landis & Reese 1983; Fischer et al. 1998; Star et al. 2002; Hotulainen & Hoogenraad 2010; Korobova & Svitkina 2010; Izeddin et al. 2011). The PSD lies at the distal tip of the spine head and includes a high density of neurotransmitter receptors, associated signaling proteins, cytoskeletal components, all stabilized and organized by a variety of scaffolding proteins (Sheng and Hoogenraad, 2007). The F-actin meshwork serves as the principal regulator of protein and vesicular trafficking (Newpher and Ehlers, 2009). To maintain stability in synapses, the actin cytoskeleton needs to be at equilibrium (cp. **Figure 6**).If

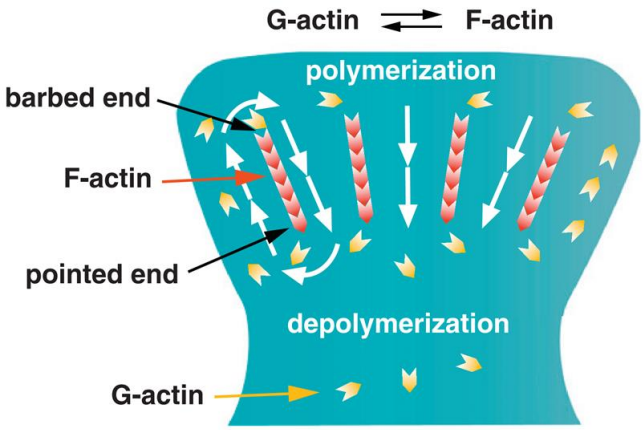

Figure 6 | Stable spines require actin at equilibrium

Constant treadmilling of actin from the periphery to the center of dendritic spines is achieved by equilibrium of F-actin polymerization/depolymerization rate (adapted from Bosch & Hayashi 2011).

association at one end and dissociation of monomers at the other end are balanced, filament length remains constant and actin filaments undergo 'treadmilling'. Growth and decay of filaments can be blocked through toxins or actin-associated proteins. The long-term stability of spine structure depends on the actin network, which in turn is regulated by a wide range of extracellular molecules that act on cell surface adhesion receptors such as Eph receptors, neurotrophin receptors, immunglobulin superfamily receptors, cadherins and integrins (cp. **Figure 7**). These receptors regulate via cytoplasmic non-receptor tyrosine kinases of the focal adhesion kinase (FAK), SRC and ABL families the activity of downstream signaling molecules including Rho-family of small GTPases and other cytoskeletal stabilizing proteins, which emerged as key integrators of environmental cues to regulate the underlying axonal and dendritic cytoskeleton (Koleske, 2013). The Rho-family of GTPases includes the most extensively characterized

RhoA, Rac1 and Cdc42, acting as binary molecular switches by cycling between an active GTP-bound state and an inactive GDP-bound state (Luo, 2000). These Rho GTPases are important determinants of dendritic structure and have profound effects on spine morphology. While Rac1 and Cdc42 promote dendrite formation, Rho acts contrarily by regulating retraction of dendrites (Da Silva et al., 2003; Govek et al., 2005). Using photoactivatable GFP, Honkura et al. could elegantly prove the existence of three distinct actin filament populations in the spine head, defined by their ultrastructure and different dynamic properties (Honkura et al., 2008). Thus, filamentous actin is classified in a dynamic, an enlargement and a stable pool based on different actin turnover rates. The dynamic pool at the tip of spines shows fast treadmilling (~40 s) and is thought to be crucial for spine volume changes. The enlargement pool appears during spine enlargement with a turnover rate of ~2-15 min and is associated with LTP (Honkura et al.,

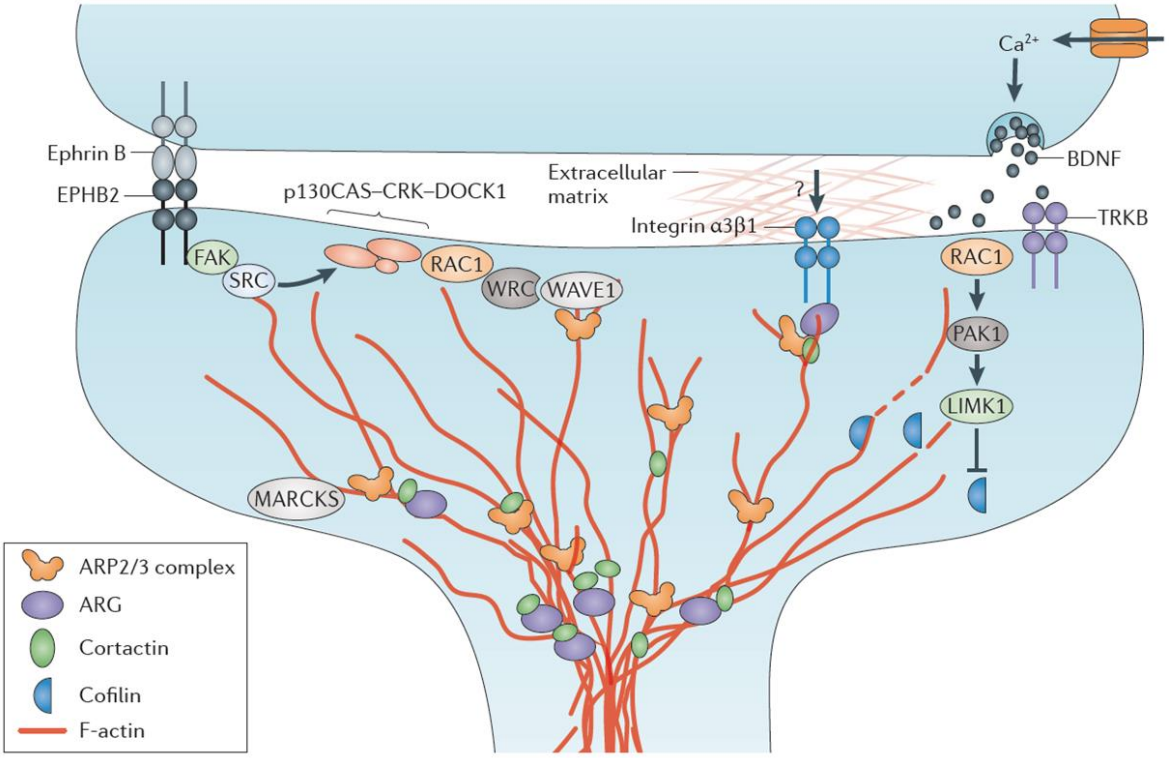

Figure 7 | Cytoskeletal signaling pathways mediate spine stabilization

Spine stability is controlled by several cytoskeletal signaling pathways. For example, binding of presynaptic ephrin B to EPHB2 activates via FAK/Src the GTPase Rac1, which in turn releases WRC from the WAVE complex. WAVE is an activator of the Arp2/3 complex responsible for creating new actin branches. ARG stabilizes newly generated actin branches and mediates phosphorylation of cortactin, thereby promoting its binding to the Arp2/3 complex. Association of cortactin with the Arp2/3 complex initiates actin branch nucleation. Upon presynaptic depolarization, calcium influx leads to release of BDNF (brain derived neurotrophic factor), which binds to its receptor TrkB. Rac1 activation regulates via PAK and LIMK1 the phosphorylation state of cofilin. As phosphorylated cofilin is inactivated, severing of actin filaments is inhibited (Koleske, 2013).

2008). This pool spans the entire spine head and initiates the enlargement of the spine. Long-term expansion of the spine head requires another pool of F-actin, the stable pool at the spine base, which displays slow actin turnover with ~17 min and provides stability and functioning of the spine (Honkura et al., 2008; Tatavarty et al., 2009).

1.3.2 Actin in activity-dependent plasticity processes at synapses

Dendritic spines remain dynamic in the adult brain and can change in response to certain forms of long-term potentiation (LTP)- or long-term depression (LTD)-inducing stimuli *in vitro* and sensory experience *in vivo* (Yuste & Bonhoeffer 2001; Matsuzaki et al. 2004; Carlisle & Kennedy 2005; Lin et al. 2005; Holtmaat et al. 2006). Interestingly, also enrichment of the environment has been shown to alter dendrite structure (Volkmar and Greenough, 1972; Greenough and Volkmar, 1973). Actin filaments are thought to be the basis for both the formation of dendritic spines during development and their structural plasticity of mature synapses (Fischer et al., 2000; Matus et al., 2000). So far, several groups have demonstrated independently that induction of LTP triggers actin polymerization and that spines are capable to undergo rapid actin-based morphological changes follwing changes in activity (Matus, 2000; Ackermann and Matus, 2003; Fukazawa et al., 2003; Okamoto et al., 2004; Lin et al., 2005). In line with this, inhibition of LTP via blocking of NMDA receptors prevented actin polymerization in spines (Lin et al., 2005). Spines can grow or shrink within minutes or hours. To enable this phenomenon, the underlying actin filaments have to be assembled or disassembled on a fast time scale which is tightly regulated via numerous actin-binding proteins (cp. **Figure 7**). Thus, it is not surprising that the dynamic pool of F-actin is at the spine tip (Honkura et al., 2008; Hotulainen et al., 2009). Interestingly, filaments grow as well toward the base of spines, indicating an antiparallel organization of filaments in the neck of spines (Hotulainen et al., 2009). It is widely believed that LTP as an enduring enhanced synaptic transmission reflects the cellular correlate of learning and memory. Induction of LTP changes the G-actin/F-actin ratio toward F-actin and increases spine volume ratio toward F-actin and increases spine volume (Lang et al., 2004; Matsuzaki et al., 2004). Changes regarding spine morphology and their postsynaptic densities are associated with LTP and underlie cytoskeletal reorganization in spines (Carlisle and Kennedy, 2005; Park et al., 2006)

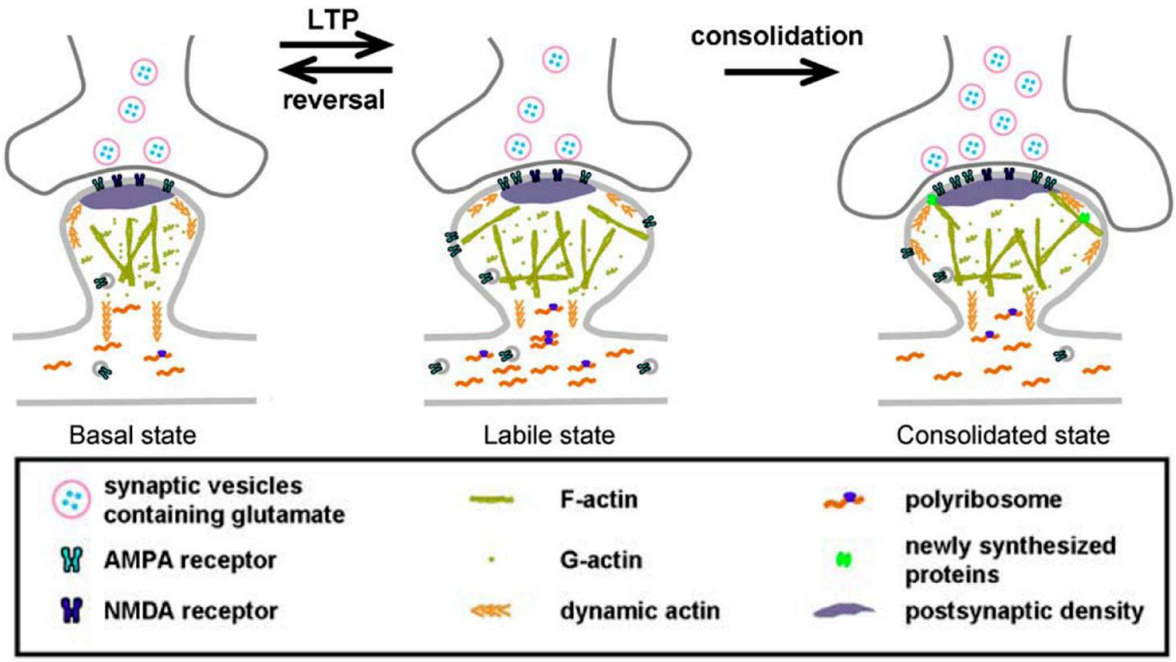

Figure 8 | Spine remodeling in plasticity processes

Spine expansion occurs upon LTP induction (middle) mediated by increased actin polymerization and enhanced actin dynamics. Right after LTP, the spine enters a labile state, where altered spine size can be reversed to the basal state (left). Trafficking and insertion of AMPA receptors into the PSD is controlled by actin dynamics and also modulates synaptic strength. Increased protein synthesis starts at this point. In the consolidated state (right), AMPAR are anchored in the membrane. Spine head enlargement is stabilized by actin-binding proteins, which link/cap filaments. At a later stage, also the presynaptic terminal is increased in size to elevate the number of synaptic vesicles docked at the active zone. In contrast, LTD results in spine shrinkage and is associated with depolymerization of F-actin and internalization of AMPA receptors (not shown) (Wang and Zhou, 2010).

Moreover, LTP is accompanied by an increased number of AMPA receptor in the PSD (Kopec et al., 2006). Since LTP occurs within 1 min and needs to be stabilized in the following 10-15 min, rapid changes in the actin organization are necessary (Lynch et al., 2007). Increased actin polymerization in dendritic spines is essential for stabilization of TBS (theta burst stimulation) induced LTP in rats and mice (Fukazawa et al., 2003; Lynch et al., 2007). In contrast to this, induction of LTD evoked a shift towards G-actin and associated spine shrinkage (Zhou et al., 2004). Low-frequency stimulation for induction of LTD resulted in spine retractions, whereas TBS evoked growth of spines (Nägerl et al., 2004). Pharmacological depolymerization of F-actin caused a decrease in spine head volume and elevated internalization of glutamate receptors. In addition to this, LTP and also spine head enlargement were abolished (Allison et al., 1998; Kim and Lisman, 1999; Krucker et al., 2000; Fukazawa et al., 2003; Rex et al., 2007; Ramachandran and Frey,

2009). Lately, sophisticated STED imaging has revealed direct evidence for morphological changes of the spine neck upon LTP. The analysis determined the spine neck as a highly dynamic structure that becomes shorter and wider upon activity, which may facilitates diffusion of second messengers from the dendrite into the spine (Tønnesen et al., 2014). Two recent studies used time-lapse two-photon imaging of fluorescently labeled synaptic marker proteins combined with electron microscopy to analyze the spatiotemporal changes in synaptic morphology upon LTP. Meyer et al. (2014) demonstrated that in persistently enlarged spines sizes of spine, PSD and bouton are correlated (Meyer et al., 2014). Bosch et al. (2014) monitored the remodeling of spine structures during LTP in single spines and showed that proteins translocate to the spine in four distinct patterns through three sequential phases. The initial phase is characterized by rapid actin remodeling and immense trafficking of cofilin to the spine. After that, cofilin forms a stable complex with F-actin and contributes to long-term spine stabilization. Interestingly, PSD scaffolding protein amounts were unaltered indicating that the PSD is remodeled independently (Bosch et al., 2014).

Application of F-actin polymerization promoting drugs such as jasplakinolide (JPK) alone was shown to be not sufficient for LTP induction and did not exert any effects on synaptic transmission (Okamoto et al., 2004). Interestingly, late-LTP is prevented in mTORC2-deficient mice which display also an abnormally low actin polymerization rate. Here, application of JPK restores late-LTP implying that actin polymerization is critically required for memory consolidation (Huang et al., 2013). More precisely, JPK application leads to conversion of early LTP to late LTP and also transforms short-term memory into long-term memory, indicating that weak stimuli are enhanced by stimulating actin polymerization. Interestingly, inhibition of the Rho/ROCK pathway prevented preferentially initial spine enlargement, whereas the blockade of the Cdc42/Pak pathway abolished the maintenance of structural plasticity (Murakoshi et al., 2011). As aforementioned, these pathways regulate the activity of essential actin-binding proteins such as profilin and cofilin, which might trigger the actin turnover rate in the long run (Saneyoshi et al., 2010). To sum up, there is good evidence that activity-dependent reorganization of the actin cytoskeleton is tightly linked to synaptic efficacy to ensure flexibility of synaptic

connections in the adult brain (Cingolani and Goda, 2008; Kasai et al., 2010). Modulations of actin structures may affect key cellular events such as insertion/removal of neurotransmitter receptors at the synapse and modifications of spine morphology. Eventually, fine-tuning of the connectivity between neurons regulates the changes in neuronal circuits clearing the way for memory storage.

1.3.3 Regulation of the actin cytoskeleton by profilins

Among a multitude of actin binding proteins, profilins (pro-filamentous, 12-16 kDa) are especially important as they directly bind to actin monomers and facilitate the addition to growing filament ends (cp. **Figure 9**) (Witke, 2004). Despite some contradictory data published concerning their effect on intracellular F-actin content, profilins are generally believed to be promoting factors of F-actin polymerization (Schlüter et al. 1997; Yarmola & Bubb 2009; reviewd in Jockusch et al. 2007). In mammals, four profilin genes encode for profilin isoforms 1-4 in a tissue-specific manner (Birbach, 2008). Ubiquitously expressed, PFN1 is the major isoform in most tissues except from neuronal tissue where PFN2a is the most abundant form (Kwiatkowski and Bruns, 1988; Witke et al., 1998). It is

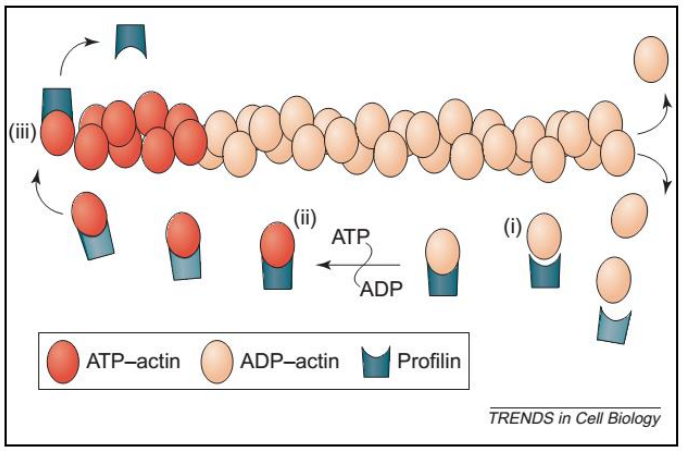

Figure 9 | Role of profilin in regulating actin structures

Three central functions of profilins are known so far. (i) Sequestration of G-actin monomers, (ii) rechargeing of ADP-actin with ATP, (iii) addition of monomers to the fast-growing end (Witke, 2004).

interesting to note that while most mammalian cells express exclusively one profilin isoform, both isoforms PFN1 and PFN2a are expressed in neurons (Lambrechts et al., 2000; Neuhoff et al., 2005). Regarding expression patterns, both profilins seem to be complementary as PFN1 is expressed ubiquitously in high amounts except from skeletal muscle, heart and brain whereas PFN2a expression occurs in heart, kidney and in the first instance in the brain (Honoré et al., 1993). Despite the fact that *pfn1* and *pfn2a* genes share approximately 65% amino acid sequence identity, affinity for G-actin is 4-5 fold higher in PFN1 (Gieselmann et al., 1995). In general, profilins offer three distinct binding

domains for the interaction with numerous binding partners besides G-actin and actin-related proteins (Dominguez, 2009).

Two additional surface-exposed binding sites bind to poly-L-proline (PLP) stretches and phosphatidylinositol-4,5-bisphosphate (PIP2) (Jockusch et al., 2007). As a consequence, profilins are involved in a variety of cell processes and actin remodeling and thus recruited to intracellular locations via binding to polyproline rich proteins associated with plasma membrane like VASP (Reinhard et al., 1995) and MENA (Gertler et al., 1996). Accelerating nucleotide exchange, profilins bind 1:1 to ADP-G-actin monomers and recharge them with ATP, resulting in a 1000 fold ATP exchange of G-actin compared to plain diffusion and replenishment of the ATP-G-actin pool (Goldschmidt-Clermont et al., 1992; Jockusch et al., 2007) (cp. **Figure 9**).

Thus, activity of profilins causes accelerated actin filament growth (Pantaloni and Carlier, 1993). Moreover, both profilins display different affinities for various ligands such as VASP (Lambrechts et al., 1997). However, it still remains to be clarified why both profilins are necessary in the brain as nowhere in the central nervous system either of them is expressed alone. Throughout development, PFN1 is expressed in high levels in nearly all tissues. Expression in the brain varies between different regions, e.g. high expression levels are found in hippocampal pyramidal cells at pre- and postsynaptic sites of synapses (Neuhoff et al., 2005). During peripheral nervous system (PNS) development controlled cytoskeletal remodeling is required and depends on PFN1 function, as knockdown of PFN1 by lentiviral-mediated shRNA delivery critically impairs Schwann cell lamellipodia formation and thereby myelination during PNS maturation (Montani et al., 2014). A recent study revealed that PFN1 associates with cortactin to regulate smooth muscle contraction and that interaction of cortactin with PFN1 is regulated by the c-Abl/cortactin pathway (Wang et al., 2014).

Approaches have begun to unravel the differential and overlapping functions of both PFN1 and PFN2a. PFN1 is essential for cell survival and development as PFN1 ablation in homozygous KO leads to early embryonic lethality (Witke et al., 2001). Hence, conventional PFN1 KO mice are not viable while PFN1 heterozygous mice show only a reduced survival rate (Witke et al., 2001). Interestingly, PFN2a cannot compensate for the lack of PFN1 indicating a more general function for PFN1 in all tissues referring to cell migration, cytokinesis, endocytosis and transcription regulation (Witke, 2004). PFN1

expression is particularly high in tissues undergoing active proliferation (Witke et al., 2001). Genetic ablation of PFN1 in neuronal and glia cell precursors during brain development ($Pfn1^{flx/flx}$, nestin-cre; E11) inhibits radial migration of neurons and brain development (Kullmann et al., 2011). The same PFN1 mutant mouse model exhibited a loss of Purkinje cells during development and associated impairments in motor coordination (Kullmann et al., 2012).

A study using conditional knockout mice with a specific deletion of PFN1 only in neurons of the adult forebrain ($Pfn1^{flx/flx}$, CaMKII-cre; E12.5) was not able to detect alterations in synaptic morphology or plasticity in the absence of PFN1. Moreover, basal synaptic transmission and presynaptic physiology were found to be unaltered in PFN1 cKO mice (Görlich et al., 2012). These findings might be attributed to the possibility that loss of PFN1 could be functionally compensated by PFN2a, supported by the fact that indeed overexpression of PFN1 can compensate for the spine loss caused by the downregulation of PFN2a (Michaelsen et al., 2010).

Numerous studies indicate that PFN1 plays an important role in processes of cellular motility. In breast cancer cells expression of PFN1 is downregulated suggesting that PFN1 could also be a tumor-suppressor protein (Janke et al., 2000; Wittenmayer et al., 2004). In line with that, overexpression of PFN1 leads to reduced migration of breast cancer cells (Roy and Jacobson, 2004). According to that, recent findings discovered that the small GTPase Rho regulates formation of R-cadherin adherens junction in epithelial cells, which may have tumor suppressor effects, via Dia1 and PFN1 (Bonacci et al., 2012). Regulatory mechanisms of profilins had been largely unknown, until PFN1 was identified as a substrate of ROCK1 (Rho-associated kinase 1), a downstream effector of the small GTPase RhoA signaling pathway. Phosphorylation at Ser-137 of profilin reduces its affinity for G-actin, identifying ROCK1 as a negative regulator of profilin activity (Shao et al., 2008). In addition, phosphorylation abolishes profilin binding to huntingtin and its activity as a suppressor of aggregation (Shao et al. 2008). As the principal phosphatase for PFN1 the protein phosphatase 1 (PP1) could be identified lately (Shao and Diamond, 2012).

Profilins are associated with various neuropathological diseases such as amyotrophic lateral sclerosis (ALS), Parkinson's disease or Huntington's disease, as the huntingtin protein affected in this disease directly interacts with PFN1 (Goehler et al., 2004). Progressive loss of both profilin isoforms was observed in the cerebral cortex of

Huntington's disease patients, and in cell culture and *Drosophila* models of polyglutamine disease (Burnett et al., 2008). Recently, a role for PFN1 in axonal remodeling during brain maturation has been confirmed, as the RNA binding protein imp controls axonal restructuring by regulating *chickadee* (the homolog of profilin in *Drosophila*) mRNA expression in *Drosophila* (Medioni et al., 2014). A matter of particular interest is the fact that both brain isoforms of profilin have been shown to be targeted to dendritic spines upon functional plasticity processes such as LTP/LTD in neurons, indicating a putative functional role of these proteins in regulating spine stabilization and synaptic plasticity (Ackermann and Matus, 2003; Neuhoff et al., 2005). Fear conditioning in rats caused the translocation of profilin into spines of the lateral amygdala (Lamprecht et al., 2006).

In contrast to the results obtained for PFN1, conventional PFN2a knockout mice are viable with normal brain development and anatomy. Learning behaviour *in vivo*, LTP and LTD *in vitro* were described to be unaffected in these animals (Pilo Boyl et al., 2007). Nevertheless, mice lacking PFN2a exhibit altered presynaptic excitability with increased vesicle exocytosis and enhanced novelty-seeking behaviour, highlighting the importance of PFN2a for the CNS (Pilo Boyl et al., 2007). Alike PFN1, PFN2a was identified to directly interact with the RhoA downstream kinase ROCK. PFN2a deficiency during development induces multiple sprouting of neurites, implying a negatively regulating function of PFN2a (Da Silva et al., 2003). To directly examine different functions of the two profilins, shRNA mediated knockdown of the neuron-specific profilin isoform PFN2a revealed diverse, isoform-specific functions of both profilins. Loss of PFN2a resulted in a reduced dendritic tree and reduction in spine number in hippocampal neurons. PFN1 expression could not compensate for decreased dendritic complexity, but restored the spine number (Michaelsen et al., 2010). The current study also revealed specific and distinct functions of both profilins downstream of pan-neurotrophin receptor p75. Spine motility experiments with PFN2a-deficient CA1 neurons revealed a stabilizing role for PFN2a in spine morphology, as spine motility was enhanced in neurons lacking PFN2a. Expected spine head growth upon induction of LTP could not be observed in shPFN2a transfected neurons, suggesting a role for PFN2a in activity-dependent structural plasticity (Remus, 2012).

1.4 The brain in disease – the fragile X syndrome

Changes in neuronal connectivity that accompany functional reorganizations both during development and in the mature CNS heavily depend on activity-dependent structural remodeling of spines. Thus, alterations in density or morphology of spines have been linked to neurodevelopmental disorders such as fragile X syndrome (FXS) or Rett syndrome, two monogenetic developmental disorders which have significant overlap with autism spectrum disorder (ASD). FXS, named after its fragile site at the end of the X-chromosome in affected individuals, is the most common inherited form of intellectual disability affecting 1/4000 males and leads to symptoms such as mental retardation, cognitive deficits ranging from mild to severe, behavioral characteristics such as stereotypic motion, epilepsy and disturbed social interaction as well as physical abnormalities such as facial dysmorphism and enlarged testicles (macroorchidism) (reviewed in (Bardoni et al., 2000; Lightbody and Reiss, 2009). FXS is caused by silencing of the *fmr1* gene upon a repeat length exceeding 200 CGGs in the 5'UTR region of the gene, which normally encodes for the fragile X-mental retardation protein (FMRP). While up to 55 CGG repeats are present in the normal population, >200 repeats result in methylation of the repeat and therefore the promoter region, accompanied by silencing of the gene (Bagni and Oostra, 2013). Predominantly expressed in the brain, FMRP is a mRNA binding protein considered to be involved in dendritic mRNA trafficking and regulation of activity-dependent synthesis of proteins. Importantly, among the proteins known to be regulated by FMRP are important modulators of synaptic plasticity and the development of dendrites and axons, thereby linking the molecular pathways of the disorder to impairments in network formation and learning and memory processes. FMRP was shown to regulate the expression of appr. 4% of all mRNAs in the brain and also interacts *in vitro* with its own mRNA (Ashley et al., 1993). Growing body of evidence indicates that modulatory control by FMRP is not solely a repressive action, but FMRP indeed is also able to positively regulate the expression of mRNAs (Fähling et al., 2009; Gross and Bassell, 2012). Strikingly, FMRP can shuttle between the nucleus and the cytoplasm of cells and translocates pre-messenger ribonucleoprotein (pre-mRNP) complexes, which were shown to be critically involved in translational control both in soma and in spines, to distant locations of the cytoplasm (Bardoni et al., 2006). Thus, in neurons FMRP mediates the binding between mRNAs and molecular motors such as

kinesins (Miyashiro et al., 2003; Dictenberg et al., 2008). Reduced rate of mRNA transport and consequently delayed local translation into distal processes and spines leads to altered protein levels, thereby affecting spine structure and plasticity as resembled by FXS patients and *fmr1* knockout mice. In accordance with that, Ascano et al. identified mRNAs as FMRP targets that are involved in neuronal disorders and gonodal development (Ascano et al., 2012). Pathological changes observed in FXS are assumed to be derived from elevated basal protein synthesis downstream of ERK1/2 signaling pathway (Bhakar et al., 2012). Consistent with these results, inhibition of Ras-Erk1/2 signaling abolishes excessive protein synthesis and exaggerated mGluR LTD in the FXS mouse model (Osterweil et al., 2013). Post mortem brain tissue examined from fragile X syndrome patients was characterized by enhanced spine density and a higher proportion of long and immature spines in the cortex, suggesting an impaired spine maturation (Hinton et al., 1991; Irwin et al., 2000, 2001).

The metabotropic glutamate receptor (mGluR) theory of FXS posits that FMRP acts downstream of group1 mGluR and represses translation (Bear et al., 2004). Hence, disturbances of spine morphogenesis in FXS might be caused by enhanced mGluR activity which may lead to more immature spines in *fmr1* KO mice. Indeed, genetically reduced mGluR5 expression or pharmacological inhibition of mGluR resulted in rescue of the spine phenotype and behavioral impairments (Dölen et al., 2007; Kao et al., 2010). Importantly, LTP is also affected in CA1 of *fmr1* KO mice, indicating a crucial role for FMRP in synaptic plasticity (Lauterborn et al., 2007).

1.5 *fmr1* KO mouse model for fragile X syndrome and structural anomalies in neurons

In the mouse model for fragile X syndrome, the *fmr1* gene was deleted resulting in the absence of FMRP (Dutch-belgian et al., 1994). *fmr1* KO mice exhibit impaired learning and memory as well as anxiety-like behavior and autistic traits similar to the phenotype seen in the human condition, making FXS an ideal disorder to study how changes in distinct signaling pathways results in impaired synaptic plasticity and dysfunctional circuits (Penagarikano et al., 2007). Up to now *fmr1* KO mice were described to show rather subtle behavioral and spatial learning abnormalities, the latter detectable in the initial

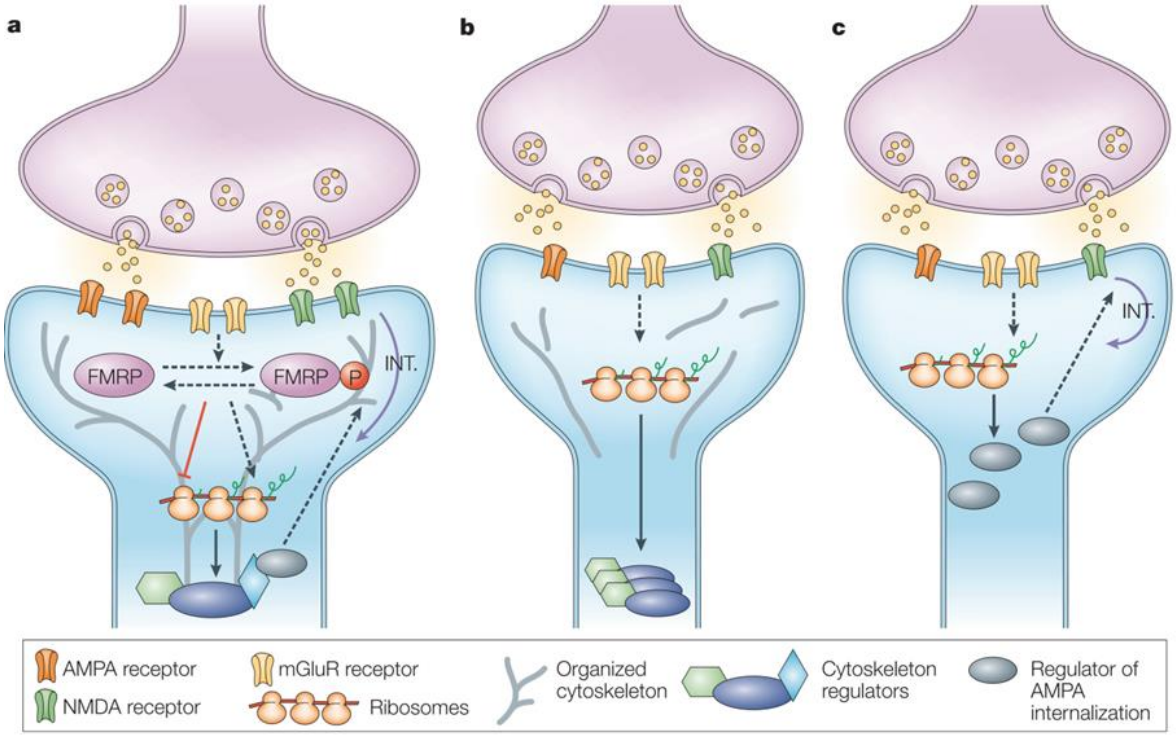

Figure 10 | FMRP at synapses

(a) *Stimulation of mGluR in wild-type synapses enhances the synthesis of FMRP, which may suppress protein translation of proteins involved in receptor internalization during LTD and proteins regulating the actin cytoskeleton.* ***(b)*** *In a spine of the FXS condition, loss of FMRP leads to imbalance of the translation of actin cytoskeleton regulators which may affect the morphology of spines.* ***(c)*** *Loss of FMRP may also result in increased synthesis of proteins responsible for AMPAR and NMDAR internalization during LTD (Bagni and Greenough, 2005).*

hybrid background but not in a pure C57BL/6 background (D'Hooge, 1997; Van Dam et al., 2005). For decades it has been a widely accepted assumption that the main pathological hallmark of FXS is a higher spine density and an increased proportion of long, immature spines. Indeed, autopsy of brain tissue demonstrated such spine abnormalities in neurons of the neocortex (Irwin et al., 2001). In addition to that, several groups used Golgi staining in fixed tissue of adult *fmr1* WT and KO mice and reported an increased spine density (Comery et al., 1997; McKinney, 2005; Dölen et al., 2007; Hayashi et al., 2007; Liu et al., 2011), with some exceptions (Irwin et al., 2002; Restivo et al., 2005). In the hippocampus, either low or normal spine density was observed with either normal or increased length of spines (Braun & Segal 2000; Segal et al. 2003; Grossman et al. 2006; Pfeiffer & Huber 2007; de Vrij et al. 2008; Bilousova et al. 2009). Despite the contradictory findings regarding spine density dependent on the brain region, method and age of mice, a consistent result seems to be the immature spine phenotype found in the cortex,

cerebellum and also hippocampus (Koekkoek et al., 2005; Antar et al., 2006; Grossman et al., 2006; de Vrij et al., 2008; Bilousova et al., 2009; Cruz-Martín et al., 2010; Pan et al., 2010). Cruz-Martin and others also reported an unaltered spine volume in *fmr1* knockout mice, but unfortunately detailed information concerning the spine structure at the subcellular level is missing so far. The FMRP is concentrated in spines, where it is believed to regulate the local translation of proteins at synapses (McKinney, 2005) (cp. **Figure 10**). *Fmr1* KO mice are transiently impaired in stabilization of spines as shown by an abnormally high turnover during the second postnatal week, when FMRP protein expression is highest in the cortex (Cruz-Martín et al., 2010; Harlow et al., 2010). In contrast to this *in vivo* study, a recent study using organotypic slice cultures of *fmr1* knockout mice demonstrated decreased basal spine turnover which could be significantly enhanced by induction of activity. Moreover, activity-induced spine stabilization was lost in FMRP lacking neurons and could be rescued by enhancement of the PI3K signaling pathway (Boda et al., 2014). In the absence of FMRP, LTP-induced signaling to the actin cytoskeleton might be impaired due to Rac1 activation and over-activation of PAK that may lead to defects in activity-dependent actin remodeling.

Collectively, dendritic spine structures and densities were described to be affected in FMRP deficient neurons in some studies, but it is still unclear to which extent neuronal morphology is altered and how these changes could be attributed to a modified signaling to the actin cytoskeleton. Remarkably, an interesting link between FMRP and the F-actin regulating protein profilin was revealed recently. In *Drosophila melanogaster*, dFMRP regulates the mRNA of *chickadee*, which is the *profilin* homolog and suppresses profilin protein expression. On the one hand, overexpression of profilin mimics the phenotype of *dfmr1* mutants while on the other hand a decrease of profilin levels suppresses *dfmr1* phenotypes (Reeve et al., 2005). Thus, findings like these point to FMRP as a regulator of actin dynamics and the absence of FMRP might also in mammals cause changes in the amount of profilin available, which could in turn affect actin polymerization process and thereby provide one explanation for the pathological alterations in the shape and size of spines in the course of this disorder.

1.6 Aim of study

Structural remodeling of the actin cytoskeleton requires a sophisticated spatial and temporal regulation mediated by numerous actin binding molecules. Among these, profilin is of key interest as it facilitates actin polymerization. In the mammalian brain, there are two profilin isoforms: prolin1 (PFN1) which is ubiquitously expressed in all cells and the brain specific isoform prolin2a (PFN2a). Interestingly, we could show recently by RNAi-mediated knockdown of PFN2a that it has indeed an isoform-specific role in mediating dendrite stability (Michaelsen et al., 2010). In order to gain a more comprehensive understanding of the specific role of PFN1 in regulating dendrite architecture and spine stability of immature and mature pyramidal neurons of the murine hippocampus, an acute RNAi-mediated knockdown of PFN1 was used. Since it has been recently shown that PFN2a is an important determinant of activity-dependent structural plasticity as well as basal spine motility, live imaging experiments with PFN1 deficient hippocampal neurons were performed to reveal differences between both isoforms regarding their function in remodeling the synaptic structure.

As morphological abnormalities in dendritic spines are in fact linked to diseases, the mouse model of the fragile X syndrome (FXS), a neurological disorder known to affect spine development and function was used to investigate *in vivo* and *in vitro* the role of actin-binding proteins like profilins and cofilin.

2 MATERIALS AND METHODS

2.1 Equipment

device type	device name	manufacturer
ApoTome		Zeiss
autoclave	Fedegari	Tecnomara
binocular	binocular	Zeiss
balance	Acculab analytical balance	Sartorius
camera (tracking)	VK-1316S/12V	Eneo
controller LSM	display SM-5	Luigs&Neumann
fluorescence microscopes	Axiovert B5 TV (HBO100)	Zeiss
	Axioplan 2 imaging	Zeiss
gel chamber		Sigma-Aldrich
gel documentation system	Herolab EASY RH	Herolab GmbH
gene gun	Helios® gene gun system	BIO-RAD
laminar flow hood	SterilGARD	The Baker Company
microscope	Axioplan 2 imaging	Zeiss
microscope LSM	BX	Olympus
microplate reader	MRX	Dynatech Medical Products
pH-meter	pH 720	Inolab
pipettes	Pipetman	Gilson
power supply	BluePower 500	Serva
semidry blotter		Fröbel
shaker	Vortex-Genie	2Scientific Industries Eppendorf, Labmate
table centrifuge	Sigma 113	B.Tech Biobraun International GmbH
thermocycler	Thermomixer 5436	Eppendorf
tubing prep station		BIO-RAD
tubing cutter		BIO-RAD
tissue chopper		McIlwain
ultrasonic cleaner		VWR
ultrasonic device	UP50H	Hielscher
UV-table	T1	Biometra
vortex	Vortex-Genie 2	Scientific Industries
vibrating microtome	VT1200S	Leica Microsystems
water maze pool	(Ø160 cm, height 60 cm)	TSE
water maze platform	Atlantis Ø10 cm	TSE

2.2 Disposables

material	manufacturer
tissue culture dishes	Techno Plastic Products AG
tissue culture 24 well plates	Techno Plastic Products AG
tube 50 ml	Greiner Bio One
tube 15 ml	Sarstedt
filter tips	Peqlab
cover glasses	VWR No. 1, diameter 13 mm, round
microtest plate 96 well F nitrocellulose	Sarstedt AG & Co.
PVDF membrane Roti-Fluoro, 0.2 µm	Carl Roth GmbH&Co. KG
sterile filter FP 30/0,2 CA-S (Ø 0.2µm)	Schleicher & Schuell
X-ray film LucentBlue	advansta

2.3 Reagents

reagents	manufacturer
5-Fluoro-2'-Deoxyuridine	S Sigma-Aldrich Chemie GmbH
AEBSF	Applichem
Ammonium persulfate	Applichem
Agar-Agar	Roth
Agarose	AppliChem
Ampicillin	MP Biomedical
ß-Mercaptoethanol	Applichem
B27 supplement	Gibco
BME medium	Gibco
Borax	Sigma-Aldrich Chemie GmbH
Boric acid	Merck
Bromphenol blue	Applichem
BSA	Roth
Calcium chloride	Applichem
Coomassie Brilliant Blue 250	Applichem
Cytosin-D-Arabinofuranosid hydrochloride	Sigma-Aldrich Chemie GmbH
DAPI	Applichem
DMEM	PAA
D-Glucose	Applichem
Disodium phosphate	Applichem
Equine donor serum	HyClone (Perbio)
Ethanol	VWR International
Fetal calf serum (FCS)	PAA Laboratories
Fluoro Gel	EMS Diasum
Glycerol	Applichem
Glycine	Applichem
Goat Serum	Invitrogen
Gold (0.6 µm)	Bio-Rad
Hank's Balanced Salt Solution	Gibco Invitrogen
HBSS (10x)	Invitrogen
Kanamycin-sulfate	MP Biomedicals
Kynurenic acid	Sigma-Aldrich Chemie GmbH
L-Glutamine	Gibco Invitrogen
Lipofectamine 2000®	Invitrogen
Luminata™ Crescendo Western HRP Substrate	Millipore Corporation
Magnesium chloride	Applichem
Magnesium sulfate heptahydrate	Applichem
Manual Fixing Bath G354	AGFA HealthCare GmbH
Methanol	Fischer Scientific UK
Monopotassium phosphate	AppliChem
Neurobasal medium	Gibco Invitrogen
N2 supplement	self-made
Nitrogen	Linde AG
N,N,N',N'-Tetramethylethylendiamin	Sigma-Aldrich Chemie GmbH
PageRuler™ Plus Prestained Protein Ladder	Thermo Scientific
Paraformaldehyde	Applichem
Pepstatin A	Applichem
Phosphatase inhibitor cocktail 2	Serva
Phosphoric acid	Applichem
Potassium chloride	Applichem
Plasmid preparation kit	Qiagen
Poly-L-lysine	Sigma-Aldrich Chemie GmbH
Polyvinylpyrrolidone (PVP)	Bio-Rad
Propan-2-ol	VWR International

Protein standard micro standard (BSA 1mg/ml)	Sigma-Aldrich Chemie GmbH
Roentogen	Tetenal Europe GmbH
Rotiphorese Gel 30	Carl Roth GmbH&Co.KG
Saccharose	Applichem
skimmed-milk powder	Sucofin
Sodium chloride	AppliChem
SDS pellets	Carl Roth GmbH&Co.KG
Sodium hydrogen carbonate	Applichem
Spermidine	Sigma-Aldrich Chemie GmbH
Titandioxid	Euro OTC Pharma
Trasylol	Bayer Vital GmbH
TRIS	Applichem
Triton X-100	Sigma-Aldrich Chemie GmbH
Trypsin-EDTA 1x	Sigma-Aldrich Chemie GmbH
Tween-20	Carl Roth GmbH&Co.KG
Tryptone	MP Biomedicals
Uridine	Sigma-Aldrich Chemie GmbH
Yeast extract	MP Biomedicals

2.4 Software

software	**manufacturer**
Adobe Acrobat 9 Pro	Adobe
Adobe Illustrator CS4	Adobe
Adobe Photoshop CS4	Adobe
Autoquant X2	MediaCybernetics
EasyWin32	Herolab GmbH
ImageJ 1.46K	NIH USA
Matlab R2009b	The Mathworks
Microsoft Office	Microsoft Corporation
Prism 5	Graphpad Software Incorporation
tracking software “TSE Videomot2 Vol. 5.76”	TSE
SPSS Statistics Client 2.0	IBM

2.5 Solutions and media

For solutions and media either demineralized water (H_2O) or purified (MQ H_2O) was used.

ACSF *(Artificial cerebrospinal fluid) used for preparation and for live imaging experiment*
125 mM NaCl
2.5 mM KCl
1.25 mM $NaH_2PO_4 * H_2O$
2 mM $MgCl_2 * 6\ H_2O$
26 mM $NaHCO_3$
2 mM $CaCl_2$
25 mM D(+)-Glucose

AEBSF
1 g AEBSF
21 ml MQ H_2O

10% Ammonium persulfate
10% in (demineralized) H_2O stored at -20°C

10x blotting buffer
0.25M Tris
1.5 M glycine
Fill up to 2 L with H_2O, pH 8.6

1x blotting buffer
100 ml methanol
100 ml 10x blotting buffer
800 ml H_2O

5x Bradford reagent
100 ml phosphoric acid
50 ml ethanol
100 mg Coomassie Brilliant Blue G250
Fill up to 250 ml with H_2O.

LB medium
10 g/l Trypton
10 g/l NaCl
5 g/l yeast extract
solid: add 15 g/l agar-agar
H_2Odest. was used as solvent.

Lyses buffer *used for the purification of genomic DNA from mice tails.*
100 mM Tris/HCl pH 8
200 mM NaCl
5 mM EDTA
0.2% SDS
100 µg/ml Proteinase K

Pepstatin A
10 mg Pepstatin A
14.6 ml EtOH 100%

Phosphate buffered saline (PBS)
2.7 mM KCl
1.5 mM KH_2PO_4
137 mM NaCl
10.4 mM Na_2HPO_4

10x SDS gel buffer
60 g Tris
288 g glycine
20 g SDS

1x SDS gel buffer
100 ml 10x SDS gel buffer
900 ml H_2O

4x SDS protein sample buffer
375 mM TRIS-HCl pH 7.6
2% SDS
12% Glycerol 87%
0.05% Bromphenol blue
10% ß-Mercaptoethanol

Separating gel
62 ml MQ H_2O
25 ml separating gel buffer
13 ml Rotiphorese gel 30
50 µl TEMED
1 ml APS 10%

Separating gel (for gradient gels)
32 ml (10%) resp. 6 ml (20%) MQ H_2O
19 ml separating gel buffer
25 ml (10%) resp. 51 ml (20%) acrylamide
20 µl TEMED
400 µl APS 10%

Separating gel buffer
1.5 M TRIS
0.4% SDS
set to pH 8.8

Stacking gel
30 ml MQ H_2O
30 ml stacking gel buffer
60 ml Rotiphorese gel 30
40 µl TEMED
800 µl APS 10%

Stacking gel (for gradient gels)
31 ml MQ H_2O
12.5 ml stacking gel buffer
6.5 ml acrylamide
50 µl TEMED
1 ml APS 10%

Stacking gel buffer
0.6 M TRIS
0.4% SDS
set to pH 6.8

STKM buffer (homogenization buffer)
250 mM Saccharose
50 mM TRIS-HCl
25 mM KCl
5 mM $MgCl_2$
set to pH 7.5 at 4 °C

STKM buffer with protease inhibitors
981 µl STKM buffer
2 µl AEBSF (1:500)
2 µl Pepstatin A (1:500)
10 µl Trasylol (1:100)
5 µl PIC2 (1:200)

10x TBS
0.2 M Tris
1.37 M NaCl
set to pH 7.6

10x TBS-T
10x TBS
0.1% Tween-20

10x TBS-X
10x TBS
0.1% Triton X-100

X-ray film developer solution
150 ml Roetogen
700 ml H_2O

X-ray film fixing solution
150 ml Manual Fixing Bath G354
750 ml H_2O

2.5.1 Primary cultures

Blocking solution
1% BSA
10% goat serum
0.2% Triton-X-100

Borate buffer pH 8.5 (glass coverslips)
1.24 g boric acid
1.9 g borax
400 ml dH_2O
set to pH 8.5

Culture medium
49 ml Neurobasal® medium
1 ml B27 supplement
125 µl L-glutamine
500 µl N2 supplement (100x)

Glucose (50%)
Dilute Glucose 1:1 with H_2O in microwave and filtrate sterile immediately.
Store 1 ml aliquots at -20 °C.

4% Paraformaldehyde (in 0.1 M phosphate buffer, pH 7.4)
For fixation solution, 40 g PFA were solved in 500 ml warm dH_2O, cooled down and filtrated. Then 500 ml of 0.2 M phosphate buffer were added before 50 ml aliquots were stored at -20 °C.

Phosphate buffer (0.2 M, pH 7.4)
0.04 M $NaH_2PO_4*2H_2O$
0.17 M $Na_2HPO_4*2H_2O$

2.5.2 Organotypic cultures

Antimitotics
2.422 mg Uridine in 10 ml dH_2O (1 M)
2.797 mg Cytosin-β-D-Arabinofuranosid Hydrochlorid in 10 ml dH_2O (1 M)
2.462 mg 5-Fluoro-2´-Deoxyuridin in 10 ml H_2O (1 M)
Stock solutions were mixed 1:1, filtered sterile and stored at -20 °C

Culture medium
100 ml BME
50 ml HBSS
50 ml Equine donor serum
1 ml L-Glutamin (200mM)
1 ml Glucose (50%)

GBSS solution (Gey's balanced salt solution)
0.22 g $CaCl_2 * 2\ H_2O$
0.37 g KCl
0.03 g KH_2PO_4
0.21 g $MgCl_2 * 6\ H_2O$
0.07 g $MgSO_4 * 7\ H_2O$
8 g NaCl
0.227 g Na_2HCO_3
0.12 g Na_2HPO_4
1 g D-glucose
Fill up to 1 l with MQ H_2O.

Kynurenic acid
946 mg Kynurenic acid
5 ml 1 M NaOH
45 ml H2O

Preparation solution pH 7.2
98 ml GBSS
1 ml glucose
1ml Kynurenic acid (in case of slice culture preparation)

2.6 Mouse strains

Fmr1 knockout and wild type mice were on FVB background. The *fmr1* gene is located on the X chromosome, therefore its deletion in one allele results in FXS in males. Female

fmr1$^{+/-}$ mice were crossed with male mutant *fmr1*$^{y/+}$ mice to generate mutant mice as well as wild-type (WT) littermates. Genotypes of offsprings resulting from a *fmr1*$^{+/-}$ x *fmr1*$^{y/+}$ breeding were determined by PCR using a tail biopsy. Dissociated neuronal cultures were prepared from embryos (E18.5) of *fmr1*$^{+/-}$ x *fmr1*$^{y/+}$ breedings or from C57BL/6 embryos at E18.5. Organotypic hippocampal cultures were produced from C57BL/6 mice at postnatal day P5. Biochemical assays were performed with P0, P7, P15 or adult (not less than 2 months) *fmr1* KO and WT mice, respectively. Hippocampal slice cultures used for biochemical analyses were derived from adult male C57BL/6 mice. Behavioural tests included adult male *fmr1*$^{-/-}$ or *fmr1*$^{y/+}$ mice at age of 12-18 weeks at the onset of experiments.

2.6.1 Genotyping of transgenic mice

Genomic DNA was obtained from distal tail tissue (tail biopsy) followed by DNA isolation. Briefly, tail tips were digested overnight in 500 µl lyses buffer at 55 °C. By centrifugation at 14.000 x g cellular debris was removed. Extraction of genomic DNA was performed using phenol/chloroform and DNA was precipitated with ethanol-sodium acetate. DNA was washed once using 70% ethanol and stored at 4 °C in 10 mM Tris/HCl (pH 8).

Table 1: PCR master mix

component	concentration
PCR buffer	10 mM
dNTPs	10 nM
forward primer	100 nM
reverse primer	100 nM
GoTaq polymerase	1 unit
DNA	1 µl

Table 2: PCR program

temperature [°C]	time
94	3 min
94	30 s
62	30 s
72	1 min
72	2 min
10	hold

(repeat 2-4 34 times)

Table 3: Primer for genotyping

primer	target	sequence (5'→3')	primer type
oIMR2060	*fmr1* KO (400 bp)	CACGAGACTAGTGAGACGTG	mutant forward
oIMR6734	*fmr1* WT (131 bp)	TGTGATAGAATATGCAGCATGTGA	wild-type forward
oIMR6735	*fmr1* WT (131 bp)	CTTCTGGCACCTCCAGCTT	common

Wild-type (131 bp) and knockout (400 bp) alleles were amplified with specific primer combinations and separated by gel electrophoresis on a 1.5% agarose gel.

2.7 Cell culture techniques

2.7.1 Preparation of primary hippocampal cultures

Preparation of cover slips

After incubation in 10 M NaOH for 3-5 h at 100 °C coverslips were washed five times with distilled water and dried for 6 h at 225 °C. Before coating with poly-L-lysine (0.5 mg/ml in borate buffer), the coverslips were allowed to cool down to room temperature. Coating was performed either at 4 °C overnight or for 2-3 h at 37 °C. The coverslips were washed five times with distilled water and dried. Coated coverslips were stored at 4 °C.

Preparation of cultures

One of the most well-established and widely used techniques for the study of hippocampal and cortical pyramidal neurons has been the primary dissociated cell culture system developed by Craig and Banker 1994 (established protocol in Kaech and Banker 2006) for the culture of embryonic rat neurons. This system allows neurons to be cultured *in vitro* in a far less complex environment than that present *in vivo*, making them highly accessible to manipulations and observations.

Cultures of hippocampal neurons were prepared from embryonic day 18 (E18.5) mouse embryos of C57BL/6 mice or, in case of *fmr1* KO mice, from a *fmr1*$^{+/-}$ x fmr$^{y/-}$ mating. After decapitation embryonic heads were placed into cold GBSS/glucose (10 cm dish). Cranium and meninges were removed. Hippocampi and parts of the cortex were rapidly taken out and transferred into 1 ml trypsin/EDTA solution. Subsequent incubation at 37 °C for 30 min. ensured dissociation of brain tissue. Trypsin was aspirated and the reaction stopped by addition of 1 ml serum medium. For mechanical dissociation, the solution was pipetted up and down without introducing air bubbles until it was homogeneous. Cell number was determined before cells could be plated at high density (70.000 cells/well = appr. 350 cells per mm^2) on each coverslip in 150 µl medium. Cells were allowed to attach for 2-3 h before 350 µl medium were added to each well. Neurons were kept in Neurobasal® medium supplemented with B27, glutamine as well as N2 in a humidified atmosphere at 36.5 °C with 5% CO_2. Once a week, 100 µl of culture medium per well were replaced by fresh medium.

2.7.2 Preparation of organotypic hippocampal cultures

Organotypic hippocampal slice cultures (OHC) represent an *in vitro* model that includes the different cell types and maintains the complex three-dimensional organization of the hippocampal network. As the central nervous system is a complex tissue, OHCs have the advantage of preserving tissue-specific cell connections compared to dissociated cell cultures. Conventional OHCs were established from C57BL/6 mice after Stoppini et al. 1991. Mice at age of 5 d postnatal were rapidly decapitated in ice-cold GBSS. Both hippocampi were cut using the McIllwain tissue chopper into 400 µm thick transversal slices. After incubation in GBSS for 15-30 min at 4 °C, a maximum of four slices were transferred onto a membrane insert (Millicell®, 0.4 µm pore size) in a 6-well plate with culture medium. At 3 days in vitro (DIV) antimitotics (15.4 µl per well) were added for 24 h to the medium to prevent glia cell division. Once a week 50% of the culture medium was replaced by fresh medium. Hippocampal slices were cultured in medium for 14-21 days *in vitro* (DIV).

2.7.3 Preparation of acute hippocampal slices

Acute slices were prepared from hippocampi of adult (2-3 months old) male C57/Bl6 mice. After a brief anesthesia with CO_2, the mice were rapidly decapitated and the brain was removed. In order to reduce oxidative stress the brain was left for 3 min in ice-cold ACSF. The solution was constantly carbogenated (95% O_2, 5% CO_2) to ensure a sufficient supply with oxygen. Both hippocampi were fixed upright with tissue-glue on a disk and leaned against an agar block. Within a buffer tray filled with ice-cold carbogenated ACSF, the hippocampi were cut horizontally into 400 µm thick transversal slices using the VT1200S vibrating microtome (Leica Microsystems, Germany). Slices were transferred into a storage chamber with gassed ACSF for 2 h at RT before starting the biopsy punching.

2.8 Transfection of hippocampal neurons

2.8.1 Biolistic transfection using the Helios® *gene gun*

The *gene gun* technique, also known as biolistic particle delivery or biolistics, was originally developed for plant transformation in the early 1980s and enables the

transfection of only a small subset of cells in slice cultures (Sanford, J.C., Klein, 1987). Organotypic slices were transfected with the Helios® gene gun system of Bio-Rad at different points in time (10 DIV and 17 DIV) with siPFN1 or control plasmid and subsequently cultured for 4 days. Gold microcarriers coated with DNA were shot onto the slices with helium at a pressure of 100 psi. Acceleration provides the necessary force to puncture the cell membrane and deliver the materials into the living neuron. A filter placed between the gene gun and the slices prevents gold clumps from reaching the tissue.

At least one day before transfection the bullets were prepared using the tubing preparation station provided with the *gene gun*. Briefly, the gold microcarriers (12.5-15 mg per tubing for one plasmid and co-transfections, respectively) were mixed with 100 µl of 0.05 M spermidine. After 10 s of sonication, 25 or 30 µg of DNA was added to the solution, respectively. 100 µl 1 M Ca_2Cl were added drop wise to the gold-DNA-mixture followed by 10 min incubation at RT. The solution was resuspended in 1 ml of ice-cold 96% ethanol and centrifuged for 60-90 s at 100 x g. The supernatant was removed and discarded. To remove residual spermidine, this washing step was repeated three times before the gold microcarriers were finally dissolved in 3 ml of ethanol containing 0.05 mg/ml PVP. A Tefzel (ethylen-tetrafluorethylene) tubing was cleaned and dried in the tubing preparation station with nitrogen flow for 10 min before the gold-DNA-suspension was injected via a syringe. Ethanol was removed after 3 min and the tubing was rotated for 30 s to ensure a homogenous gold distribution. Finally, the tubing dried by nitrogen flow for 5 min and was cut into appr. 50 bullets per tubing with the tubing cutter (Bio-Rad). Bullets were stored at 4 °C in the presence of a dessicant pellet for several weeks.

2.8.2 Transfection of primary dissociated hippocampal and cortical neurons

Dissociated hippocampal or cortical neurons were transfected using Lipofectamine2000® at various time points. Shortly before transfection, culture medium was exchanged with Neurobasal® medium without supplements. For transfection, 0.8 µg DNA and 2 µl Lipofectamine2000® per well were diluted separately in 50 µl of Neurobasal® medium. After 5 min both components were combined and incubated for 20 min at room temperature. Lipofection solution (100 µl per well) was added to each well dropwise

followed by a subsequent incubation for 45 min in a 36.5 °C and 5% CO_2 atmosphere. Reaction was stopped by replacing the medium with prior preserved culture medium. The cells were used for experiments at various points in time after transfection ranging from 48 h (for overexpression of PFN1/PFN2a) to 72 h (for knockdown of PFN1) and 7 days (for knockdown of PFN2a). Cells were fixed post transfection using 4% paraformaldehyde (in PB) overnight at 4 °C or 15 min at RT. The cultures were washed three times with PBS for 20 min, mounted onto microscope slides and stored in the dark at 4 °C.

2.9 Immunohistochemistry of primary cultures

After fixation the cells were washed three times in PBS and permeabilized using 0.2% Triton X-100 in PBS. Blocking was performed with 10% goat serum and 1% BSA in PBS for 1 h. The primary antibody was diluted in blocking solution without BSA and incubated overnight at 4 °C. The secondary antibodies were diluted in PBS and incubated for 2 h at RT. The coverslips were washed three times with PBS and once with H_2O before being mounted onto microscope slides.

Table 4 | Primary and secondary antibodies for immunohistochemistry and western blotting. (*= cross-absorbed)

used primary or secondary antibody	species	manufacturer	dilution
anti-Cofilin	rabbit	Abcam plc	1:10.000
anti-GAPDH	rabbit	Acris Antibodies GmbH	1:6000
anti-LaminA	rabbit	Sigma-Aldrich Chemie GmbH	1:2000
anti-PFN1 C-terminus	rabbit		1:5000
anti-PFN1 clone1A11	mouse	Sabine Buchmeier (AG Jockusch)	1:100
anti-PFN2a clone4H5	mouse	Sabine Buchmeier (AG Jockusch)	1:75
anti-PFN2a antiserum	rabbit	Bioscience Göttingen	1:20.000
anti-Tubulin DM1a	mouse	Abcam plc	1:10.000
anti-mouse IgG Cy3*	goat	Dianova (Hamburg)	1:100
anti-mouse IgG Cy2*	goat	Dianova (Hamburg)	1:100
anti-mouse IgG Peroxidase	goat	Sigma-Aldrich Chemie GmbH	1:20.000
anti-rabbit Cy3*	goat	Dianova (Hamburg)	1:100
anti-rabbit Cy2*	goat	Dianova (Hamburg)	1:100
anti-rabbit Cy5*	goat	Dianova (Hamburg)	1:100
anti-rabbit IgG Peroxidase	goat	Sigma-Aldrich Chemie GmbH	1:20.000
used agents			
Alexa Fluor 350 Phalloidin		Invitrogen (Karlsruhe)	1:100
DAPI		Applichem (Darmstadt)	1:1000

2.10 Image acquisition and analysis

2.10.1 Fixed tissue

For morphological analysis of dissociated or OHC neurons only cells without any signs of degeneration like swellings of the soma or retraction bulbs were chosen. Images of hippocampal neurons were collected with the Axiocam MRm and a Zeiss Axioplan 2 microscope using a 20x objective (0.8 NA Plan-APO, Zeiss) and a z-sectioning of 1 µm. For spine analysis, parts of the dendritic tree were imaged with a 63x oil immersion objective (1.4 NA Plan-APO, Zeiss) and a z-stack thickness of 0.5 µm. An associated ApoTome apparatus (Zeiss) removed blur arising from out of focus fluorescence signal, therefore causing a higher resolution. To determine spine density and spine types, spines on three dendrites per cell (secondary or tertiary dendrites) were counted and measured manually.

Dendritic morphology was analyzed using Neurolucida Software (MBF Bioscience) by tracing dendrites manually. Further analysis of Neurolucida data was done with NeuroExplorer. Total dendritic length and total number of nodes or endings were analyzed. In addition, *Sholl analysis* (Sholl, 1953) was performed. This method quantifies the number of dendritic intersections with concentric spheres or circles around the cell body and allows analysis of a detailed neuronal complexity profile.

To determine spine geometry, independent traces were drawn for the neck and the head of each spine with the segmented line tool of ImageJ (NIH). The total length was measured from the tip of the spine head towards the base of the spine where it connects to the adjacent dendrite.

The data were statistically evaluated with Microsoft Office Excel (version 2010) or GraphPad Prism (version 5.01). Statistical significance was evaluated by applying an unpaired, two-tailed Student's *t* test and significance levels were set at *$p<0.05$, **$p<0.01$, ***$p<0.001$. For *Sholl analysis*, significance was only considered if two or more adjacent points showed p values below 0.05. Behavioural tests were statistically evaluated by one-way ANOVA with repeated measures in SPSS.

2.10.2 Live imaging of spines

Spines are highly motile structures. The formation of dendritic spines during development or activity-induced structural changes of spines are critical aspects of synaptic plasticity. Thus, spine dynamics of pyramidal neurons in CA1 and CA3 region as well as of granule cells in the dentate gyrus of the hippocampus were analyzed with *live imaging* experiments using a confocal laser scanning microscope (model: Fluoview 1000, Olympus). The imaging chamber (RC-22, Warner Instruments, Connecticut, USA) was heated to 35 °C and perfused with carbogenated ACSF via a peristaltic pump at a flow rate of 1 ml/min. Hippocampal slices were preincubated for 20 min in the chamber and hold in place with a slice anchor (Warner Instruments) to reduce movement.

The imaging system was equipped with a low numerical-aperture (NA) objective for low resolution images of whole cells (20x, 1.4 NA) and a high NA objective (60x, NA 1.0) for detailed imaging of dendritic spines.

Transfected pyramidal neurons were randomly selected and were encoded for blind analysis. Basal dendrites as well as proximal dendrites from the apical compartment (identified as processes up to a distance of 200 µm from the neuronal cell body) were selected for analysis of the spine mobility in case of CA1 and CA3 pyramidal cells. Z-stacks (interval for z-sectioning = 0.35 µm) of dendritic sections were captured at 5 min intervals for 25 min (pixel size = 0.071 µm). In addition to spine mobility monitoring under basal conditions, spine changes were analyzed before and 60 min after chemically induced long-term potentiation (cLTP). cLTP was induced by application of 10 mM glycine in ACSF for 10 min. 60 min after cLTP induction, spine mobility was recorded again as described above.

Subsequently, morphological changes upon cLTP induction as well as mobility of spines were determined by measuring spine length and spine head width with ImageJ (NIH). For analysis of global spine mobility, the following equation after Chierzi et al. 2012 was used:

$$\text{motility index} = \frac{(|L2-L1|+|L3-L2|+|L4-L3|+|L5-L4|)}{\left[\frac{L1+L2+L3+L4+L5}{5}\right]}$$

Using this equation, the motility index of either spine head or spine length can be determined.

2.11 Molecular biology

2.11.1 Preparation of DNA

To chemically transform cells, 30 µl of competent *E.coli* cells are mixed with 1 µl of DNA (on ice), followed by a brief heat shock for 30 s at 42 °C. Cells were incubated with LB medium without antibiotics for 30-60 min prior to plating. After incubation at 37 °C overnight one single colony was picked and transferred into 3 ml of LB medium supplemented with appropriate antibiotics. The starter culture incubated for 6-8 h at 37 °C with vigorous shaking (225 rpm) before it was used for inoculation of the main culture (100-200 ml LB medium with the appropriate selective antibiotic). Bacteria were incubated at 37 °C overnight on a shaker. Plasmid DNA was prepared and purified using Qiagen Plasmid Midi Kit (Qiagen GmbH, Hilden) as recommended by the manufacturer. Bacteria were lysed and the filtered lysate cleared using a Qiagen column. Finally, DNA purity and concentration were measured by UV absorption with a photometer and also verified via gel electrophoresis. **Table** gives an overview of all plasmids used in this work.

Table 5 | Plasmids used in this work

plasmid	description	reference
pmCherry-f	farnesylated fluorescent protein mcherry (CMV promoter)	Shaner et al., 2004; O'Brien, 2007
peGFP-f	farnesylated enhanced green fluorescent protein (CMV promoter)	Clontech
pRNAT_siFluc	firefly luciferase siRNA vector (control vector) for shPFN1	Genescript
pRNAT1.3	Profilin1 specific RNAi, GFP-f	Murk K., 2008
pRNAT_1.3_ΔmApple	Profilin1 specific RNAi, mApple(truncated CMV promoter)	Schweinhuber S., 2014
pRNAT2.13eGFP-f	polycistronic vector: 1. Profilin2a-specific shRNA sequence (CMV/U6.3 promoter), 2. Reporter fGFP (CMV promoter)	Murk K., 2008
pΔCMV-YFP-mPFN2amod	mouse profilin2a (truncated CMV promoter)	Boshart et al., 1985; Murk K., 2008
PFN1	mouse profilin1	Murk K., 2008

2.11.2 Biopsy punching of acute slices and sample preparation

Since resulting morphological changes can be hippocampal region-dependent or even differ between distinct compartments of a CA neuron (basal and apical parts), the underlying mechanisms could be attributed to locally different regulated protein levels.

As the cytoarchitecture of the hippocampus is well preserved in acute slices, it was possible to perform tissue biopsy dissection ("punching") of three subregions of the hippocampus (DG, CA3, and CA1). In addition, samples of basal as well as apical dendritic compartments were prepared in case of the CA1 and the CA3 region. Thus, the biopsy punch application by removing precisely discrete parts of hippocampal slice tissue enables the analysis of protein amount in the above-mentioned hippocampal regions and compartments of pyramidal neurons.

Figure 11 | Biopsy punching setup

(A) *The Zivic tissue biopsy punch is a stainless steel cannula (circular sectioning diameter 0.5 mm) for dissection or removal ("punch") of defined tissue regions. The apparatus was connected to an expulsion tube with attached syringe allowing the release and collection of the tissue.* ***(B), (C)*** *Hippocampal acute slices from adult male C57BL/6 mice were kept in carbogenated ACSF for 2 h to reduce oxidative stress. The biopsy punching was performed in ice-cold PBS (supplemented with protease and phosphatase inhibitors) on ice.*

In total, hippocampal acute slices from 5 adult male C57BL/6 mice were used and merged for one sample. Tissue was collected in ice-cold PBS supplemented with protease inhibitors as well as phosphatase inhibitor cocktail on ice. Samples were lysed in homogenization buffer (STKM supplemented with protease and phosphatase inhibitors) via sonication (80% amplitude, 3 pulses with 5 min intervals). After centrifugation for 30 min at 4 °C (19.000 x g) the supernatant was collected and stored at -80 °C for further processing. Protein levels for PFN1 and PFN2a were analyzed via SDS-PAGE and western blot. In total, 5 independent experiments were performed.

2.11.3 Preparation of hippocampal nuclei

After the probe trial of the Morris water maze (MWM) training (see below for details), mice were sacrificed by cervical dislocation and only the right hippocampi were prepared and rapidly collected in ice-cold homogenization buffer (STKM) with phosphatase inhibitors. The tissue was homogenized manually with a pestle on ice. Differential

centrifugation is a process involving multiple centrifugation steps with increasing speed of centrifugation each time. Hence, collection of both nuclear pellets as well as cytosomal fractions from the hippocampi was possible according to the following protocol: homogenates were centrifuged at 10 min at 680 x g (all centrifugation steps were performed at 4 °C), supernatants were collected on ice. Sediments were resuspended, centrifuged again and all the supernatants were pooled. Since each fraction obtained was only partially-pure and contaminated with particles derived from previous fractions, repeated washing steps were crucial for clarification (three times with STKM + NP-40). The low speed sediments contained the nuclei and were resuspended in 50 µl STKM. The nuclear fraction contains all material found in the nucleus including genomic DNA, proteins involved in replication and transcription, as well as other nuclear proteins and materials. Subsequently, the supernatants were centrifuged at higher speed at 10.000 x g for 10 min. The pellets of this fraction (the second pellets of the cell fractioning procedure) corresponded to the mitochondrial fractions and were discarded. Further cell fractionation by differential centrifugation usually requires the use of an ultracentrifuge, which could have not been involved in this experiment owing to the small volumes. A centrifugation at max. speed (39.800 x g) for 1 h yielded a pellet (microsomal fraction), which was discarded while the supernatant consisting of the cytosolic fraction was saved at -80 °C for further processing. The supernatants that remained after the other cellular fractions were removed by sedimentation steps in previous rounds of centrifugation consist of soluble components of the cytoplasm, including mainly soluble proteins, salts and small macromolecules.

2.11.4 Preparation of whole brains, hippocampi and the medial prefrontal cortex

To prepare brain samples for running on a SDS gel, tissues need to be lysed to release the proteins of interest. Therefore, either whole brains or the brain region of interest was processed according to the following protocol. After the probe trial at day 9 of the Morris water maze training, adult male mice (3-5 months) were sacrificed by cervical dislocation and rapidly decapitated. In the case for swim controls, preparation was performed on the next day directly after the swim training. Both hippocampi and the medial prefrontal cortex (mPFC) were dissected and frozen immediately on liquid nitrogen (for age-

dependent protein level detection whole brains were collected). Frozen tissue samples were weighed and placed in homogenization buffer (pre-cooled STKM buffer containing protease and phosphatase inhibitors) at a ratio of 1 mg tissue: 1 µl buffer set on ice. Following three cycles of "freeze/thaw" (freeze in liquid nitrogen and thaw at 37 °C for 1 min, mix well on ice), the tissue was homogenized mechanically with a pestle. The homogenate was centrifugated for 30 min at 4 °C (19.000 x g) and the resulting supernatant was transferred into a new tube. Samples were stored at -80 °C.

2.11.5 SDS-PAGE and western blot

Bradford protein assay

The Bradford protein assay is a rapid and sensitive method for protein quantitation based on the binding of Coomassie Brilliant Blue G-250 dye to proteins. Under acidic conditions the dye is red, but due to its binding to proteins it is converted into a blue form. The amount of the formed complex of proteins with the dye present in the solution can be measured by absorbance at 595 nm, which reflects proportionally the protein amount. Briefly, 20 µl of several dilutions of the sample were mixed with 100 µl Bradford solution in a 96-well plate and incubated for 5 min at RT. Following readout via ELISA, the protein concentration was calculated referring to the standard curve resulting from solutions with defined BSA concentrations (25-200 µg).

SDS-PAGE

Sodium dodecyl sulfate polyacrylamide gel electrophoresis (SDS PAGE) is the most widely used analytical method to resolve separate components of a protein mixture. In SDS PAGE, proteins are denatured and separated according to their molecular weight solely. As protein samples are heated before electrophoresis with SDS, an anionic detergent binding to hydrophobic regions of proteins, their positive charges are covered with an evenly negative net charge. Additionally, a molecular weight marker is also loaded onto the gel providing a reference by which the mass of sample proteins can be determined. Electrophoretic gels are made of acrylamide, which forms a crosslinking network if the polymerizing agent ammonium persulfate (APS) is added. TEMED (N,N,N,N'-tetramethylenediamine) catalyzes the polymerization reaction. SDS-bound proteins with less mass travel more quickly through the gel matrix than those with greater mass due to the sieving effect. In contrast to uniform concentration gels, gradient gels exhibit two

important advantages: firstly, proteins are fractionated over a wider range of molecular weights and secondly, the gradient in pore size leads to a significant sharpening of protein bands during migration. Brain samples were prepared in 4x SDS buffer, ß-Mercaptoethanol and PBS and incubated at 95 °C for 5 min. 10-20 µg of protein per lane were loaded on the gel. Settings: 225 V, 100 W and 20 mA per gel. Protein gel electrophoresis was stopped when the first reference band at 10 kDa reached the edge of the separating gel. Once separated by electrophoresis, proteins can be transferred onto a nitrocellulose or polyvinylidene fluoride membrane (PVDF) membrane for detection.

Western blotting

The separated polypeptides are transferred via active semi-dry electroblotting to a nitrocellulose or PVDF membrane, thereby retaining the same pattern of separation they had on the gel. For this purpose, the gel and membrane are "sandwiched" between three stacks of filter paper and placed in a blotter apparatus with direct contact to plate electrodes. The applied electric charge (10 W; 100 mA and 100 V for 1 h) causes the protein transfer out of the gel onto the membrane. Subsequently, unoccupied binding sites on the membrane were blocked with 5% milk in TBST for 1 h at RT to prevent nonspecific binding of antibodies. After washing with TBST, diluted antibodies were applied to the membrane and incubation occurred overnight at 4 °C on a shaker. Primary antibodies used in this work were essentially anti-Cofilin, anti-Cortactin, anti-Profilin1, anti-Profilin2a as well as anti-GAPDH to control gel loading (cp. **Table 4**). Between the two antibody incubations and prior to detection, the membrane must be washed thoroughly to remove excess antibody in order to prevent nonspecific binding. Therefore, the membrane was washed again with 1 L TBST before the corresponding HRP-conjugated secondary antibody diluted in TBST was incubated for 2 h at RT on a shaker. Following multiple washing steps with TBST, TBSX and DM H_2O, excessive liquid was removed by Whatman paper and Luminata™ Crescendo HRP substrate solution was poured directly onto the membrane for 2 min. Briefly, the location of the antibody is revealed by application of the substrate, which is converted to a visible product by the HRP enzyme. Visualization of the product was performed as follows: X-ray film was placed for various periods onto the blot and then exposed to developer and finally fixing solution. Afterwards, the films were imaged and analyzed using ImageJ (NIH) or EasyWin32.

2.12 Behavioural analysis

2.12.1 The Morris water maze navigation task

The hippocampus represents, together with the entorhinal cortex (EC), the spatial navigation system of the brain. Rodents with lesions in the hippocampus are impaired in spatial memory tasks such as the Morris water maze (MWM). The MWM is a behavioural test to investigate hippocampus-dependent learning and memory as well as search strategies. Developed in 1984 by Morris and McNaughton, it is one of the most widely used models to study spatially cued learning and memory in mice or rats (Morris, 1981, 1984; McNaughton and Morris, 1987). In brief, it represents a spatial navigation task, which requires an animal placed in different starting positions to find the location of the hidden escape platform within the pool. Indeed, mice and rats are highly motivated to escape as soon as possible and find the invisible, submerged platform.

2.12.1.1 Build-up and pre-training

At least one day prior to pre-training started mice were kept separated in the same room as the water maze setup to ensure habituation to the new environment. Animals were maintained on a 12:12 h light/dark cycle provided with food and water *ad libitum*. All behavioral tests were carried out in the light phase.

The MWM task was conducted by usage of a black circular pool (diameter = 160 cm, height = 60 cm) filled with water made opaque by addition of titanium oxide and kept at 22±2 °C. The maze was virtually divided into four equivalent quadrants: north-east (NE), north-west (NW), south-east (SE) and south-west (SW). For visual orientation, three different extra-maze-cues (enabling “triangulation”) were placed on the room walls (triangle, circle, stripes; black on white) and were visible from inside of the pool for the entire experiment.

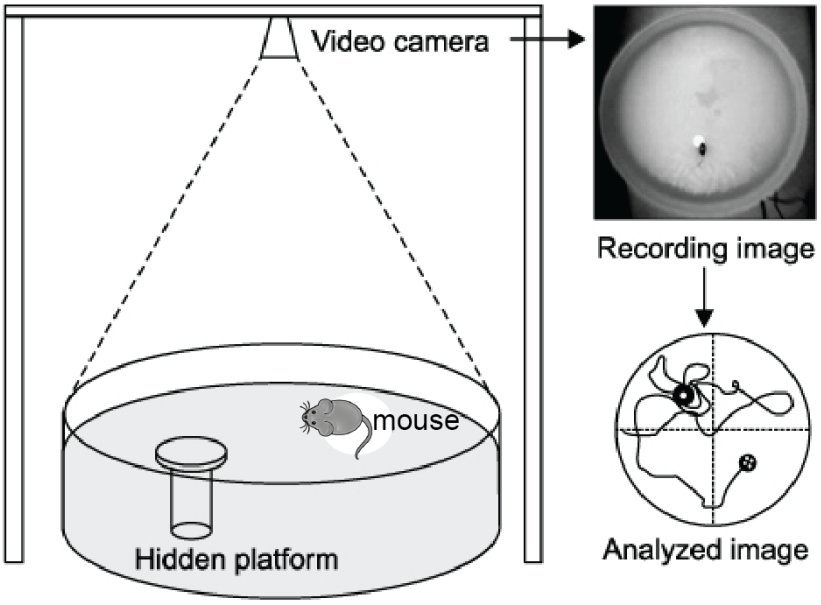

Figure 12 | Build-up water maze system (TSE)

Collection and analysis of data from training sessions and probe trials were obtained by the video tracking system (TSE) and the software "TSE Videomot2". By using the time-tagged xy-coordinates analysis of mice performances were carried out. Analyses included general measurements such as global latency, global distance, quadrant preference, swim speed, swim length and platform crossings (scheme adapted from Koo et al. 2007).

The pre-training took place on three consecutive days with a visible platform (diameter = 10 cm, covered with grip material) 1 cm above the water surface marked with a colored flag. Each mouse received 2 trials per day with an interval time of 5-10 min between the trials, starting on the opposite position from the platform and the position of the platform was changed between trials. If the animal was not successful in finding the rescue platform within 90 s, it was guided manually onto it and rescued after 15 s by the experimenter. Following pre-training, mice were allowed to recover for 2 d before the training started.

2.12.1.2 Memory formation in the MWM

The experiment was performed twice over 8 days with two groups of animals, the *fmr1* KO (total n=13) and their respective WT littermates (total n=11), serving as control animals (cp. **Figure 13**). Swimming control mice (*fmr1* KO and *fmr1* WT in each case total n=9) were allowed to swim in the maze in the absence of the platform for 30 s each day of training. Experimenter was blind to the genotype during the entire sessions. The task

for the mouse was to find the submerged hidden platform positioned 1 cm below the water surface within 90 s while using the extra-maze cues on the walls for navigation. While the platform was located in the center of the north-west (NW) quadrant constantly, the start position changed in a pseudo-random order. Mice were placed into the maze at one of these four different start points around the pool: north-east (NE), east (E), south (S), south-west (SW) (cp. **Figure 14**). Each mouse had to perform four trials per day from each start point with an interval of 5-10 min. After staying on the platform for 15 s, the animal was rescued and returned to its home cage. The animal's movement was recorded as swim path via a video tracking system above the water maze requiring a high contrast between the animal's fur and the water. To quantify the capacity of mice to learn spatially-encoded information, one of the most common measurements is the escape latency to find the platform. Latency describes the average time per day the mouse required to find the platform. Besides that, another parameter was the average global distance each mouse was swimming per training day. Both parameters decreased over time as an indicator of memory formation regarding the platform position. Swim speed was analyzed as well to guarantee the physical integrity of the mice.

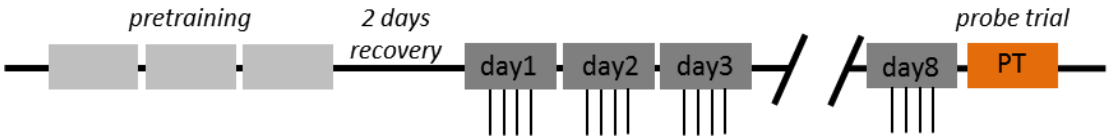

Figure 13 | Scheme of the experimental design and conditions

Pretraining (platform visible) was performed for three days. After two days of recovery, training was carried out with four trials per day (platform submerged). On day nine, probe trial was performed and mice were sacrificed.

On day 9 the platform was removed and the reference memory test ("probe trial") was performed over a cutoff time of 45 s. Here, the time spent in the target quadrant (the NW quadrant where the platform has been before) was measured to test for quadrant preference. Without training, the preference for each quadrant should be close to 25%. In addition to global latency and distance, the number of annulus crossings to former platform location was also taken as a measurement of memory formation.

2.12.1.3 Analysis of MWM performance & searching strategies

How did the mice solve the problem of locating the platform? Considering the qualitative aspects of learning, the different behavioral strategies for finding the platform were analyzed. In some cases, the subtle but significant differences between mutant mice and control mice might be rather found in the learning strategies used than in escape latency or the distance traveled. A parameter-based algorithm was used to classify the swim patterns into different search strategies. For this purpose, the pool was divided into distinct zones and variables were determined as described by Garthe and colleagues before (cp. **Figure 14;** Garthe, Behr & Kempermann 2009).

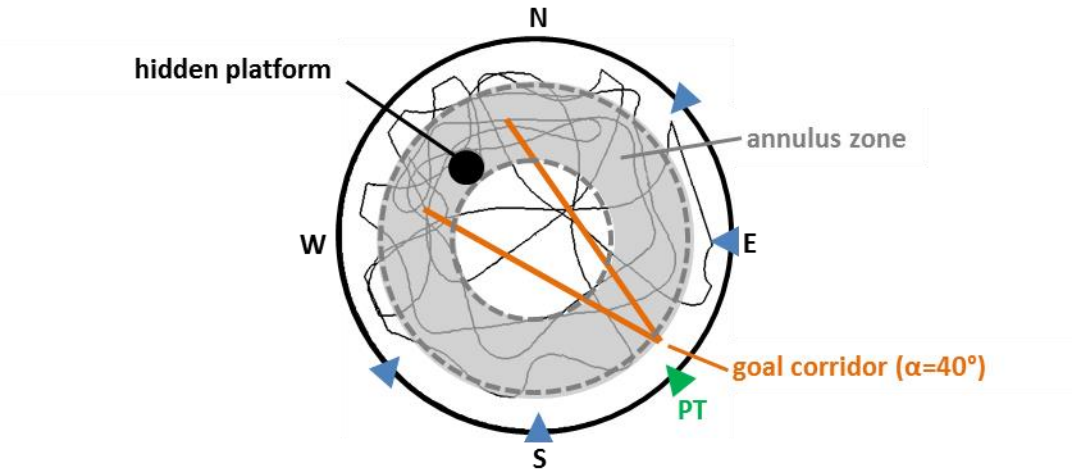

Figure 14 | Schematic drawing of the water maze pool

The pool was divided in different zones in order to classify the search strategies. Spatial strategies with d direct targeting to the platform were identified with a triangular shaped goal corridor (orange triangle ranging from the starting point (indicated by blue filled triangles) to the hidden platform (black filled circle in the NW quadrant. Annulus zone is indicated by grey circle (scheme modified after Garthe et al. 2012).

Identification of each search pattern was mainly based on the amount of time spent in respective areas. Since some strategies were lacking defined key properties, the algorithm provided a particular order to exclude other strategies (cp. **Figure 15**). By graphic output of the program it was possible to verify results manually.

This parameter-based classification of search patterns demonstrated the progressive use of spatially precise search strategies during learning as with increased training time, the mice used more spatial strategies and less random search.

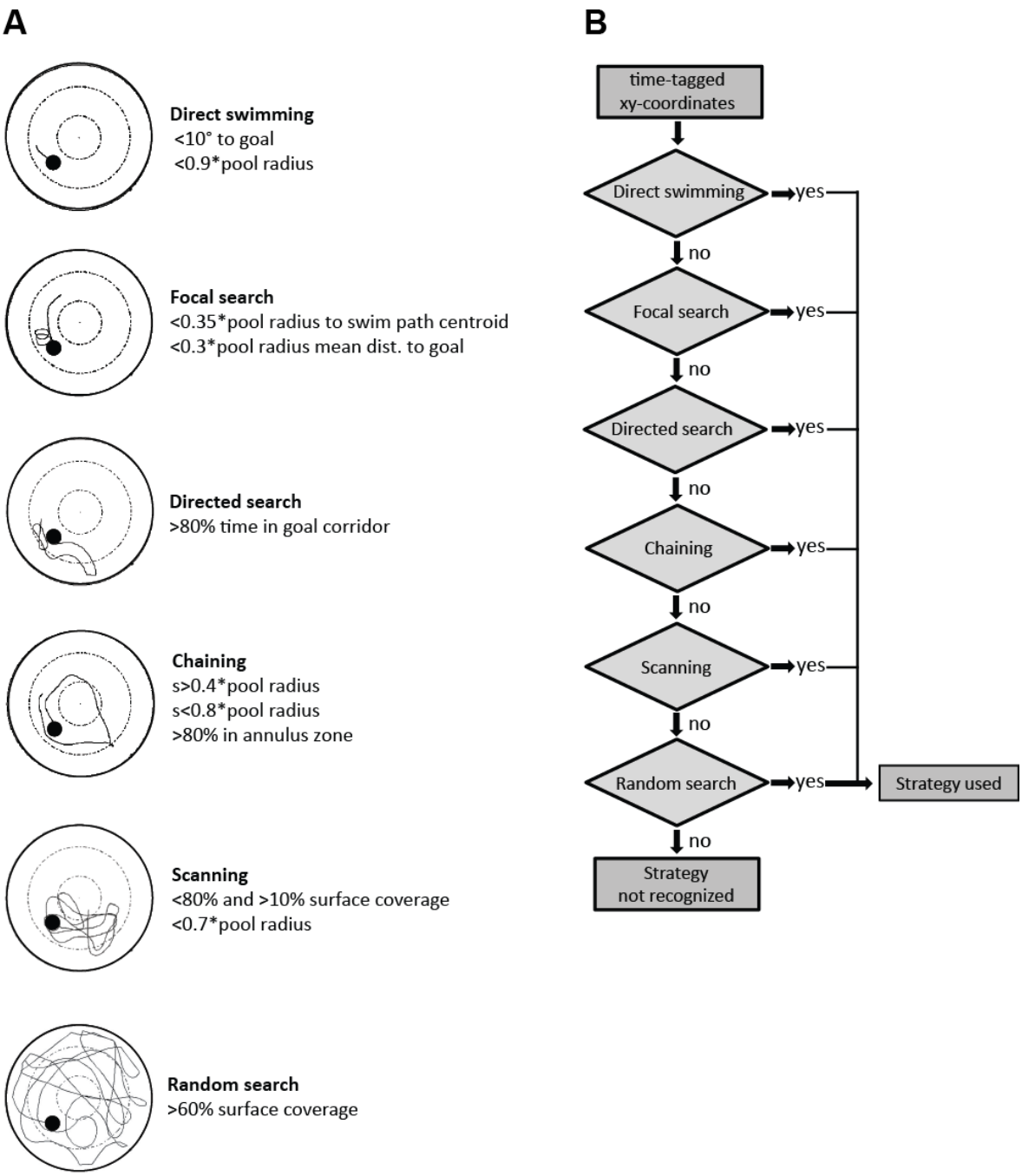

Figure 15 | Search strategies

(A) *Analysis of performance in navigating through the water maze. Search strategies were identified by using one or two parameters.* ***(B)*** *Some strategies are identified by exclusion of other strategies, therefore a particular hierarchy of the different searching strategies is required. If a search strategy could not be identified automatically, it was classified by hand (adapted from Garthe et al., 2009)*

3 RESULTS

3.1 Role of profilin1 in dendritic morphology of the hippocampus

3.1.1 PFN1 *vs* PFN2a

In the mammalian brain overall and also specifically in hippocampal neurons two profilin isoforms (PFN1 and PFN2a) exist. While the specific function of the brain-specific isoform PFN2a was elucidated regarding dendrite morphology and spine stability in mature hippocampal CA1 neurons (Michaelsen et al., 2010), much less is known about the role of the ubiquitously expressed profilin isoform PFN1 in neurons of the CNS. More precisely, PFN2a deficient neurons (CA1) showed a significantly reduced overall dendritic complexity as well as a reduced spine density of the basal and proximal apical dendrites (Michaelsen et al., 2010). Originally defined as G-actin sequestering protein, several others functions of profilins were discovered, including mRNA splicing, cell motility, trafficking of actin between nucleus and cytoplasm as well as vesicular endocytosis (Carlsson et al., 1977; Witke et al., 1998, 2001). One widely accepted function is its main role in promoting actin polymerization by catalyzing the exchange of ADP for ATP on the G-monomer (Witke, 2004). Research has focused in particular on its role in tumor cell

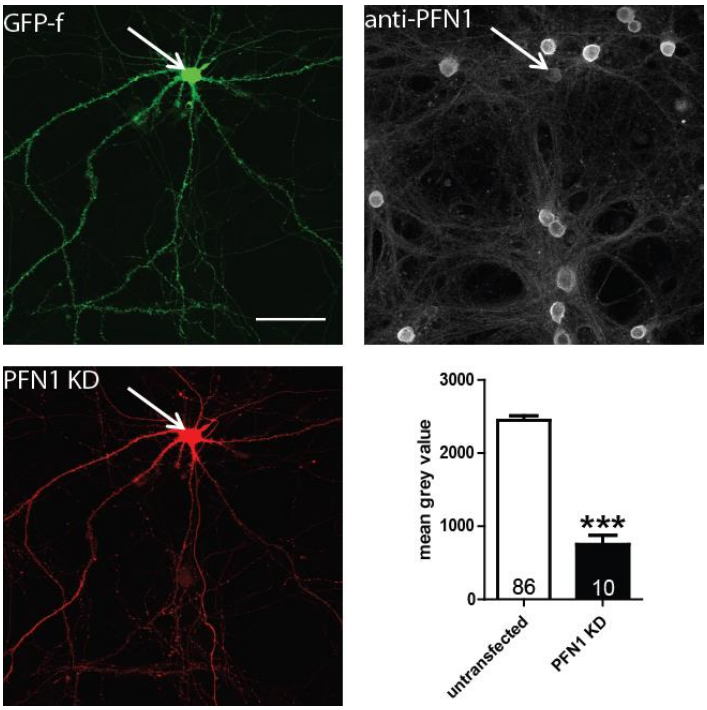

Figure 16 | Knockdown of PFN1 in primary hippocampal dissociated neurons led to a reduction in the protein amount by approx. 70%

*Cells were co-transfected with shRNA vector against PFN1 and GFP-f. Immunostaining with anti-PFN1 enabled the quantification of PFN1 amount in the soma of transfected cells. Nearby untransfected neurons were measured as controls. Quantification of fluorescence signals revealed a high significant reduction in protein level to approx. 31% in comparison to control cells. Scalebar = 50 µm, ***p<0.001*

invasion and metastasis as the expression levels of PFN1 are downregulated in several invasive breast, pancreatic and hepatic cancer cell types (Roy and Jacobson, 2004; Wittenmayer et al., 2004). Interestingly, silencing PFN1 leads to a higher motility and tumor progression.

Acute knockdown of PFN1 was achieved via a vector-based RNAi approach. The RNAi vector for PFN1 is based on pRNATU6.3-siFluc (pRNAT_1.3) and targeted PFN1 mRNA while simultaneously expressing GFP or mApple (pRNAT_1.3-ΔmApple) (Murk 2008; Schweinhuber 2014). Immunohistochemistry using anti-PFN1 and anti-PFN2a antibodies confirmed that the knockdown of PFN1 by shRNA was specific to PFN1 and did not interfere with PFN2a expression levels. The antibody signal quantified in the soma of dissociated hippocampal neurons demonstrated a significant reduction in PFN1 expression level to approx. 31% (cp. **Figure 16**). Primary cultures were co-transfected at DIV14 for 72 h with PFN1-KD (pRNAT_1.3-ΔmApple) and GFP-f. Previous studies expressing the shPFN1 in HeLa cells for 96 h led to a nearly complete loss of PFN1 signal, however, transfected neurons became apoptotic over time (Murk, 2009). For this reason the expression time in dissociated neurons was reduced to 72 h to ensure viability of the cells at this time point. Analysis of the anti-PFN1 antibody fluorescence signal in the soma of transfected neurons (n=10) resulted in a mean grey value of 752.9 ± 125.1 in comparison to control cells with 2448 ± 66.41 (as controls, neighboring untransfected neurons were chosen; n=86). Thus, PFN1 protein level in hippocampal neurons was reduced by 69% upon shPFN1 expression for 72 h.

3.2 Acute knockdown of profilin1 affects neuronal structure in a subregion- and age-dependent manner

3.2.1 Dissociated neurons

The dissociated primary neuronal cultures provide a system with all kinds of hippocampal cell types, e.g. pyramidal neurons, granule cells, glia cells or GABAergic interneurons. Many dissociated pyramidal neurons form a normal polarity as they develop extensive axonal and dendritic arbors as well as numerous synaptic connections. Thus, compared to the *in vivo* situation, this system can be manipulated in a much more convenient way enabling the investigation of cellular and molecular mechanisms of dendrite and spine

structure. Importantly, overexpression of proteins or the acute knock-down of protein expression by RNAi can be accomplished relatively easily in this culture system to study the function of specific proteins.

Neurons were transfected with the respective plasmids for 4 d and fixed at two different developmental stages (DIV 17 and DIV 34) to examine if knockdown or overexpression of PFN1 affects neuronal structure in a developmental manner. Subsequently, *Sholl* analysis was performed to determine the complexity of the dendritic tree structure by counting the occurrence of branches along concentric spheres. Thus, the number of intersections was used as a direct measurement for dendritic complexity.

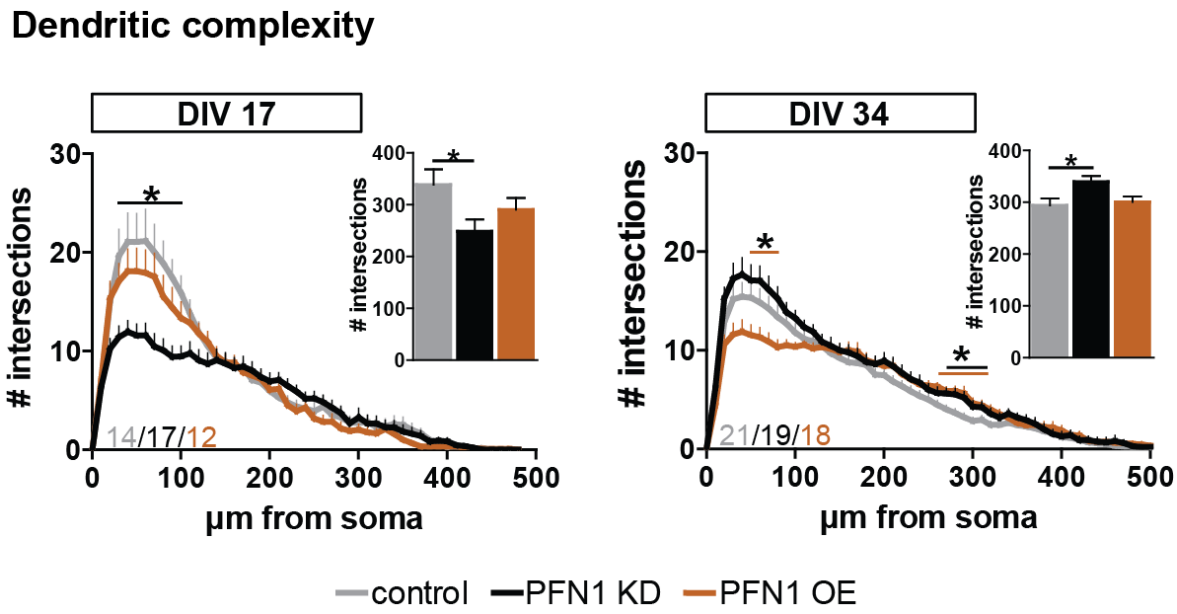

Figure 17 | Acute knockdown (KD) and overexpression (OE) of PFN1 in dissociated hippocampal neurons of different developmental stages affects dendritic structure

*Sholl analysis and total number of intersections of hippocampal dissociated neurons at DIV 17 (left) and DIV 34 (right) revealed significant alterations in dendritic architecture upon PFN1 KD and PFN1 OE. *p<0.05*

Less mature hippocampal neurons at DIV 17 showed a significantly reduced complexity of the dendritic tree at 30 – 100 µm from soma when PFN1 level was reduced via RNA interference (cp. **Figure 17**).

In line with this, also the total number of intersections was significantly reduced (~338.7 ± 29.4 for control cells compared to ~248.5 ± 22.9 for PFN1 KD cells). PFN1 overexpression led to no significant changes in dendritic architecture of immature neurons. Interestingly, fully mature neurons were not reduced in their complexity by knockdown of PFN1, but showed a reduction in dendritic complexity upon the overexpression of PFN1, which

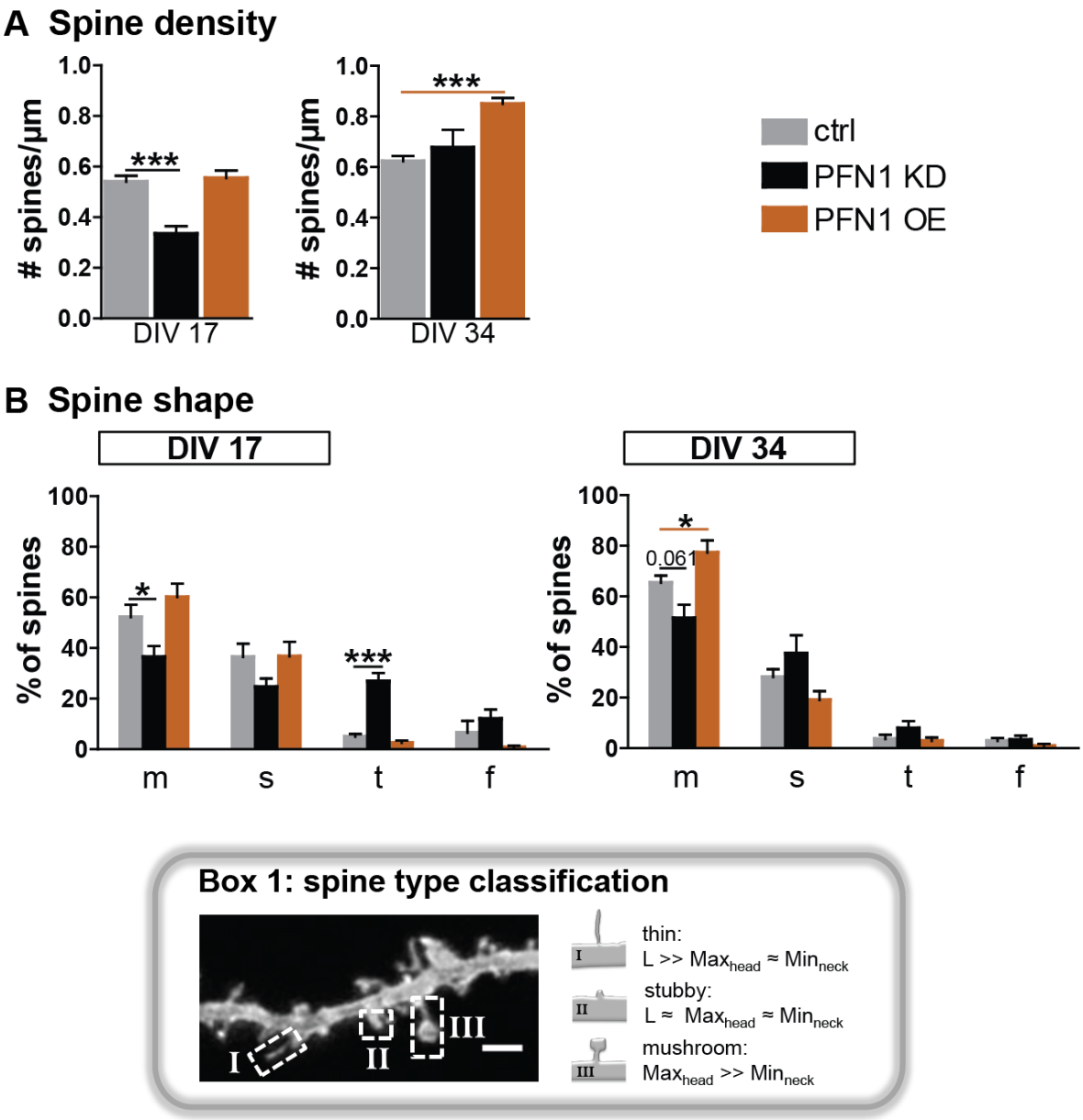

Figure 18 | Acute knockdown (KD) and overexpression (OE) of PFN1 in dissociated hippocampal neurons of different developmental stages affects number and shape of spines

*__(A)__ Spine density was significantly reduced due to PFN1 KD in immature neurons (left), whereas PFN1 OE had no effects. Neurons at DIV 34 were not affected in spine number upon PFN1 KD, but showed significantly increased spine numbers in case of PFN1 OE (n=10 for each approach). __(B)__ Spine morphology was altered in PFN1 deficient neurons at DIV 17 (left) and at DIV 34 (right). n=10 for each approach. m=mushroom spine; s=stubby spine; t=thin spine; f=filopodium; *p<0.05, **p<0.01, ***p<0.001. __(C)__ Box 1: spine type classification. According to the ratio between spine head width, spine neck length and total spine length dendritic spines were classified as thin, stubby or mushroom spines; scalebar = 2 µm.*

reached level of significance at a distance of 50 – 80 µm from the soma. More distally at 270 – 310 µm from the soma, dendritic complexity was significantly increased in PFN1 KD cells (~293.8 ± 13.6 for control cells compared to ~339.5 ± 11.3 for PFN1 KD cells; p= 0.0145). Spine density of DIV 17 neurons was significantly reduced in PFN1 KD cells but unaffected by the overexpression of PFN1 (~0.54 ± 0.02 for control cells cp. to ~0.33 ± 0.02 for PFN1 KD cells and ~0.55 ± 0.02 for PFN1 OE cells) (cp. **Figure 18 A**). Opposing to this, the loss of PFN1 had no effect on the spine number in mature neurons at DIV 34 (~0.62 ± 0.02 for control cells cp. to ~0.67 ± 0.07 for PFN1 KD cells). Interestingly, PFN1 overexpression in mature cells led to a significant elevation of spine number (~0.85 ± 0.02 cp. to ~0.62 ± 0.02 for control cells).

Spines were classified into mushroom, stubby and thin spines as well as filopodia according to their morphology (cp. **Figure 18 Box 1**) (Zagrebelsky et al., 2005). PFN1 deficient neurons at DIV 17 showed significantly fewer mushroom spines compared to control (~52.2% ± 4.9% for control cells cp. to ~36.4% ± 4.3% for PFN1 KD cells). In return, the proportion of thin spines was significantly increased in PFN1 KD cells (~4.9% ± 1.1% for control cells cp. to ~26.9% ± 3.3% for PFN1 KD cells). Overexpression of PFN1 induced no alterations in spine type distribution at this stage. Similar to this, in mature neurons at DIV 34 the loss of PFN1 led to a reduced number of mushroom spines close to statistical significance, whereas the overexpression of PFN1 showed the opposite trend by significantly increasing the relative number of mushroom spines in comparison to control cells (~64.8% ± 2.5% for control cells cp. to ~54.9% ± 4.2% for PFN1 KD cells and ~78.4% ± 4.9% for PFN1 OE cells; p=0.061 for PFN1 KD and p=0.016 for PFN1 OE) (cp. **Figure 18 B**). Simple classification schemes of spine types do not accurately reflect the broad range of spine shapes and size. Thus, a more detailed structural analysis was achieved by separating the dendritic spines according to their stage of maturation into different binning categories based on the spine head width and on the spine length, respectively (cp. **Figure 19**). Separation of spines revealed unaltered spine head width in immature cells, as most spines were found to be in the range of either <0.5 µm or 0.5-1 µm regardless of changes in protein expression (cp. **Figure 19 A**). While the proportion of short spines (0.5-1 µm) was significantly reduced upon PFN1 KD, more spines with length of 1-1.5 µm or even 1.5-2 µm could be found (cp. **Figure 19 B**).

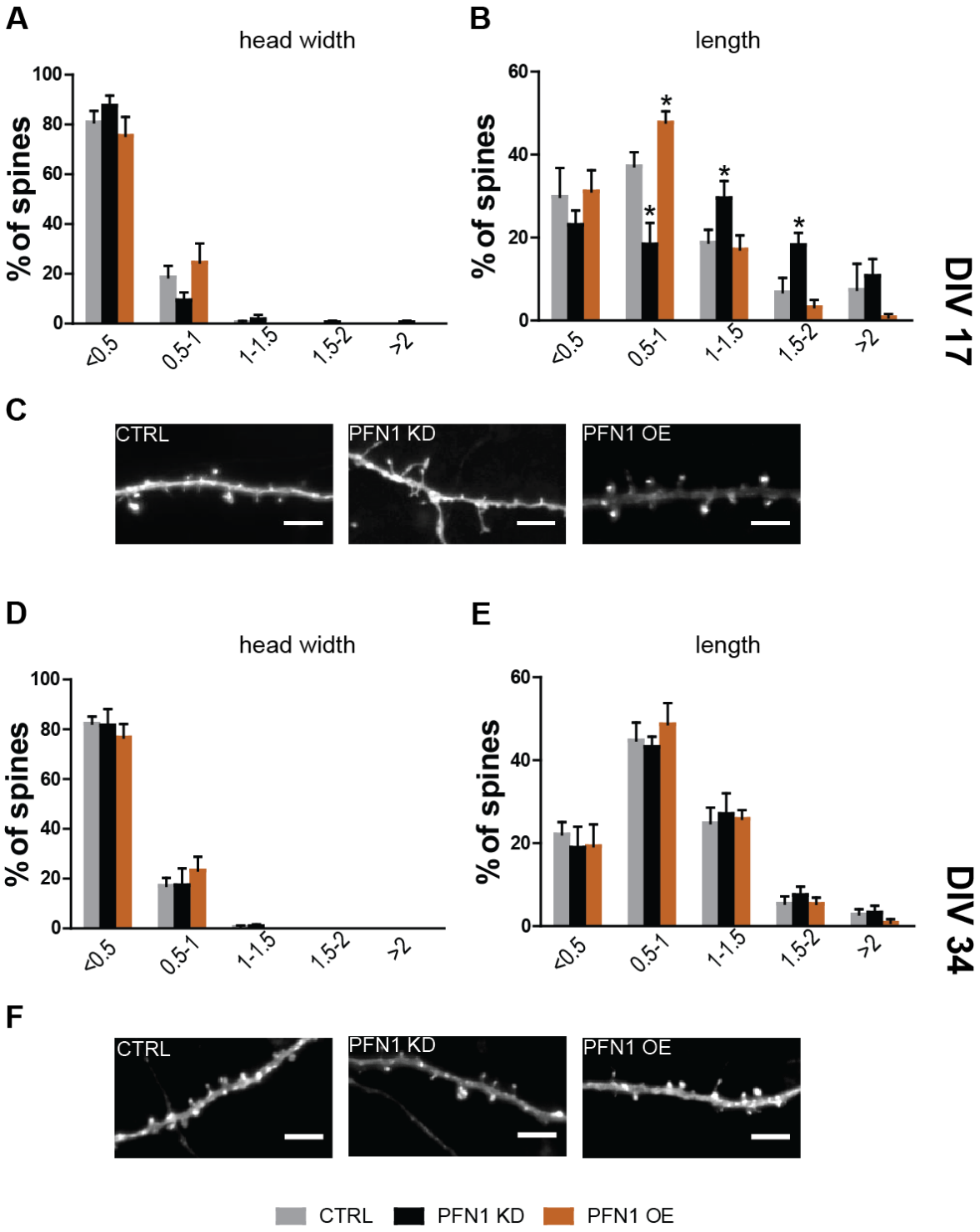

Figure 19 | Detailed spine morphology following acute knockdown or overexpression of PFN1 in hippocampal neurons

*Binned data concerning **(A)** spine head width and **(B)** length of DIV 17 neurons; **(C)** showed representative dendrite stretches of control, PFN1 KD or PFN1 OE cells at that age. **(D)** Spine head width and **(E)** spine length of DIV 34 neurons and **(F)** representative images of dendritic segments. *p<0.05; scalebar = 10 µm.*

Representative images of dendritic segments clearly indicate that the proportion of elongated, thin spines was increased in younger neurons upon PFN1 knockdown (cp. **Figure 19 C**). In mature neurons at DIV 34 neither spine head width (cp. **Figure 19 D**) nor spine length was altered in PFN1 overexpressing or deprived cells (cp. **Figure 19 E**).

Collectively, loss of PFN1 led to a decreased dendritic arborization and spine number in immature pyramidal neurons of the murine hippocampus. Spine type distribution was changed to fewer mushroom spines and, in return, was shifted to a more immature spine phenotype with longer spines. No changes in dendritic or spine structure could be observed in mature neurons. Thus, it becomes apparent that the effects of PFN1 knockdown were age-dependent and only transient pointing to a specific role of PFN1 in spine maturation during development.

3.2.2 Amount of profilin isoforms in subregions of the hippocampus

The murine hippocampus is anatomically divided into different subregions: dentate gyrus, CA3 and CA1 region. Especially pyramidal neurons of the CA1 and CA3 region exhibit a unique cellular architecture as their two different dendritic compartments – basal versus apical - show distinct morphological features indicating possibly distinct functions. Indeed, different “tag proteins” were found in apical and basal compartments, as calcium/calmodulin-dependent protein kinase II was identified as the first LTP-specific and extracellular signal-regulated kinase 1/2 as LTD-specific tag molecules in apical dendritic CA1 compartments, whereas either protein kinase A or protein kinase M were described to mediate LTP-specific tags in basal dendrites (Sajikumar et al., 2007). In this respect, morphological analyses of manipulated hippocampal neurons, e.g. following changes in gene expression, often demonstrated subregion-dependent effects. In case of pyramidal neurons, studies show that dendrites either of the basal compartment or of the apical compartment can be affected (Michaelsen, 2009). To examine if protein levels of the two profilin isoforms are differentially expressed either within the hippocampus or even in distinct compartments of CA neurons (*stratum oriens* and *stratum radiatum*), biopsy punching of hippocampal acute slices was performed to determine protein amounts of discrete parts. Indeed, analysis of the subregions and compartments of the dendritic tree revealed that the expression levels of both isoforms are partially regulated in opposing fashions (cp. **Figure 20**).

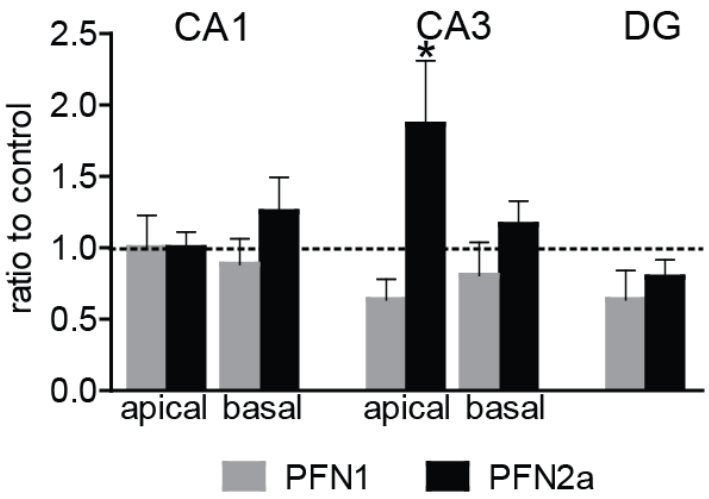

Figure 20 | Profilin isoforms differ between hippocampal subregions regarding protein content

*PFN1 and PFN2a protein amounts were found to be different within hippocampal subregions and dendritic compartments. Protein amounts were normalized to the amount of the CA1 apical part. *p<0.05*

The values for the respective isoform were normalized to the apical dendritic tree of CA1 cells set as reference levels. The *stratum oriens* demonstrated less PFN1 (88 ± 18%) and an elevated level of PFN2a (125 ± 24%) compared to profilin levels of apical dendrites. Contrary to CA1, apical dendrites in CA3 neurons showed significantly different protein levels between PFN1 (64 ± 14%) and PFN2a (186 ± 45%; p=0.023). Similar to CA1, the basal compartment of CA3 cells displayed opposing tendencies for both profilins: PFN1 level was found to be reduced (81 ± 23%), whereas PFN2a level was elevated (116 ± 16%) compared to reference. Both profilins were found to be reduced in the dentate gyrus, but to a different extent (PFN1: 64 ± 20%; PFN2a: 79 ± 12%).

3.2.3 Organotypic cultures

The hippocampal formation comprises the CA (CA1, CA2, CA3) fields within the hippocampus and distinct adjoining regions as the dentate gyrus, subiculum, presubiculum, parasubiculum and the entorhinal cortex. The one-way flow of information starts via the perforant path to the dentate gyrus and involves also CA3 and CA1, therefore called the trisynaptic circuit. The striking anatomical differences between the hippocampal regions CA1 and CA3 (the principal pyramidal cell fields in the hippocampus) as well as the dentate gyrus point to different functions of these subregions. Interestingly, pyramidal neurons are found in most mammalian forebrain structures that are associated with advanced cognitive functions indicating a crucial role in the correct functioning of the brain.

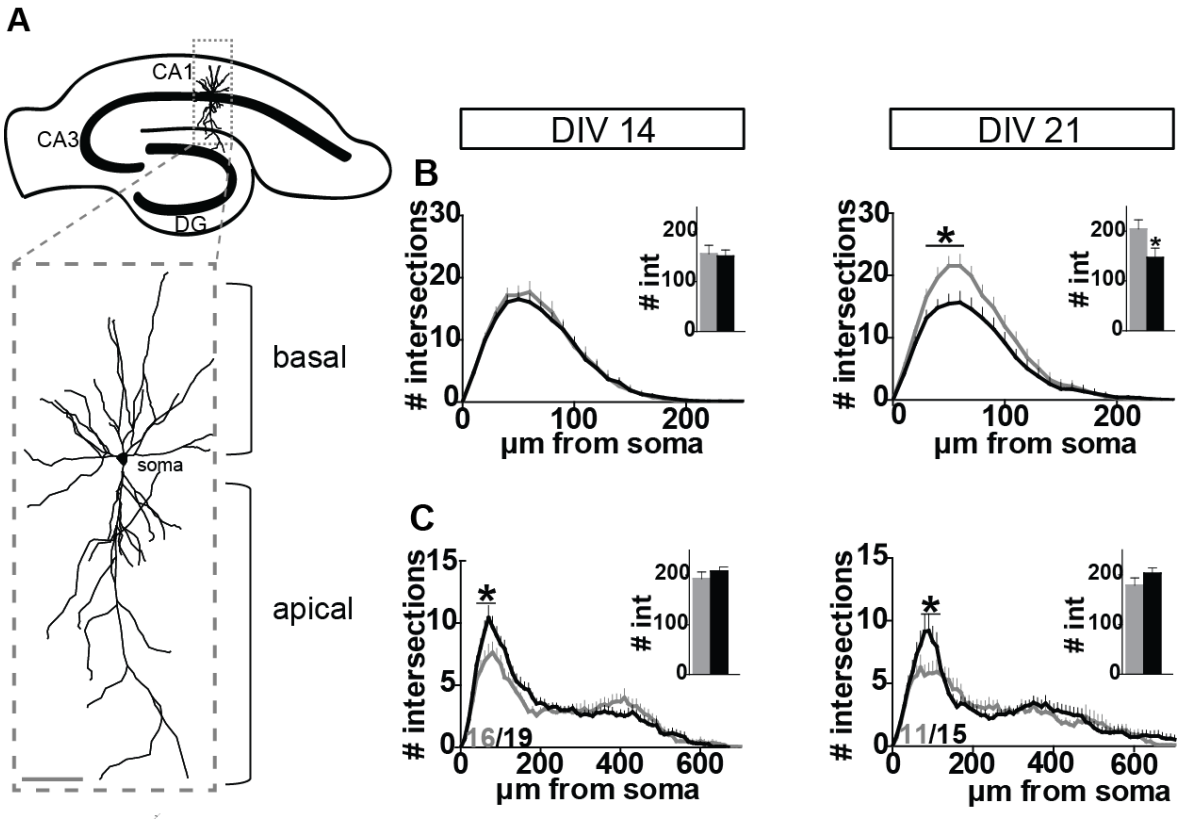

Figure 21 | Morphological analysis of PFN1 deficient CA1 neurons revealed age- and region-dependent alterations

(A) *Schematic morphologies of a hippocampal slice cultures and a principal neuron in the CA1 region. Grey rectangle shows reconstruction of a 14 DIV CA1 cell. Basal and apical compartments of cells were analyzed regarding dendritic complexity.* ***(B), (C)*** *Results obtained from different developmental stages (14 DIV and 21 DIV) of organotypic cultures revealed age-dependent effects of PFN1 knockdown on dendritic architecture. Bar graphs show the average total number of intersections per neuron. *p>0.05; scale bar = 100 µm; int = intersections*

Typically, two distinct branched dendritic trees emanate from the soma of a CA1 neuron. Firstly, the apical part consists of one primary apical dendrite, which bifurcates either in the *stratum radiatum* or in the *stratum lacunosum-moleculare* and gives rise to oblique and tuft dendrites. Secondly, the basal part where several primary dendrites branch several times close to the soma. Therefore, morphological variety of these two distinct compartments indicates different functions for both. In order to investigate if the knockdown of the profilin isoform 1 has effects on the dendritic architecture of CA1 pyramidal neurons, arborization of dendritic trees was analyzed by *Sholl* analysis. Additionally, possible developmental effects were investigated by using neurons of different developmental ages (DIV 14 and DIV 21). Indeed, lack of PFN1 did not affect the

basal compartment in DIV 14 neurons, but led to a significantly elevated apical dendritic arborization in PFN1 knockdown cells at a distance from 60 µm to 120 µm from the soma, whereas the remaining more distal apical tree displayed no alterations. In mature CA1 neurons at DIV 21, basal dendritic complexity was reduced compared to control cells at a distance of 30 µm to 60 µm from the soma (cp. **Figure 21**). Consequently, the total number of intersections per neurons was also significantly reduced in PFN1 deficient cells (204.4 ± 18.39 total intersections in control cells cp. to 147.0 ± 19.42 in PFN1 KD cells; p=0.0436). In contrast to the basal compartment of neurons, the apical tree showed enhanced complexity of dendrites upon PFN1 knockdown at a proximal distance of 70 µm - 110 µm from the soma.

Another part of the CA band contains the CA3 region. Similar to CA1, CA3 neurons consist of pyramidal-shaped somata with two distinct emerging dendritic trees. Notably, a typical CA3 neuron is larger in size and the apical dendrites start to branch closer to the soma than their counterparts in CA1 cells. Despite the fact that average dendritic length and complexity is comparable to CA1 cells, CA3 neurons exhibit a wide range of dendritic complexity, which can be attributed to the various subregions of CA3. Collectively, cells descending from the CA3 regions were less affected than CA1 cells. CA3 neurons lacking PFN1 at DIV 14 showed no structural changes in the basal compartment. Structural alterations were found to be exclusively in the apical dendritic tree of younger pyramidal neurons resctricted at a distance of 270 µm to 350 µm from the soma (cp. **Figure 22 C**). CA3 cells at DIV 21 exhibited neither changes in the basal nor in the apical dendritic compartment.

Since the dentate gyrus is the major termination of projections from the entorhinal cortex (EC), it is therefore considered as the first step in information processing before its convey to the CA3 field. The principal excitatory cell type of the dentate gyrus is the granule cell, which comprises in contrast to CA1/CA3 neurons a small, non-pyramidal cell body. Only one single elliptic tree of apical dendrites emanates from the soma with significantly shorter dendrites compared to CA1 or CA3 neurons. In granule cells PFN1 knockdown did not affect the dendritic branching complexity, irrespective of theirl developmental age (cp. **Figure 23**).

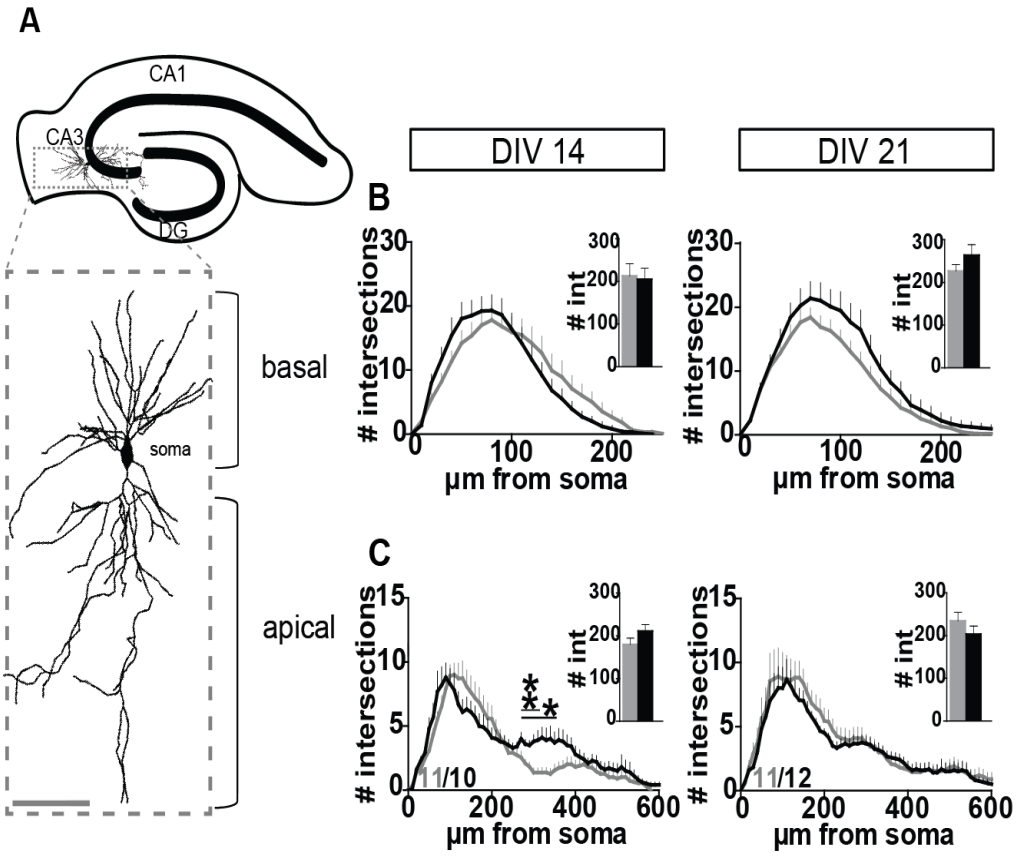

Figure 22 | Morphological analysis of PFN1 deficient CA3 neurons revealed only minor age- and region-dependent alterations

(A) *Schematic morphologies of hippocampal structure and principal neurons in the CA3 region. Basal and apical compartments of cells were analyzed regarding dendritic complexity.* ***(B), (C)*** *Results obtained from different developmental stages (14 DIV and 21 DIV) of organotypic cultures revealed age-dependent effects of PFN1 knockdown on dendritic architecture. Bar graphs show the averaged total number of intersections per neuron. *p>0.05; scale bar = 100 µm; int = intersections*

Detailed *Sholl* analysis revealed a subregion- and age-dependent effect of PFN1 knockdown on hippocampal neurons, as the deficit of PFN1 affected dendritic morphology of pyramidal cells in CA1 or CA3 area differentially. However, dendritic architecture was only affected mildly by PFN1 knockdown at both developmental stages indicating only a minor role for PFN1 in establishing and maintaining the dendritic tree of principal hippocampal neurons.

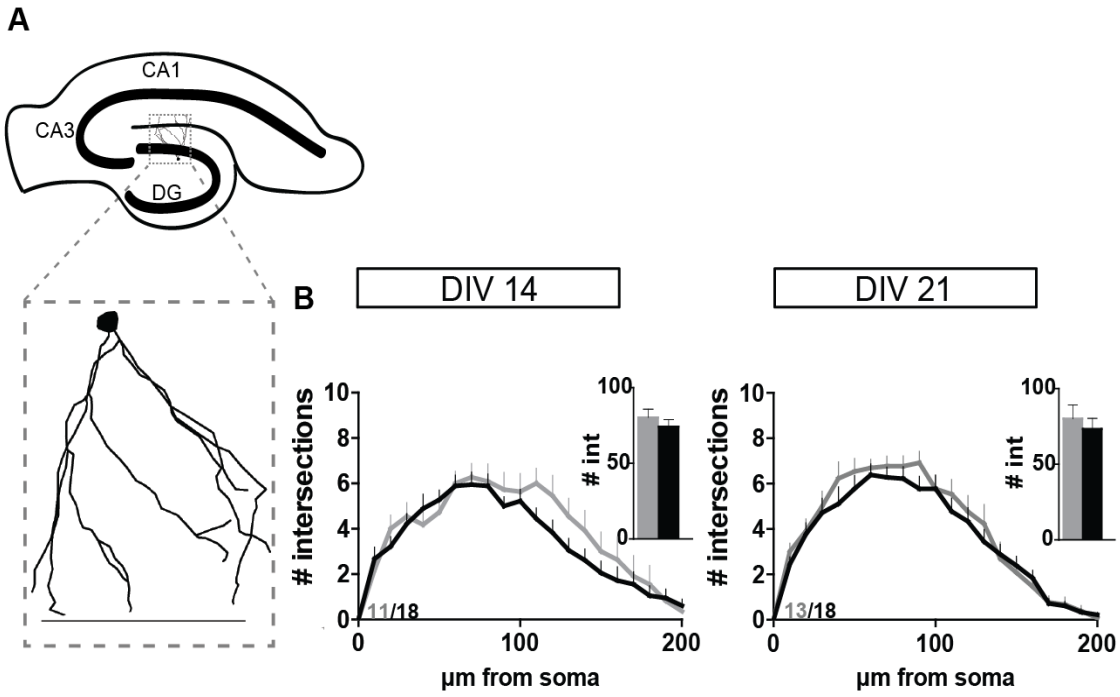

Figure 23 | Morphological analysis of PFN1 deficient dentate gyrus neurons

(A) *Schematic representation of the hippocampal formation with principal neurons of the DG region. Granule cells of this region were analyzed regarding their dendritic morphology.* ***(B)*** *Results obtained from different developmental stages (14 DIV and 21 DIV) of organotypic cultures revealed no age-dependent effects of PFN1 knockdown on dendritic complexity. *p>0.05; scalebar = 100 µm; int = intersections*

In order to study the role of PFN1 in regulating the spine number of hippocampal neurons in an age- or region-dependent manner, spine density of basal and apical dendrites was evaluated in CA1, CA3 and DG cells at DIV 14 and DIV 21. Spine density is an important determinant of network function, as with increasing spine number, also the number of neuronal connections increases. Thus, changes in spine density might consequently lead to network dysfunction.

Thus, the apical dendritic tree was categorized into two parts: firstly, spines were counted on the shorter proximal apical dendrites at a distance of appr. 200 µm from the soma (mid-apical dendritic part) and secondly, spines were counted on the apical tufts at a distance of appr. 400 µm from the soma (distal-apical dendritic part). To ensure counting was accurate, z-stacks were analyzed by scrolling through the individual image of the stack. Quantification of spine density in the CA1 area revealed a significant reduction in PFN1 deficient cells, as spine number was decreased in basal and apical dendrites compared to control transfected cells (cp. **Figure 24 A**).

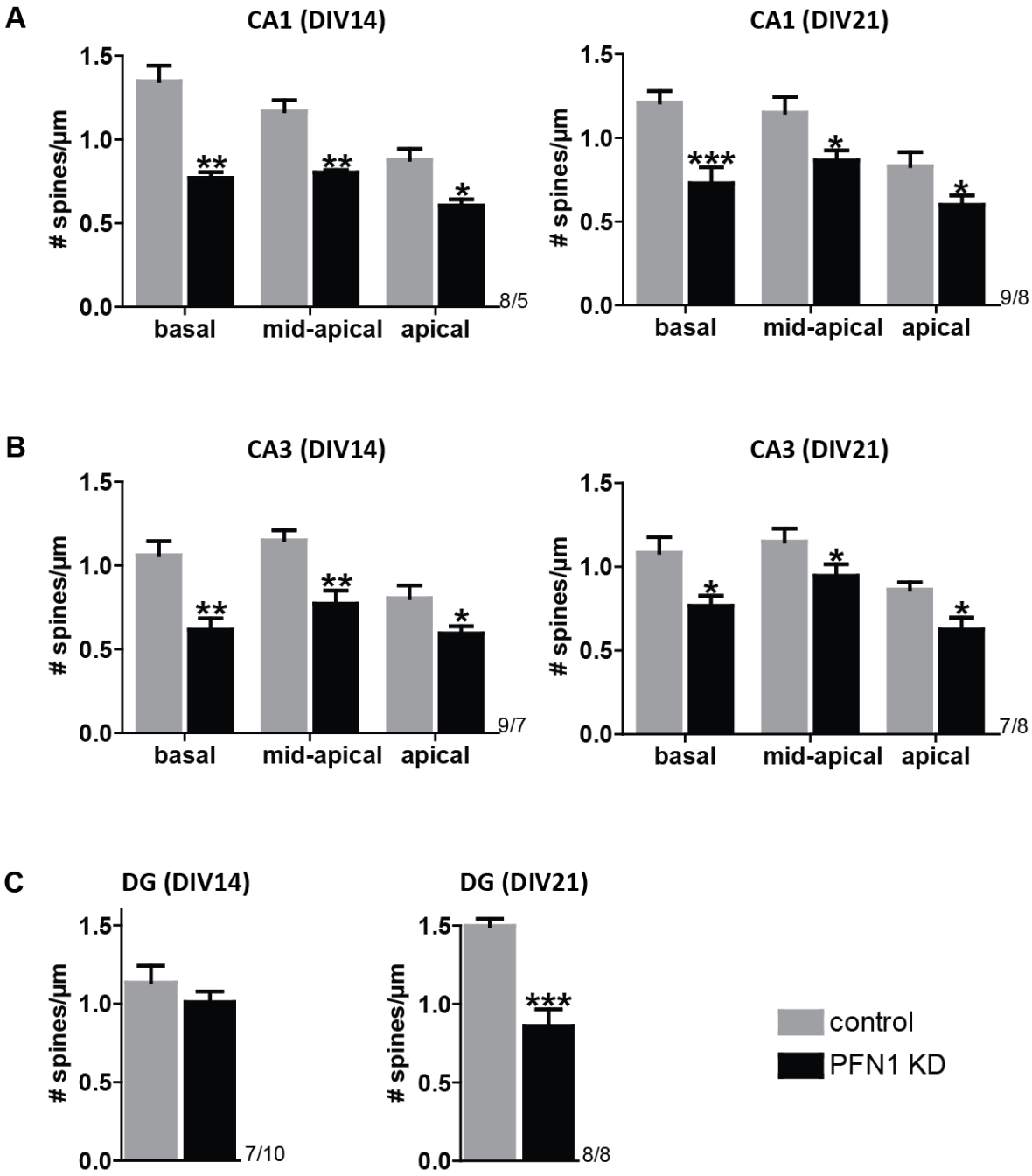

Figure 24 | Spine density is reduced in pyramidal neurons and granule cells of the hippocampus upon PFN1 depletion

(A) *Pyramidal neurons of the CA1 region showed a significant reduction in spine density compared to neurons transfected with a control plasmid expressing GFP-f. The differences could be observed in all three dendritic compartments (basal, mid-apical and distal-apical) of DIV 14 and DIV 21 cultures.* ***(B)*** *CA3 neurons were affected similarly, as the spine number was reduced regardless of the dendritic compartment or the developmental stage.* ***(C)*** *Granule cells of the dentate gyrus were not affected regarding spine number by a reduced PFN1 level at DIV 14. In contrast to this, spine number was significantly decreased compared to control at DIV 21 upon knockdown of PFN1. *p<0.05, **p<0.01, ***p<0.001*

Interestingly, the degree of reduction in spine number was similar between the two developmental ages DIV 14 and DIV 21. In line with this, in CA3 neurons similar effects on spine density could be observed as it was the case for CA1 cells (cp. **Figure 24 B**). Interestingly, granule cells of the dentate gyrus exhibited an age-dependent alteration of spine density. While spine numbers were comparable between PFN1 deficient cells and control transfected cells at DIV 14, PFN1 KD neurons had significantly less spines than control neurons at a later age (cp. **Figure 24 C).** All in all depletion of PFN1 in hippocampal neurons led to a significant reduction in the number of spines, regardless of the subregion or developmental age, except from granule cells being affected only at DIV 21 (see **Suppl. Table 1** for detailed results regarding spine density).

To determine if an acute knockdown of PFN1 alters not only spine density but also morphology, spines on CA1 and CA3 pyramidal neurons as well as granule cells were classified according to morphological parameters. Randomly selected GFP-labeled dendrite segments from the basal, mid-apical and distal-apical compartments of CA1 and CA3 neurons were imaged as described above for spine density analysis and dendritic spines were categorized according to their morphology as thin, mushroom, or stubby, according to aforementioned criteria (cp. **Figure 25**). For each cell, approximately 150 µm of total dendrite length were analyzed. Spine type distribution analysis revealed a slight but not significant decrease of mushroom spines on basal, mid-apical and distal-apical dendrites of CA1 DIV 14 neurons upon PFN1 KD (cp. **Figure 25**). Similarly, a slight but not significant increase of stubby spines was detected after PFN1 depletion. These tendencies could be also observed in more mature neurons of DIV 21. Here, significantly more stubby spines were found at distal-apical dendrites of PFN1 KD CA1 cells (~31.2% ± 3.0% for control cells cp. to ~43.7% ± 4.1% for PFN1 KD cells).

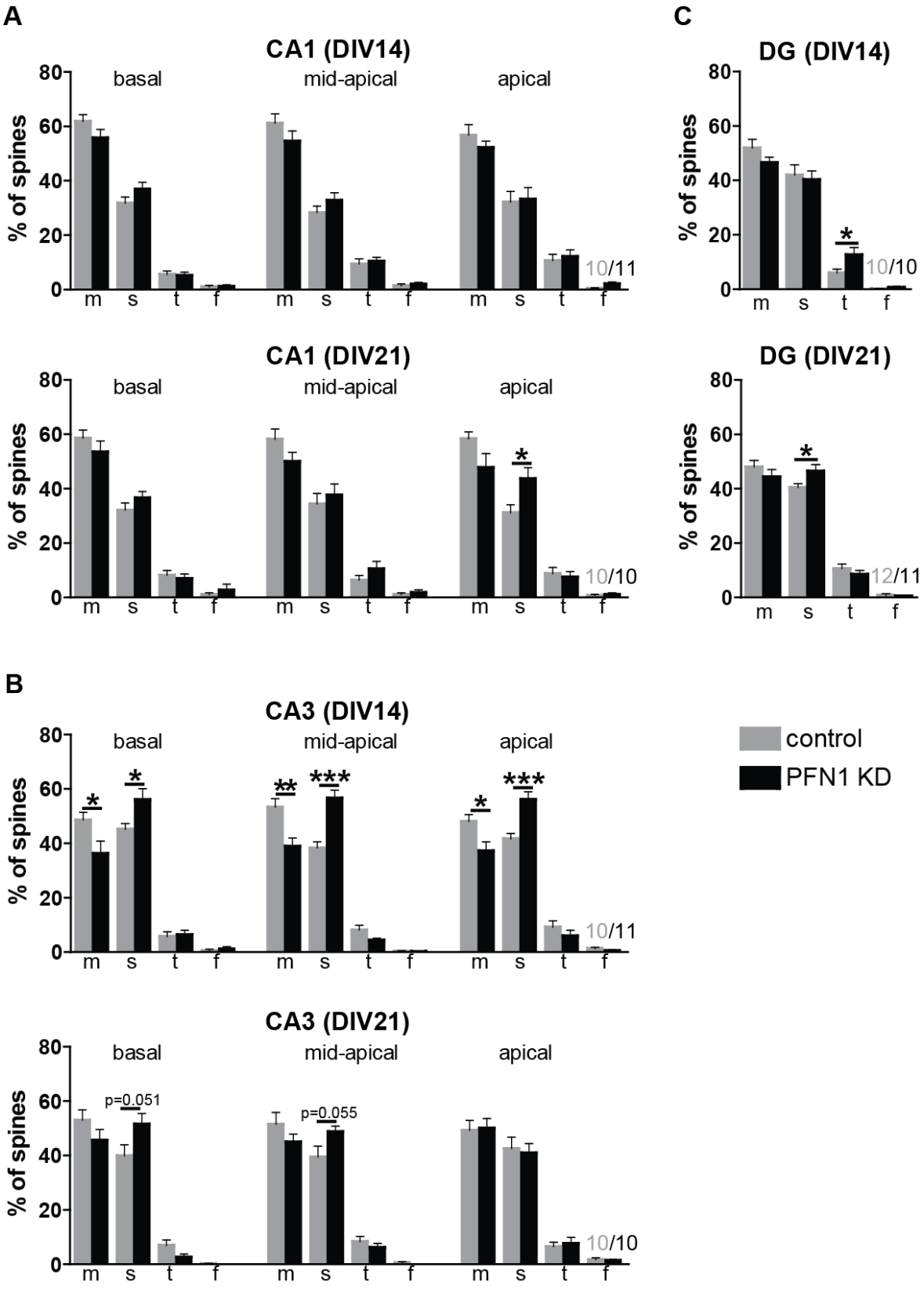

Figure 25 | Spine types are altered in pyramidal neurons and granule cells upon PFN1 knockdown

(A) *Pyramidal neurons of the CA1 region from different developmental stages (14 DIV and 21 DIV) were only mildly affected concerning spine morphology by PFN1 depletion.* – to be continued on the following page -

- continued from the previous page - *Only apical dendrites of DIV 21 PFN1 KD neurons exhibited significantly more stubby spines.* ***(B)*** *CA3 neurons at DIV14 showed a significantly higher proportion of stubby spines and a reduced proportion of mushroom spines when PFN1 was depleted. These alterations in spine type distribution were abolished at DIV 21.* ***(C)*** *Granule cells lacking PFN1 showed an increased number of thin spines at DIV 14, but not at DIV 21. Here, number of stubby spines was significantly increased in PFN1 KD cells. m=mushroom; s=stubby; t=thin; f=filopodium; *p<0.05, **p<0.01, ***p<0.001*

In contrast to this, the phenotype was much stronger in CA3 cells deprived of PFN1. In immature CA3 cells (DIV 14), a significantly reduced proportion of mushroom spines with a concurrent enhanced proportion of stubby spines could be detected in all examined dendritic compartments. At a later developmental stage (DIV 21) these significant changes in spine type distribution could not be observed to this extent. Interestingly, spine type distribution of PFN1 depleted distal-apical dendrites seemed to be not affected at all, while basal and mid-apical dendrites showed a tendency towards an increase in the number of stubby spines as was observed for the more immature state. Granule cells of the dentate gyrus demonstrated enhanced numbers of thin spines in response to PFN1 KD (~5.98% ± 1.41% for control cells cp. to ~12.61% ± 2.71% for PFN1 KD cells). In contrast to this, the number of thin spines was found to be unaffected in DIV 21 granule cells. PFN1 KD cells revealed a significantly elevated proportion of stubby spines (~40.4% ± 1.4% for control cells cp. to ~46.5% ± 2.4% for PFN1 KD cells).

Taken together, the loss of PFN1 led to a significant decreased proportion of mushroom spines in immature CA3 cells whereas the reduction in mushroom spines did not reach the level of significance in mature CA3 cells or in CA1 cells. Thus, effects on changes in spine shape seemed to depend on the hippocampal cell type as well as the developmental age of cultures.

3.3 Acute knockdown of profilin1 alters spine dynamics

3.3.1 Role of profilin1 in basal motility of spines

As spines are not rigid, but morphologically highly dynamic structures, also spine motility was analyzed upon PFN1 knockdown. To investigate spine dynamics in detail, time lapse imaging of defined dendritic branches of the apical and basal compartment was performed every 5 min for 20 min in total. Length and head width of spines were

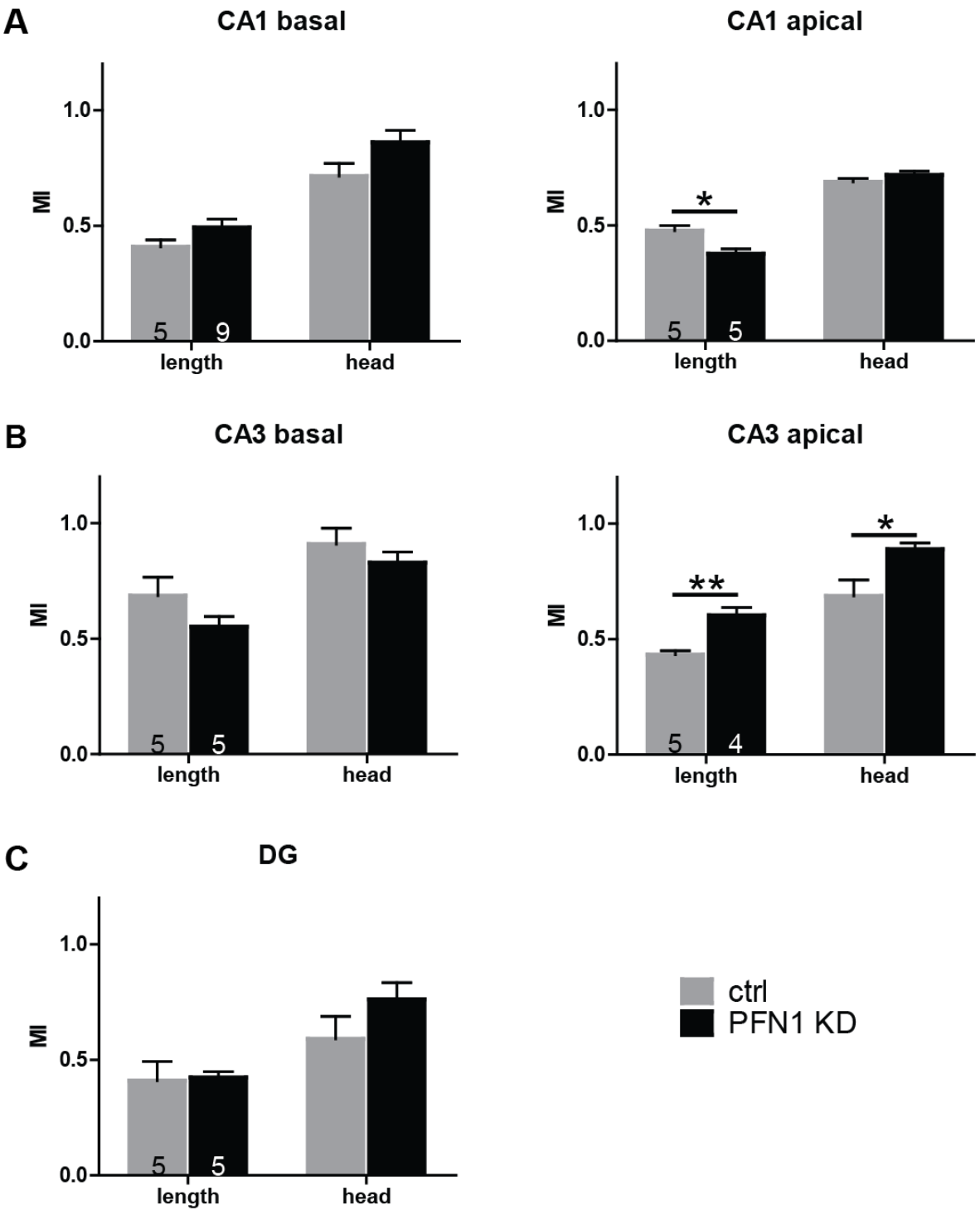

Figure 26 | Spine motility is affected upon PFN1 knockdown depending on the pyramidal cell type and the dendritic compartment

(A) *Pyramidal CA1 neurons showed decreased spine head motility upon PFN1 knockdown at apical dendrites.* ***(B)*** *Pyramidal CA3 neurons showed increased spine head and length motility upon PFN1knockdown at apical dendrites.* ***(C)*** *Granule cells were not affected in their motility upon PFN1 knockdown. *p<0.05, **p<0.01*

measured at different time points to quantify spine dynamics as the changes in spine length or spine head width per 5 min. The motility index indicated the differences in length over the entire imaging session. Basal (absence of stimulation) motility of spine length and spine head width was not changed in spines at basal dendrites of PFN1 depleted CA1 neurons compared to control cells (cp. **Figure 26 A**). In contrast to basal dendrites, spine length motility at apical dendrites was significantly reduced due to PFN1 KD (~0.47 ± 0.02 in control cells cp. to ~0.37 ± 0.02 in PFN1 KD cells). Similar results were obtained for CA3 cells, as no changes could be detected in spines of basal dendrites regarding spine length and head width (cp. **Figure 26 B**). On the contrary, spines at apical dendrites of PFN1 deprived cells exhibited significantly enhanced motility of length and head diameter (spine length: ~0.43 ± 0.02 in control cells cp. to ~0.88 ± 0.02 in PFN1 KD cells; spine head: ~0.69 ± 0.07 in control cells cp. to ~0.60 ± 0.03 in PFN1 KD cells). Interestingly, CA1 and CA3 cells seemed to act in an opposing fashion, as lack of PFN1 led to a higher motility index in case of CA3 and to a lower motility index in case of CA1. In addition to that, motility of spines at basal dendrites appeared to be contrary between CA1 and CA3, as PFN1 KD led to slightly increased motility in CA1 cells and slightly decreased motility in CA3 cells by tendency; however, alterations were not significant in both cases. Neither spine length nor spine head basal motility were significantly affected in granule cells upon acute knockdown of PFN1 (cp. **Figure 26 C**).

3.3.2 Role of profilin1 in activity-dependent structural plasticity

3.3.2.1 In contrast to PFN2a, the actin binding protein PFN1 is not crucial for activity induced spine changes

Remarkably, it was shown before that both profilin isoforms were targeted to dendritic spines in an activity-dependent manner (Ackermann and Matus, 2003; Neuhoff et al., 2005). In this respect, recent investigations point to a fundamental role of PFN2a in regulating activity-induced structural modulations such as spine head growth upon chemical induction of LTP (cLTP; Remus 2012). Thus, cLTP was induced to analyze the role of PFN1 in processes of activity-dependent structural plasticity in CA1 neurons at DIV 14-17. Here, a widely known and effective protocol based on glycine application was used to

induce NMDA receptor-dependent LTP in hippocampal slice culture comparable to LTP induction by theta-burst stimulation (Shahi et al., 1993; Fortin et al., 2011). Analysis included exclusively basal dendrites of CA1 pyramidal neurons.

Interestingly, A. Remus could prove in our lab that PFN2a is crucially involved in activity-induced structural plasticity. The spine head diameter of control cells showed an increase after stimulation, whereas in PFN2a deficient neurons this increase could not be detected (Remus 2012). In contrast to this, application of 10 mM glycine led to increased spine head diameters in control cells as well as PFN1 KD CA1 neurons 50 min after the stimulation (cp. **Figure 27 A**). More precisely, control transfected CA1 cells showed an average spine head diameter increase of ~18.4% ± 3.7% compared to ~20.3% ± 4.1% in PFN1 KD cells (cp. **Figure 27 B**).

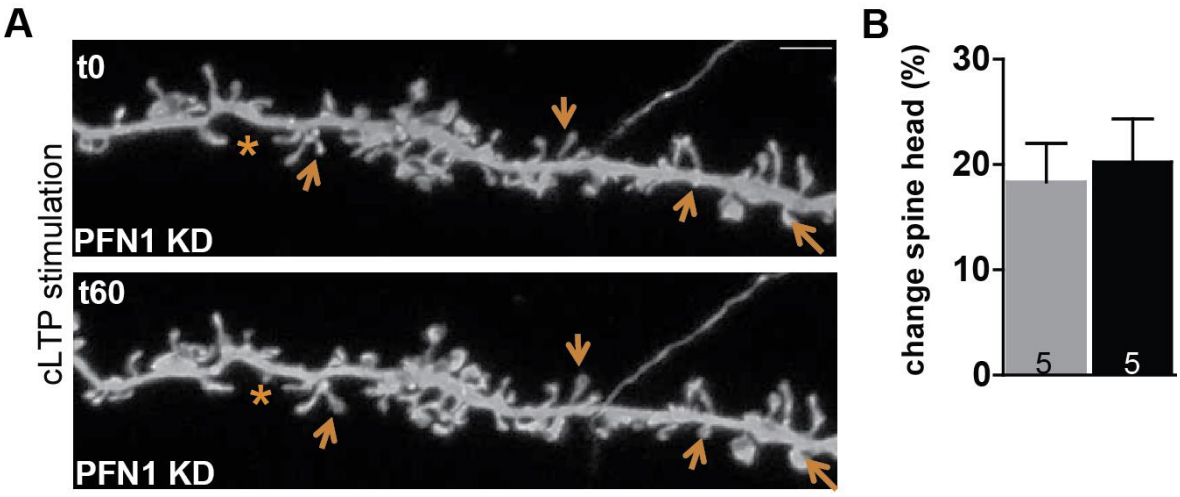

Figure 27 | PFN1 deficient CA1 neurons can undergo activity-induced spine head growth

(A) Induction of cLTP by acute glycine application triggered spine head increase in CA1 neurons (indicated by arrows) and growth of new spines (indicated by asterisks) within 60 min (scalebar = 4 µm). **(B)** Quantification of spine head growth upon cLTP revealed no significant difference between control transfected and PFN1 deficient neurons.

Motility of dendritic spines was analyzed before and 50 min after induction of cLTP. While in control cells motility was slightly, but not significantly, decreased, PFN1 KD cells did not exert any significant effect upon cLTP concerning their motility (cp. **Figure 28**).

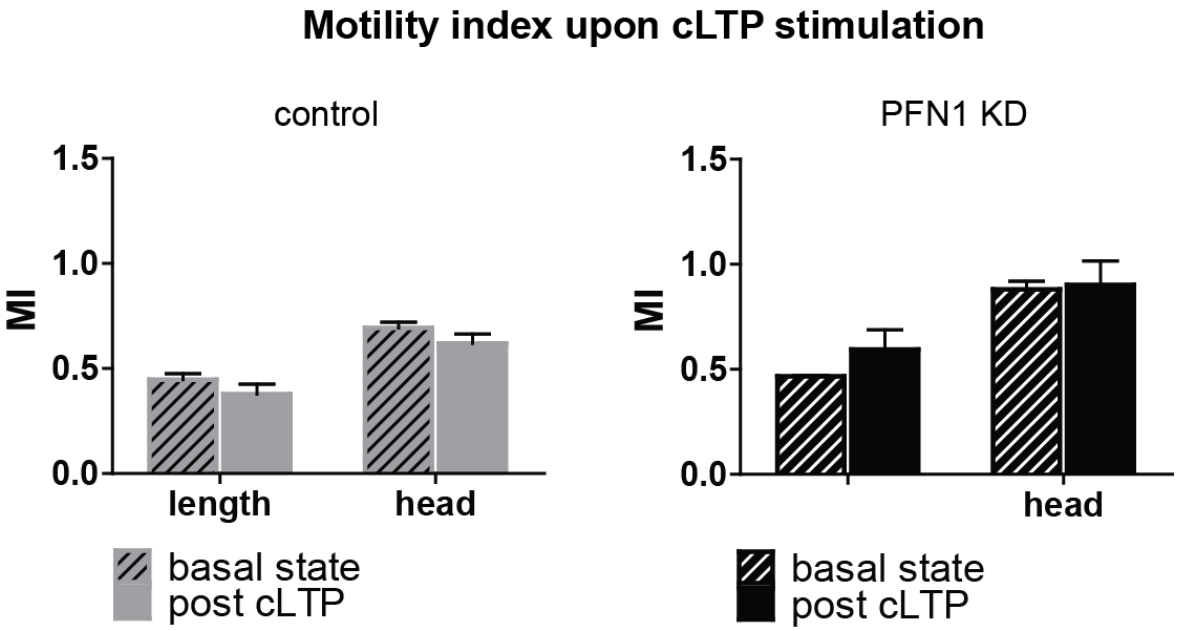

Figure 28 | Motility index of basal CA1 spines before and after induction of cLTP

Analysis of motility index before and after induction of cLTP via glycine application in control cells (left) and PFN1 deficient cells (right). Control cells showed reduced motility by tendency. In case of PFN1 KD, the MI of length increased slightly but not significantly over imaging time.

3.4 Actin binding proteins in the context of the fragile X syndrome

In *Drosophila*, the PFN1 homologue *chickadee* was shown to be bound and regulated by FMRP. Thus, protein levels of important actin-regulating proteins such as PFN1, PFN2a, CFL (cofilin) and CTTN (cortactin) were examined in brains of adult *fmr1* WT and KO mice. To determine the total protein level of whole brain lysates, SDS PAGE and western blotting were performed as described above.

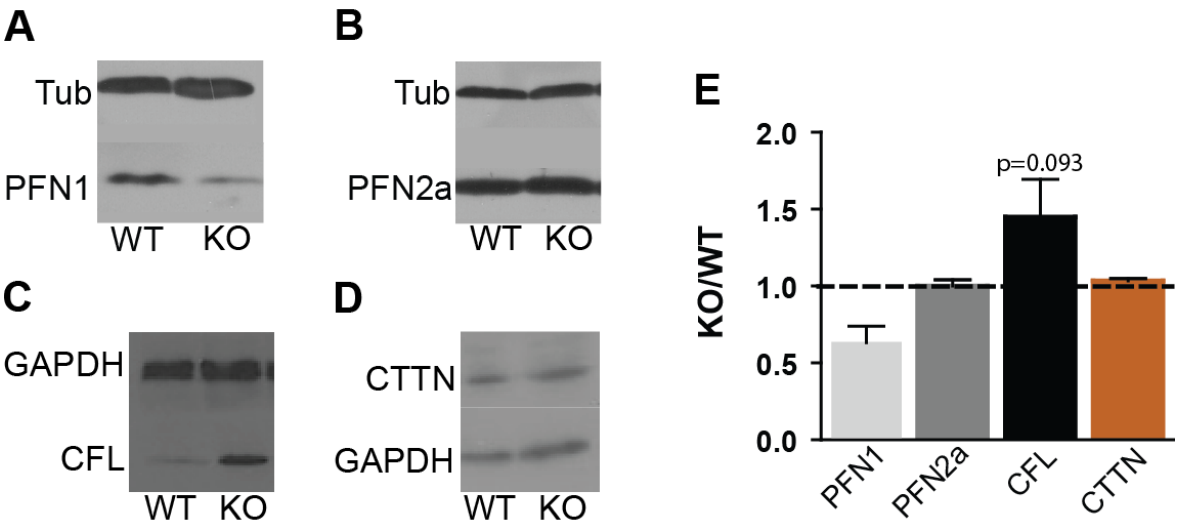

Figure 29 | Protein amounts of brain lysates from adult *fmr1* WT and *fmr1* KO mice

Representative western blots of important actin-regulating proteins such as PFN1 ***(A)****, PFN2a* ***(B)****, cofilin (CFL)* ***(C)*** *and cortactin (CTTN)* ***(D)****.* ***(E)*** *Quantification of protein amounts were normalized to fmr1 WT. Tubulin and GAPDH were used as loading controls.*

Quantification of protein levels revealed that the PFN1 expression level was decreased in brains of knockout mice, while PFN2a protein content was not different between WT and *fmr1* KO (PFN1 ratio ~0.63 ± 0.09; PFN2a ratio ~1.00 ± 0.04) (cp. **Figure 29**). Interestingly, also cortactin level was not altered in knockout mice CTTN ratio (~1.04 ± 0.02). Opposing to this, cofilin amount was increased in comparison to WT, pointing to the fact that also cofilin mRNA might be regulated by FMRP (CFL ratio ~1.45 ± 0.25; p=0.093). These results indicate that important modulators of the actin cytoskeleton such as PFN1 and CFL were dysregulated in the *fmr1* knockout mice, but most notably with contrary effects. Other actin regulators like PFN2a and CTTN, displayed comparable protein amounts in WT and *fmr1* KO brain lysates pointing to the fact that among the broad diversity of actin

modulating proteins only some might be directly under control of FMRP while others are not.

3.5 Spine morphology of FMRP-deficient hippocampal neurons

3.5.1 Profilin1 overexpression reverses the spine phenotype in *fmr1* KO neurons

Dendritic spines are identified to be abnormal in patients with the fragile X syndrome as well as in the well-studied mouse model for this disorder (Irwin et al., 2000; Nimchinsky et al., 2001; Antar et al., 2006; Cruz-Martín et al., 2010). Especially the number of spines was examined as changes in spine density are often linked to neuropsychiatric disorders. Also the size and shape of spines are critical parameters of proper neuronal functioning and connectivity, as a large spine head diameter can be in general correlated to bigger presynaptic terminals and larger postsynaptic currents (for a review see Hotulainen and Hoogenraad, 2010). However, until today, the exact extent of the spine defect in FXS is still controversial. During the last two decades many studies in the mouse model for FXS have been conducted using intact brain tissue sections, organotypic slice culture and dissociated neurons, which characterized alterations in the density, size, shape and turnover of spines in FXS or *fmr1* KO mice, but unfortunately with contradictory results (for a review see Portera-Cailliau and He, 2012). Most studies examining spines in FXS were performed by Golgi staining of pyramidal neurons from the neocortex and hippocampus upon post-mortem brain tissue from individuals with FXS or in adult *fmr1* KO mice and described elevated spine density across different layers of the neocortex (Comery et al., 1997; Irwin et al., 2001; Galvez et al., 2003; McKinney, 2005; Dölen et al., 2007; Hayashi et al., 2007). More recent developmental studies focused on morphological analyses of spines during early postnatal development in *fmr1* KO mice and relied rather on advanced microscopy techniques than on Golgi staining. Strikingly, these studies could not detect any differences in spine density of *fmr1* KO pyramidal neurons (Meredith et al., 2007; Cruz-Martín et al., 2010; Harlow et al., 2010; Pan et al., 2010). Thus, no common phenotype concerning spine density could be found in the literature so far, as conflicting data were obtained from the adult brain, from the developing brain (P≤20) or from dissociated hippocampal neurons in culture which either report increased (Comery et al., 1997; Nimchinsky et al., 2001; McKinney, 2005; Antar et al., 2006; Dölen et al., 2007;

Levenga et al., 2011), normal (Braun and Segal, 2000; Restivo et al., 2005; Grossman et al., 2006; de Vrij et al., 2008; Cruz-Martín et al., 2010; Harlow et al., 2010; Pan et al., 2010) or even lower (Segal et al., 2003) density in different cortical layers or in the hippocampus of *fmr1* knockout mice.

In this study, no alterations in spine numbers could be identified in dissociated hippocampal and cortical cell culture between *fmr1* WT and KO, neither in immature nor in mature neurons. These findings are in line with several publications which also described spine density to be unaffected in *in vitro* hippocampal cultures (Braun and Segal, 2000; Segal et al., 2003; de Vrij et al., 2008; Levenga et al., 2011; Su et al., 2011).

However, it is likely that changes in size and/or shape of spines might affect synapse and therefore network function to an equal degree like alterations in spine number. Since spine head size correlates with synaptic strength and is able to change during synaptic plasticity processes, spine morphology is indeed tightly related to synapse function (Matsuzaki et al., 2001, 2004; Lang et al., 2004; Nägerl et al., 2004; Oh et al., 2012). The literature shows no consensus on spine morphology in *fmr1* KO mice, which means that a variety of spine abnormalities have been reported. Several publications displayed an immature spine phenotype in *fmr1* KO mice by showing a higher proportion of longer spines in the KO; which matches what has been observed in autopsy of patients with fragile X syndrome. It is important to note that not all studies agree with the described immature spine phenotype; contradictory results concerning the immaturity of spines might be dependent on the brain region (or even subregion) being examined, or might be influenced by the age of cultures or different methods to label neurons (Golgi staining, diolistic labeling, STED microscopy of transgenic animals). In addition to that, one should carefully consider that *in vitro* studies do not fully reflect the *in vivo* situation.

The data yielded by this study provide evidence that the morphology of spines was changed in *fmr1* KO neurons, as the proportion of long, thin spines was increased and less mature (mushroom) spines could be detected compared to WT control cells (cp. **Figure 30 A3**). As it could be shown here that PFN1 levels are reduced in whole brain lysate of *fmr1* KO mice (cp. **Figure 20**) and as it could be shown as well that PFN1 can influence both spine number as well as spine morphology, the question was raised whether a PFN overexpression would be sufficient to attenuate or even rescue the FXS phenotype.

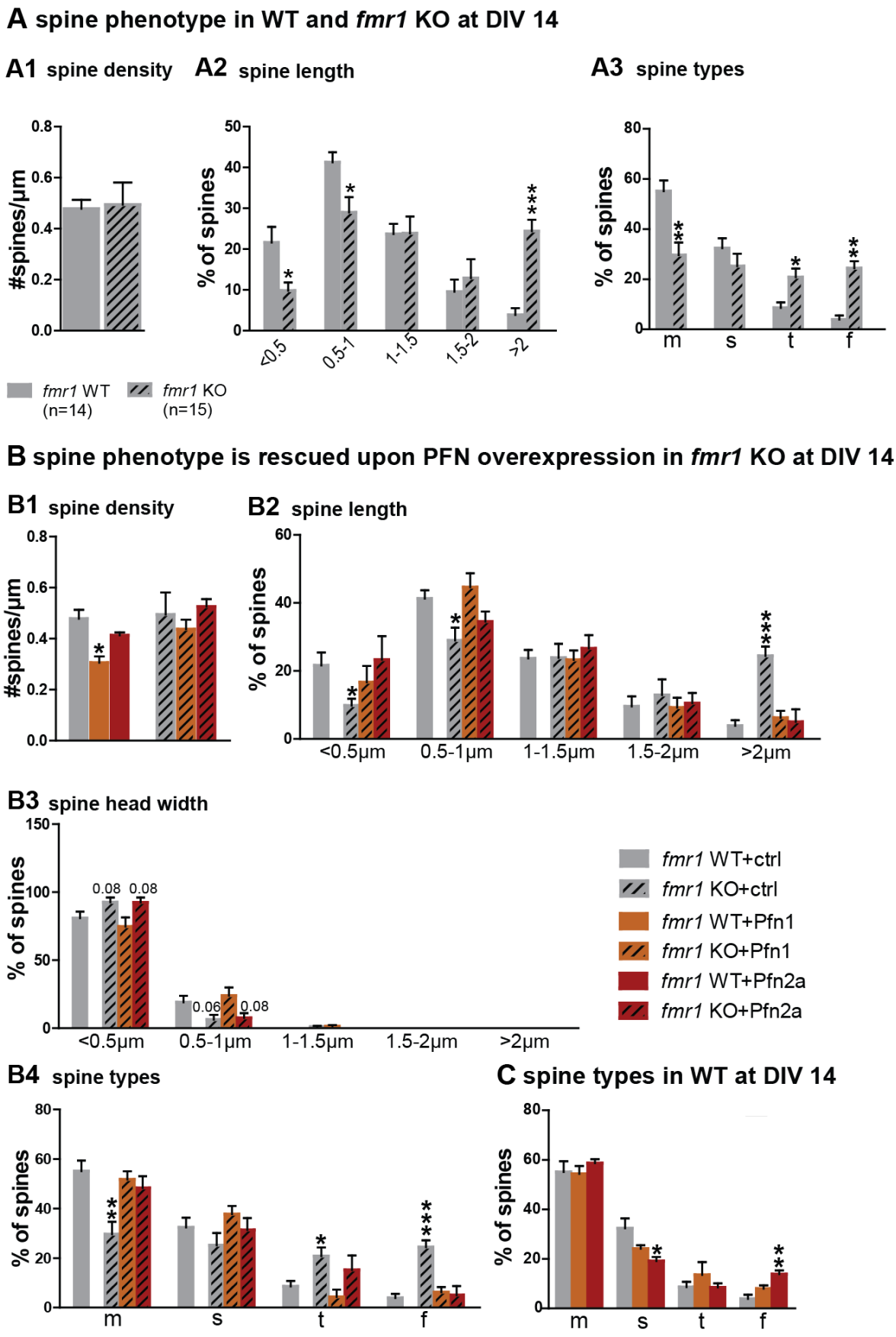

Figure 30 | Spine density and shape at DIV 14 in dissociated hippocampal neurons derived from WT and *fmr1* KO animals *- to be continued on the following page -*

- continued from the previous page - ***(A)*** *Spine phenotype in dissociated fmr1 WT and KO hippocampal neurons.* ***(A1)*** *Spine density showed no differences between fmr1 WT and KO neurons.* ***(A2)*** *Length of dendritic spines was significantly altered in case of KO neurons, as proportions of spines with a length below 0.5 µm and a length between 0.5-1 µm were significantly decreased in the KO. In turn, KO neurons showed significantly more long (> 2 µm) spines than WT cells.* ***(A3)*** *Spine type distribution was significantly altered in the KO, as number of mushroom spines was significantly decreased in the KO. Both, long spines and filopodia, were significantly enhanced in KO neurons.* ***(B)*** *Spine phenotype was rescued upon PFN1 overexpression in fmr1 KO neurons.* ***(B1)*** *Spine density showed no major differences between WT and fmr1 KO neurons. PFN1 overexpression led to a significant reduction of spine density in WT cells* ***(B2)*** *Alterations in the spine length, spine head width* ***(B3)*** *and* ***(B4)*** *alterations in the spine type distribution of fmr1 KO cells were restored upon overexpression of either PFN1 or PFN2a.* ***(C)*** *Spine type distribution in fmr1 WT was only slightly changed upon PFN2a overexpression. *p<0.05, **p<0.01, ***p<0.001*

To analyze spine type distribution in the *fmr1* knockout, dissociated hippocampal and cortical neurons were prepared from WT and *fmr1* KO animals and transfected at two different developmental ages (DIV 14, DIV 21). To further investigate if profilins might play a role in the spine phenotype, overexpression experiments were performed with either PFN1 or PFN2a. In general, spine density of control cells was lower at DIV 14 than at DIV 21 (0.48 ± 0.03 at DIV 14 cp. to 0.93 ± 0.04 spines/µm at DIV 21; cp. **Figure 30** and **Figure 31 A1**). Binning of spine lengths into different categories revealed a significant decrease in the frequency of shorter spines in the *fmr1* KO (21.6% ± 3.8 in WT cp. to 9.8% ± 2.0 in KO for spines <0.5 µm, p=0.0253; 41.3% ± 2.5 in WT cp. to 28.98% ± 3.7 in KO for spines 0.5-1 µm, p=0.0255; cp. **Figure 30 A2**). In return, *fmr1* KO cells exhibited a highly significant elevation of the number of long (>2 µm) spines (3.87% ± 1.7 in WT cp. to 24.41% ± 2.8 in KO, p=0.0002).

Spine type distribution was significantly altered between WT and *fmr1* KO as mushroom spines were significantly decreased in the KO (55.2% ± 4.3 in WT cp. to 29.6% ± 5.0 in KO, p=0.0049). Consequently, proportions of thin spines and filopodia were significantly increased in *fmr1* KO cells (thin spines: 8.6% ± 2.2 in WT cp. to 20.8% ± 3.5 in KO, p=0.018; filopodia: 3.8% ± 1.7 in WT cp. to 24.4% ± 2.8 in KO, p=0.0002; cp. **Figure 30 A3**). While mushroom and stubby spines are thought to be more mature spine types, thin spines are most likely immature spines and filopodia might represent precursors of spines. Spine density was not significantly different between both genotypes, but was affected differentially by overexpression of PFN1 which led to a significant reduction in case of WT compared to control condition (0.48 ± 0.03 cp. to 0.31 ± 0.02, p=0.0118; cp. **Figure 30 B1**). In contrast to this, PFN2a overexpression had no effects on spine number, neither in WT

nor in KO cells. In cortical neurons, spine density was not significantly different between WT and KO at DIV 14 or DIV 21, but was significantly elevated by PFN1 overexpression in *fmr1* KO neurons at both ages (cp. **Suppl. Fig. 2 E**). Strikingly, the expression of profilin isoforms resulted in a reversal of the spine length phenotype observed in the *fmr1* KO cells, as the frequency of short spines was significantly increased there and did not longer differ from the WT. Moreover, the proportion of filopodia, which was significantly higher in *fmr1* KO cells than in the WT, was strongly reduced close to WT level (cp. **Figure 30 B2**). Spine head width showed a tendency to be different between genotypes, as KO cells exhibited more small spine heads (< 0.5 µm; 80.9% ± 4.8 in WT cp. to 92.6% ± 3.5 in KO, p=0.08) and less spine heads with a size of 0.5 – 1 µm (19.1% ± 4.8 in WT cp. to 6.3% ± 3.4 in KO, p=0.08; cp. **Figure 30 B3**). Interestingly, these alterations between WT and KO were abolished by PFN1 expression, but not by PFN2a expression pointing to the fact that only PFN1 is able to fully rescue the spine phenotype. Similar to this, spine type distribution was also rescued by overexpression of either PFN1 or PFN2a (cp. **Figure 30 B4**). On the one hand, the proportion of mushroom spines was significantly increased in *fmr1* KO cells by exogenous expression of either PFN1 or PFN2a. On the other hand, the number of immature spine types was reduced and therefore significantly different from control transfected *fmr1* KO cells and not any longer from the WT. Importantly, PFN isoforms appeared to act differentially, as exogenous expression of PFN1 led to a complete rescue while only a partial rescue could be achieved by the expression of PFN2a. Interestingly, while overexpression of PFN1 had no influence on spine type distribution in WT neurons, PFN2a overexpression led to a significant decrease of stubby spines with a concomitant increase of filopodia (cp. **Figure 30**). Similar to the results obtained for DIV 14, also spine density at DIV 21 exhibited no significant changes between the two genotypes (cp. **Figure 31 A1**). Moreover, spine length of *fmr1* KO neurons was comparable to WT cells, with the exception of the frequency of very short spines (<0.5 µm of length), which was significantly reduced in the KO (22.2% ± 3.4 in WT cp. to 8.3% ± 3.3 in KO, p=0.0199; cp. **Figure 31 A2**). Remarkably, spine type distribution was not affected at all in the *fmr1* KO at this stage (cp. **Figure 31 A3**) and remained unaffected in the case of PFN overexpression (cp. **Figure 31 B4**). In general, spine density was comparable between *fmr1* WT and KO, but was significantly reduced upon PFN2a expression in WT neurons (0.93 ± 0.04 in WT ctrl cp. to 0.75 ± 0.03 in WT with PFN1, p=0.0112; cp. **Figure 31 B1**).

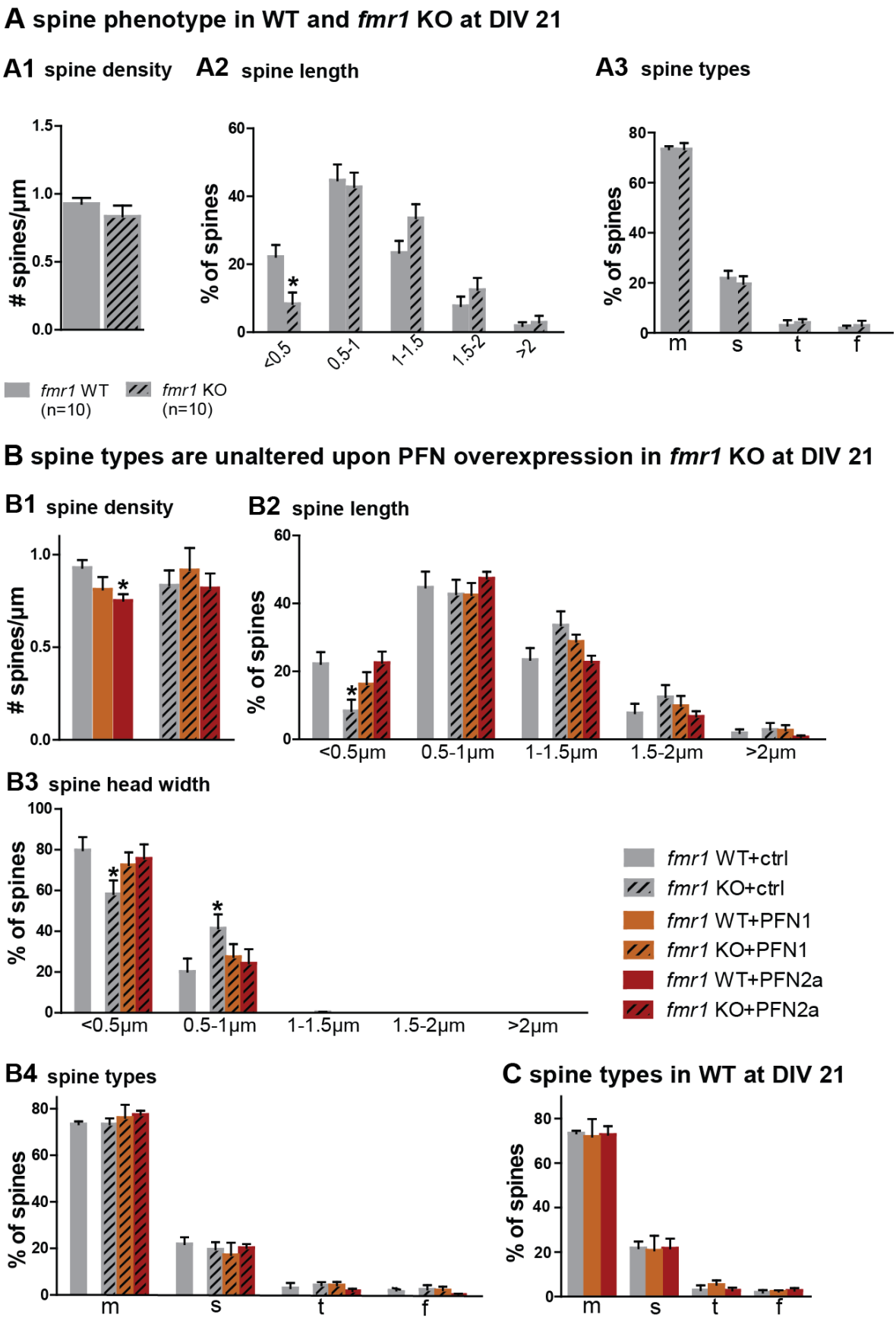

Figure 31 | Spine density and shape at DIV 21 in dissociated hippocampal neurons derived from *fmr1* WT and KO animals *- to be continued on the following page -*

- continued from the previous page - ***(A)*** *Dendritic spines exhibited no major differences between mature hippocampal WT and fmr1 KO neurons.* ***(A1)*** *Spine density in control transfected dissociated WT and fmr1 KO cells showed no significant differences. PFN1 overexpression did not affect spine number.* ***(A2)*** *Binning of length of spines revealed a significant reduction of short spines with a length below 0.5 µm in fmr1 KO cells.* ***(A3)*** *Spine type distribution was identical in both genotypes.* ***(B1)*** *Spine density was comparable between genotypes and only affected by PFN2a overexpression in the WT.* ***(B2)*** *Spine length was comparable between genotypes and remained unaffected upon PFN overexpression.* ***(B3)*** *Spine head width was significantly different between genotypes.* ***(B4). (C)*** *Spine type distribution did not change upon PFN overexpression in the KO or in the WT cells n equals number of neurons; *p<0.05*

Control transfected cells as well as PFN1 or PFN2a overexpressing cells demonstrated spine lengths similar to WT cells (cp. **Figure 31 B2**). Spine head width was significantly different between genotypes, as KO cells exhibited less small spine heads (< 0.5 µm; 79.8% ± 6.4 in WT cp. to 58.3% ± 6.7 in KO, p=0.049) and significantly more spine heads with a size of 0.5 – 1 µm (20.2% ± 6.4 in WT cp. to 43.1% ± 5.8 in KO, p=0.026; cp. **Figure 31 B3**). Overexpression of profilins abolished these alterations in the *fmr1* KO cells. All in all, no major differences in the spine phenotype between *fmr1* WT and KO hippocampal neurons occurred at the developmental stage of DIV 21. However, exogenously expression of PFN isoforms did not influence spine shape or spine number neither in the WT nor in the KO.

These results provide evidence for a transient effect of FMRP during the development of dendritic spines in the hippocampus, as spine maturation was found to be delayed in *fmr1* KO neurons. Strikingly, a complete or partial, rescue of the spine phenotype observed in *fmr1* KO neurons was achieved by exogenous expression of either PFN1 or PFN2a, respectively, in immature neurons. Taken together, these results suggest that there might be indeed a close association between the immature spine phenotype in *fmr1* KO neurons and a dysregulation of profilin isoforms.

3.6 Lack of FMRP affects hippocampal and cortical neurons in an age-dependent manner

Over the past decade most research in FXS has focused on characterization on the spine phenotype. This study also investigated the dendritic architecture of dissociated hippocampal neurons of *fmr1* KO mice or WT littermates. At two different developmental ages (DIV 14 and DIV 21) cells were transfected with control plasmids as well as

overexpression vectors for PFN1/PFN2a or knockdown vectors against PFN1 or PFN2a to analyze the phenotype of FMRP-deficient hippocampal neurons in dissociated culture and reveal possible effects on dendritic complexity. In immature neurons, overexpression as well as knockdown of one of the profilin isoform resulted in decreased dendritic complexity to the same extent in *fmr1* WT and KO neurons. Concomitantly, total number of intersections and total length of dendrites per neurons were significantly reduced (cp. **Supplement Fig. 1**). Similar to this, also *fmr1* WT neurons of DIV 21 showed less complex dendrites if PFN1 or PFN2a was reduced in contrast to *fmr1* KO neurons which were not affected. Moreover, overexpression of either PFN1 or PFN2a did not exert any effects on the dendritic tree.

Besides dissociated neurons from the hippocampus also cortices were prepared to gain primary cortical neurons of *fmr1* WT and KO animals (cp. **Supplement Fig. 2**). Overexpression of PFN1 did not affect dendritic architecture of cortical *fmr1* WT and KO neurons at DIV 14 or DIV 21. Interestingly, while *fmr1* WT cortical neurons increase their dendritic tree with increasing age, this is not the case for cortical neurons derived from *fmr1* KO animals as dendritic complexity was not enhanced compared to DIV 14.

3.7 Spatial memory formation in the mouse model for fragile X syndrome

Since *fmr1* KO mice exhibit a broad range of behavioral phenotypes such as elevated locomotor activity (Bakker et al., 1994), increased stereotypic behavior (Spencer et al., 2011) or impaired attention (Moon et al., 2006). In addition, they show altered synaptic plasticity in brain areas involved in learning and memory processes, therefore these deficits might indeed contribute to impaired performances in standardized test of memory (D'Hooge & De Deyn 2001). Spatial learning abilities as tested in the Morris water maze are thought to rely significantly on the hippocampus and parallel episodic memory in humans. Interestingly, in previous studies it could be demonstrated that *fmr1* KO mice reflect several behavioral traits of those of FXS patients, as shown by mildly impaired spatial learning performances in the Morris water maze as well as trace fear memory tests (Zhao et al. 2005; D'Hooge 1997; Kooy et al. 1996). To investigate the physiological function of the *fmr1* gene regarding its role in spatial learning and resulting memory formation, the well-established Morris water maze test was conducted with *fmr1* KO mice and corresponding *fmr1* WT littermate controls in a few studies, which presents partially controversial results. Some studies using the classic Morris water maze test to assess spatial learning found impairment exclusively in the reversal trial in *fmr1* knockout mice (Bakker et al., 1994; D'Hooge, 1997), whereas other studies could not observe any difference between both genotypes in the learning and the reversal task (Paradee et al., 1999). Moreover, near-normal performances of knockout animals were apparent in the probe trial of other studies (Kooy et al. 1996; D'Hooge 1997; Paradee et al. 1999).

Thus, general findings point to learning and memory deficits in *fmr1* KO mice, yet the magnitude of which still needs to be clarified. A precise evaluation of spatial learning in these mice could further profit from new methods to analyze MWM data sets by the assessment of different learning strategies. Here, search strategies were studied for the first time in *fmr1* KO animals in detail as a comparison only between latencies and path lengths could fail to reveal rather subtle yet important impairments in spatial memory acquisition. The efficient use of non-spatial egocentric strategies can sometimes result in reduced latency times almost comparable to those achieved by the use of allocentric direct search strategies without significant contribution of the hippocampus (Gallagher et

al., 1993; Wolfer et al., 1998). In order to clarify the actual extent of learning deficits regarding acquisition, retrieval and use of spatial information, we examined spatial learning in the *fmr1* knockout mice using the hippocampus-dependent Morris water maze paradigm. Additionally, alterations in hippocampal and cortical protein levels induced by spatial learning in the water maze should be determined to address the relationship between hippocampus-dependent memory and actin-binding proteins in the mouse model of the fragile X syndrome.

3.7.1 *fmr1* KO mice show a significant impairment in spatial reference memory formation

Testing in the water maze revealed that *fmr1* KO mice were able to acquire spatial memory, as the performance of both genotype groups in locating the hidden platform improved over time (cp. **Figure 32 A, B**). No significant differences in general swimming ability could be observed (cp. **Figure 32 C, D**). During the acquisition phase, performances of *fmr1* KO mice showed no significant differences compared to WT littermates in the parameters evaluated such as escape latency to reach the platform, global distance travelled and swimming speed (cp. **Figure 32**).

Escape latency of *fmr1* WT animals decreased significantly from ~25 ± 6.0 s on the first day to ~5 ± 1.7 s on training day 8 ($F_{(7, 70)}$=5.03; p<0.0001). Interestingly, *fmr1* KO mice needed more time to reach the platform already at the onset of training. Latencies of *fmr1* KO mice were higher on the first day of training (~35 ± 5.8 s) than in control animals, but also gradually decreased over time to ~8 ± 2.3 s ($F_{(7, 84)}$=7.333; p<0.0001) (cp. **Figure 32 A**). Although *fmr1* KO mice showed higher latency times at days 1 and days 5-8, there was no significant difference between genotypes (latency, $F_{(1,23)}$=0.507, p=0.484). The average distance travelled in the water maze decreased as well throughout training in both groups, as it was reduced from ~693 ± 111 cm at day 1 to ~126 ± 40 cm at day 8 for *fmr1* WT ($F_{(7,70)}$=6.229; p<0.0001) and ~934 ± 152 cm to ~208 ± 62 cm for *fmr1* KO ($F_{(7,84)}$=5.49; p<0.0001) on average per trial (cp. **Figure 32 B**). The evaluation of the swim speed proved the physical intactness of mice and was similar among genotypes, as both control littermates and knockouts started with a speed of ~26.93 ± 2.19 cm/s (WT) and ~27.00 ± 0.85 cm/s (KO) (cp. **Figure 32 C**). With training time, both groups reduced their speed until the last day of training: a significant decrease to ~17.9 ± 1.9 cm/s in case of *fmr1* WT

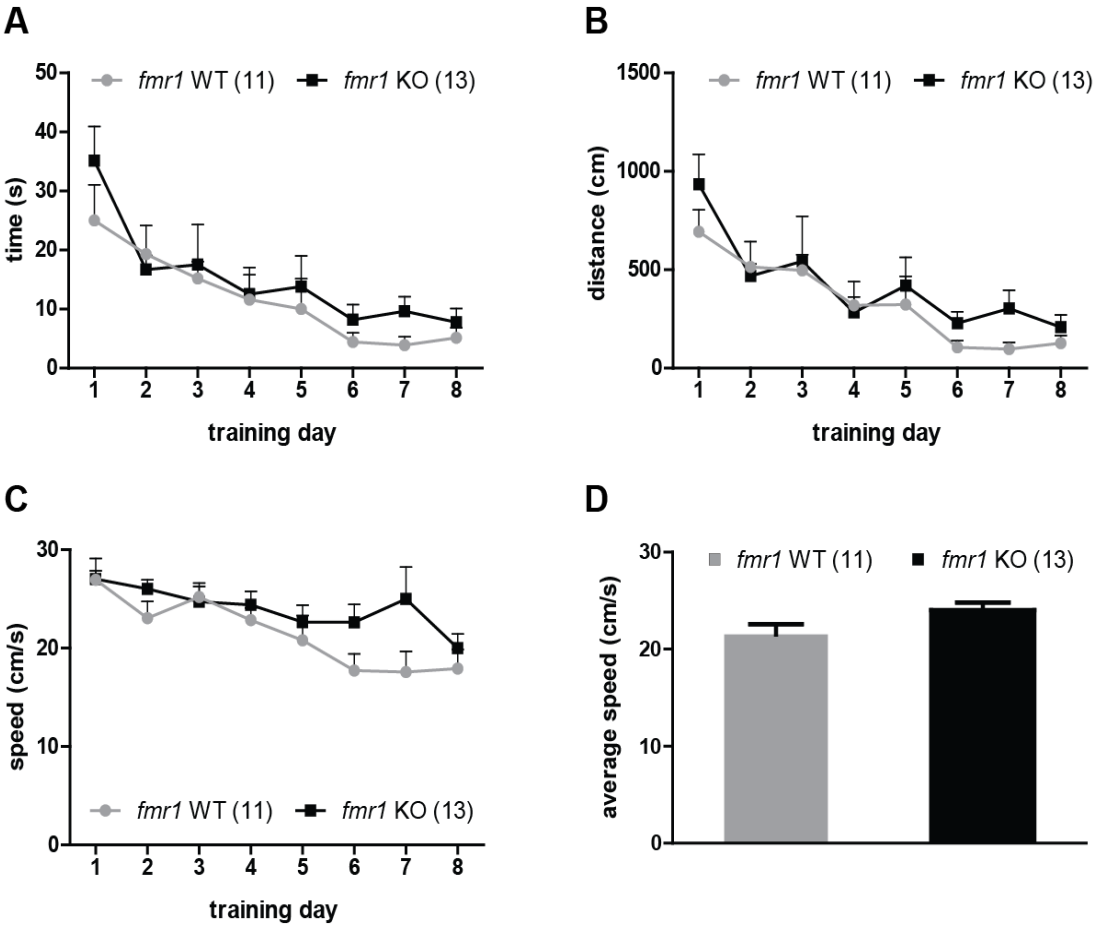

Figure 32 | Spatial learning in the water maze of *fmr1* WT and *fmr1* KO animals

(A) *Escape latency described the average time to find the platform. During the 8 days of training, latency of both genotypes decreased. Although fmr1 KO mice showed in general higher latency times there was no significant difference between fmr1 WT and KO.* ***(B)*** *The average distance per trial travelled in the water maze decreases with training in both groups.* ***(C)*** *The swim speed was used as a measurement for physical integrity of mice. Both fmr1 WT and KO mice reduced their swim speed throughout training to a similar extent.* ***(D)*** *Average swim speed during the training exhibited no significant differences between fmr1 WT and KO mice (two independent experimental series, fmr1 WT n=11, fmr1 KO n=13).*

animals ($F_{(7,70)}$=4.806; p=0.0002) and a non-significant decrease from ~20 ± 1.4 cm/s in case of *fmr1* KO mice ($F_{(7,84)}$=1.743; p=0.1101). Average speed was not altered significantly between groups (*fmr1* WT: ~21.5 ± 3.6 cm/s; *fmr1* KO: ~24 ± 2.8 cm/s; p=0.1014) (cp. **Figure 32 D**).

By measuring escape latency and path length, the course of the spatial navigation learning process could be investigated. While this gave information on the goal-finding speed during the acquisition phase, a probe trial administered 24 h following the last acquisition day provided a measure for the spatial reference memory at this point of time. The formation of this long-lasting spatial reference memory was shown to be linked

to hippocampal and cortical function and is represented by a clear preference for the target quadrant. Since only one probe trial was conducted at the end of training, the final condition of the animals regarding memory formation was measured.

For the probe trial at day 9 the platform was removed and the mice were allowed to swim freely in the pool for 45 s. To assess spatial memory retrieval during the probe trial the time spent in the quadrant that previously contained the platform as well as crossings of the previous platform position were measured and compared between genotypes. Detailed analysis of the reference memory test revealed that wild-type mice spent most of the time in the target quadrant (~67.74 ± 4.7 s) and highly significant less time (p-value < 0.001) in the other quadrants such as NE quadrant (~13.90 ± 2.7 s), the SE quadrant (~4.57 ± 1.7 s) as well as the SW quadrant (~13.79 ± 2.6 s; cp. **Figure 33 A**). Similar results were found for the knockout mice, as they spent significantly more time in the target NW quadrant (~45.69 ± 4.7 s) than in the other quadrants (SE quadrant 10.56 ± 2.5 s, SW quadrant ~9.02 ± 2.6 s) (cp. **Figure 33 B**). In fact, results obtained in *fmr1* KO were quite similar as they exhibited a significant difference between target and remaining quadrants (~45.69 ± 4.7 s compared to ~18.10 ± 1.6 s), too (cp. **Figure 33 D)**.

Collectively, both genotypes were above chance probability (>25%) in visiting the target quadrant but to a different amount. Strikingly, when comparing both genotypes, *fmr1* KO spent significantly less time in the target and significantly more time in the other quadrants than WT littermates.

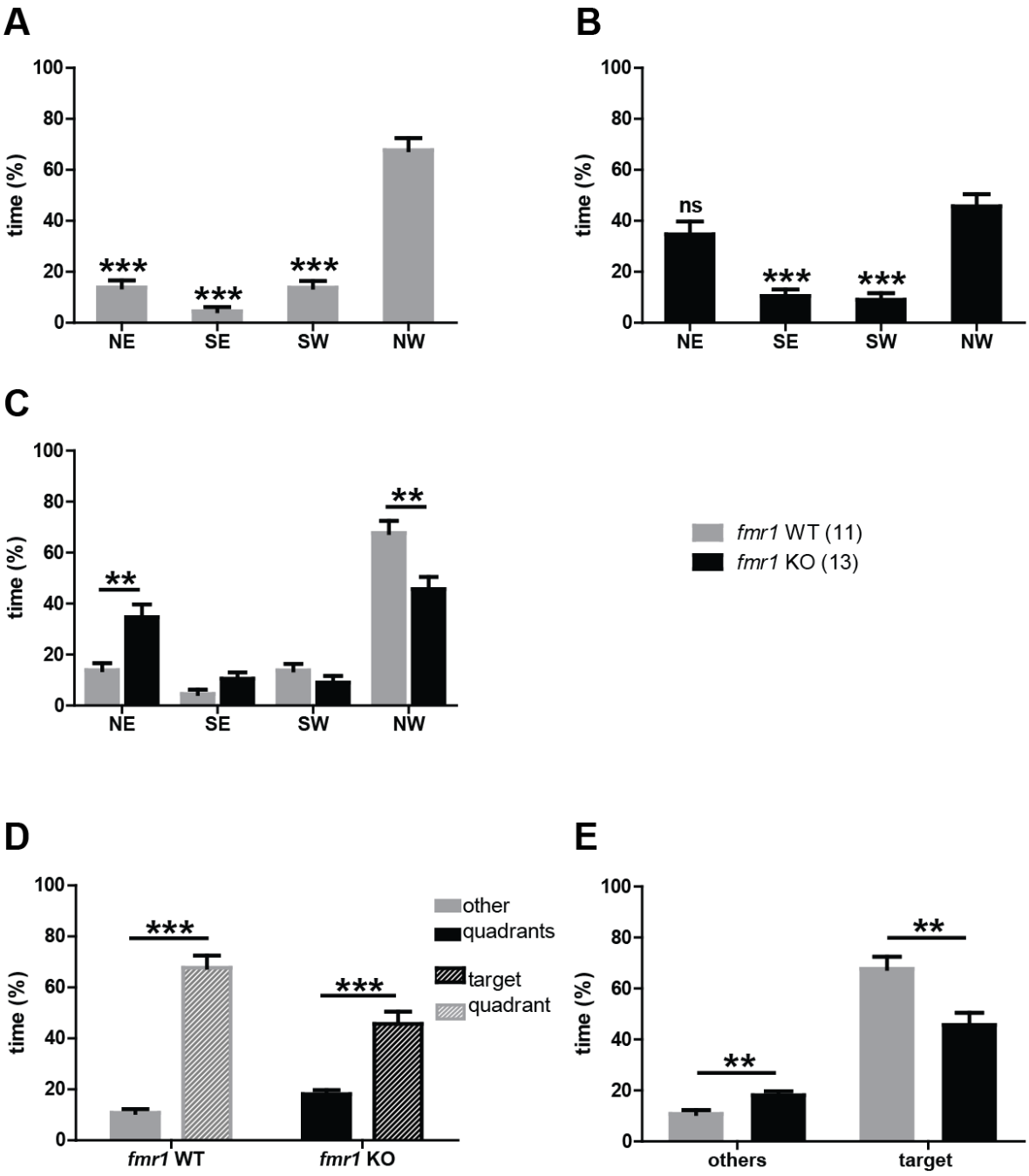

Figure 33 | Reference memory test (probe trial) at day 9 of training

(A) *Time spent in each quadrant. fmr1 WT mice spent significantly more time in the target quadrant than in the remaining three quadrants.* ***(B)*** *fmr1 KO mice spent more time in the NW quadrant than in the other quadrants.* ***(C)*** *fmr1 WT animals spent highly significant more time in the target quadrant than fmr1 KO littermates. Instead, knockouts spent time in the NE quadrant.* ***(D)*** *The differences between fmr1 WT and fmr1 KO were both highly significant for the target quadrant preference and the duration of stay in other quadrants.* ***(E)*** *fmr1 WT showed a significantly higher preference for the target quadrant than fmr1 KO mice, while the latter stayed significantly longer in the other quadrants than WT littermates. *p<0.05; **p<0.01; ***p<0.001*

An additional and even more precise parameter to assess the accuracy of spatial memory retrieval during the probe trial is an assessment of the number of "platform" crossings. Entries into the area of the previous platform were considered as platform crossing (cp. **Figure 34 B**). Interestingly, *fmr1* WT mice visited the previous platform position during the probe trial on average ~6.7 ± 0.5 times (cp. **Figure 34 A**), whereas *fmr1* KO animals showed a significantly reduced number of platform crossings with ~5.0 ± 0.6 times compared to the WT (p=0.0358). Example swim paths of *fmr1* WT as well as *fmr1* KO animals demonstrate that both genotypes display a clear preference for the target quadrant and learned to find the platform almost comparably, however displaying significant difference in spatial precision (cp. **Figure 34 B**).

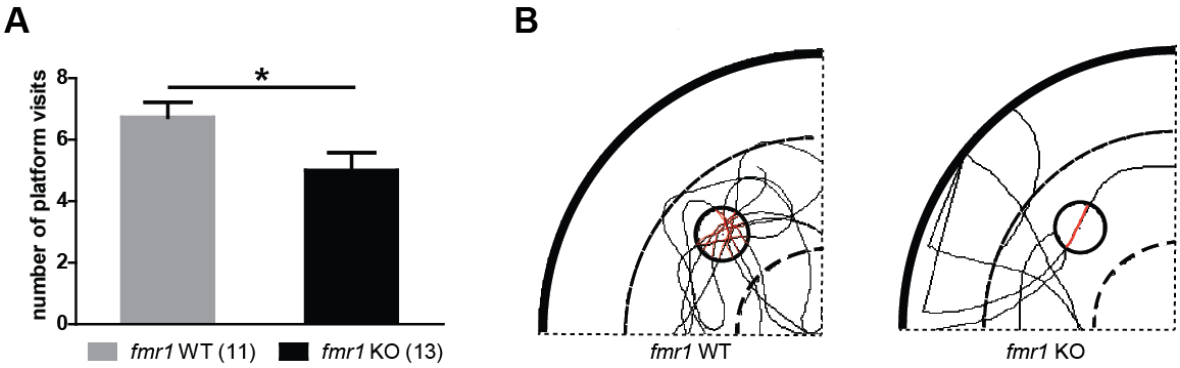

Figure 34 | Spatial memory retrieval during the probe trial: number of platform visits

(A) *Probe trial for 45 s revealed that fmr1 WT mice significantly more often visited the platform position than fmr1 knockout mice.* ***(B)*** *Representative traces of one fmr1 WT animal and one fmr1 KO animal, respectively. In each case only the target quadrant is shown depicted. The previous platform position is indicated by a black circle, platform crossings are highlighted in red. *p<0.05*

Interestingly, phenotypic inter-animal variation was observed in *fmr1* knockout mice. To further elucidate the role of FMRP in learning and memory processes, the knockout animals group was subdivided into two subgroups on the basis of their probe trial performance. For this, the weakest probe trial performance within the WT group was set as a threshold for classification of *fmr1* KO mice subgroups. Thus, the first group (*fmr1* KO) consisted of mice demonstrating wild-type-like behavior and therefore displayed a similar target quadrant preference (n=5). *fmr1* KO mice with a quadrant preference below the threshold were assigned to the second group named *fmr1** KO (n=8).

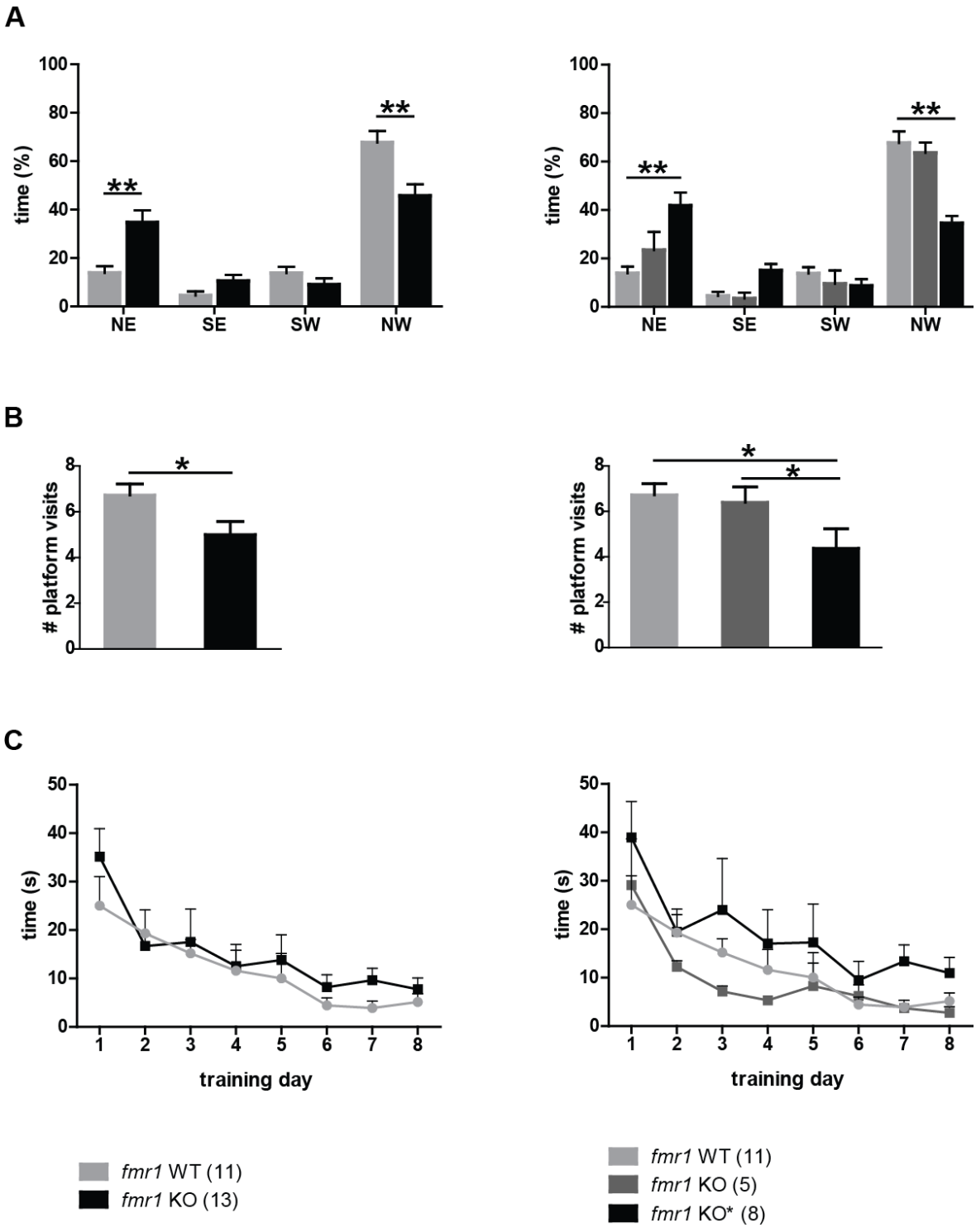

Figure 35 | Subgroup of *fmr1* knockout mice displays severe impairments in spatial learning

Testing group of fmr1 knockout animals was divided into two subgroups. ***(A)*** *Quadrant preference test revealed no difference in preference for the target quadrant between controls and the wild-type-like subgroup of fmr1 KO mice, whereas the fmr1* KO group showed no clear preference for the NW quadrant (right).* ***(B)*** *Number of platform crossings differs between both subgroups of fmr1 knockout mice (right).* ***(C)*** *Latencies of fmr1 KO subgroups exhibit different deviations from control.*

This group included *fmr1* knockout animals with an impaired learning behaviour indicated by a reduced target quadrant preference. Based on this classification, reference memory test resulted in a near-normal performance of the *fmr1* KO group (cp. **Figure 35 A**) with a highly significant preference for the target quadrant. In contrast to this, *fmr1** KO mice demonstrated no clear preference (~34.5% in *fmr1** KO compared to ~63.6% in *fmr1* KO and ~67.7% in *fmr1* WT). In accordance with this, subdivision yielded in a higher number of platform crossings in *fmr1* KO and simultaneously in reduced platform visits of *fmr1** KO (cp. **Figure 35 B**). Latency did not differ between KO and WT mice, regardless of the introduction of knockout subgroups. Surprisingly, latencies of WT lay in between both subgroups. While *fmr1** KO performed inferior to controls, the second KO group showed even better latency times. Thus, separation of *fmr1* knockout mice revealed an even stronger phenotype restricted to only a subpopulation of *fmr1* KO animals. These findings further help to understand the wide range of phenotypes previously described for *fmr1* KO animals ranging from close-to-control-performances to a strong impairment in memory formation and inaccuracy.

Taken together, these findings reveal despite previous controversial publications that significant differences in spatial memory formation exist between *fmr1* WT and KO mice. While *fmr1* KO exhibited a near-normal performance in the water maze during the acquisition phase concerning common measures as latency and distance travelled, they presented a decreased accuracy for the platform position after removal of the platform, indicating impaired precise memory retrieval. The reference test clearly illustrated that exact retrieval of learned information was impaired referring to accuracy after loss of FMRP, while *fmr1* knockouts revealed only minimal changes in their capability to learn the task in general.

3.7.2 *fmr1* KO mice use a lower percentage of hippocampus dependent searching strategies during the acquisition phase

Besides the common measurements to assess spatial memory formation in the water maze (global latency, global distance in the acquisition phase and time spent in the target quadrant as well as platform crossings during the probe trial), additional information can be gained by examining the different search strategies used by mice to locate the hidden platform throughout consecutive training days. Mice can use both allocentric and egocentric strategies to learn a spatial task such as the water maze. Analysis of swimming paths was based on the algorithm used in the publication by Garthe et al. 2009 and allowed the differentiation between highly hippocampus-dependent allocentric (*direct search, direct swimming* and *focal search*) and hippocampus-independent egocentric search strategies (*random search, scanning* and *chaining*; cp. **Figure 15**). According to annulus zone and swimming corridor, the prevailing strategies were assigned automatically by the parameter-based algorithm using time-tagged xy-coordinates. Search strategies were defined as described above (cp. **Figure 15 A**). At the beginning of the water maze training, the majority of mice used non-spatial search paradigms such as *random search* (covering the entire pool area) or *scanning* to find the platform (cp. **Figure 36 A**). *Scanning* depicts swimming behaviour that is restricted to the central area of the pool. *Chaining* describes the swimming within a circular path at a constant distance from the wall. Since in this case the animal has only learned the correct distance of the platform to the wall, this strategy was described previously as “least-effort-principle”.

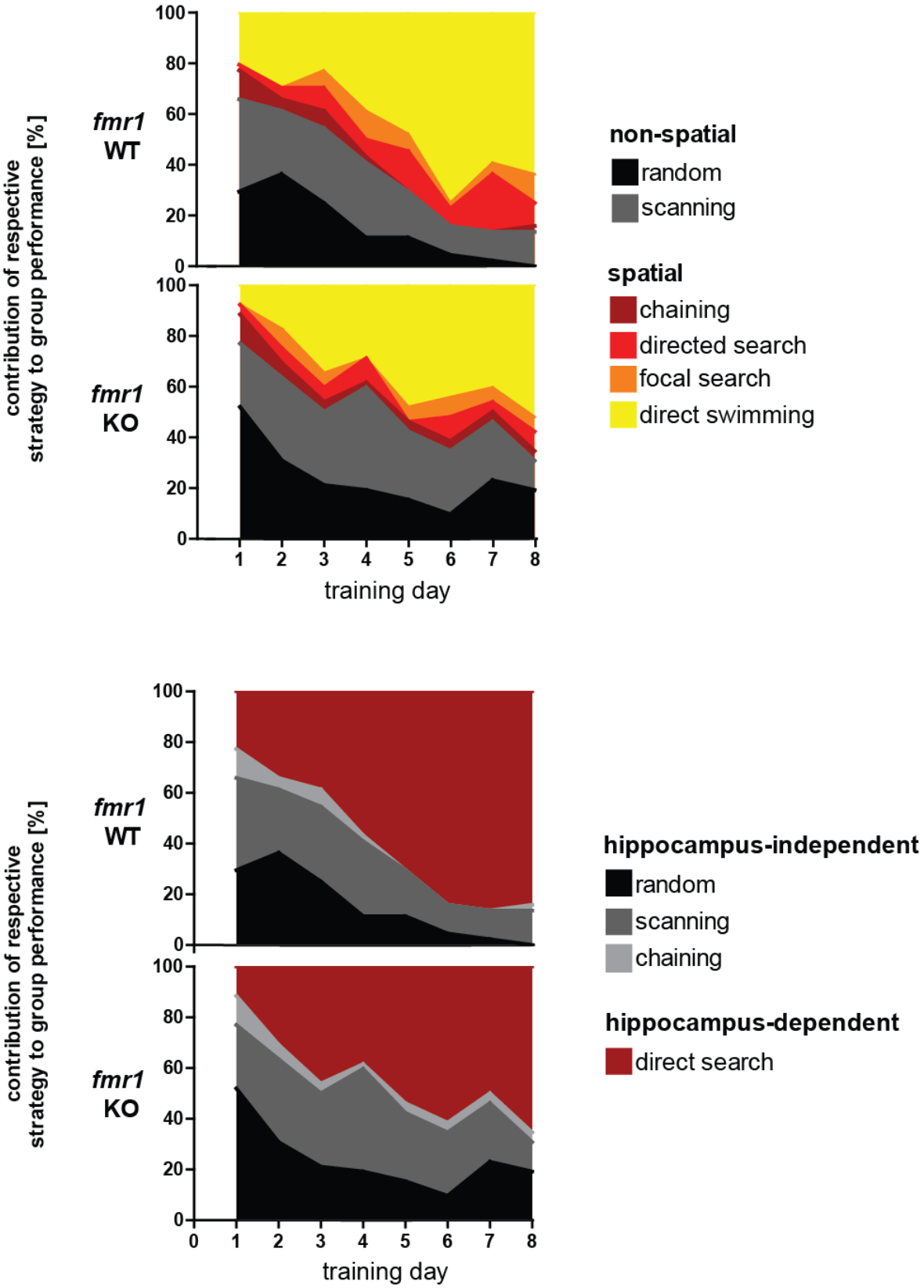

Figure 36 | Usage of various search strategies in *fmr1* WT and *fmr1* KO mice

(A) *Strategies are color-coded. Contribution of non-spatial (random and scanning) and spatial (direct swimming, chaining, directed search, focal search) strategies over training days.* ***(B)*** *Search strategies were categorized into hippocampus-independent (random, scanning and chaining) and hippocampus-dependent (direct search) strategies.*

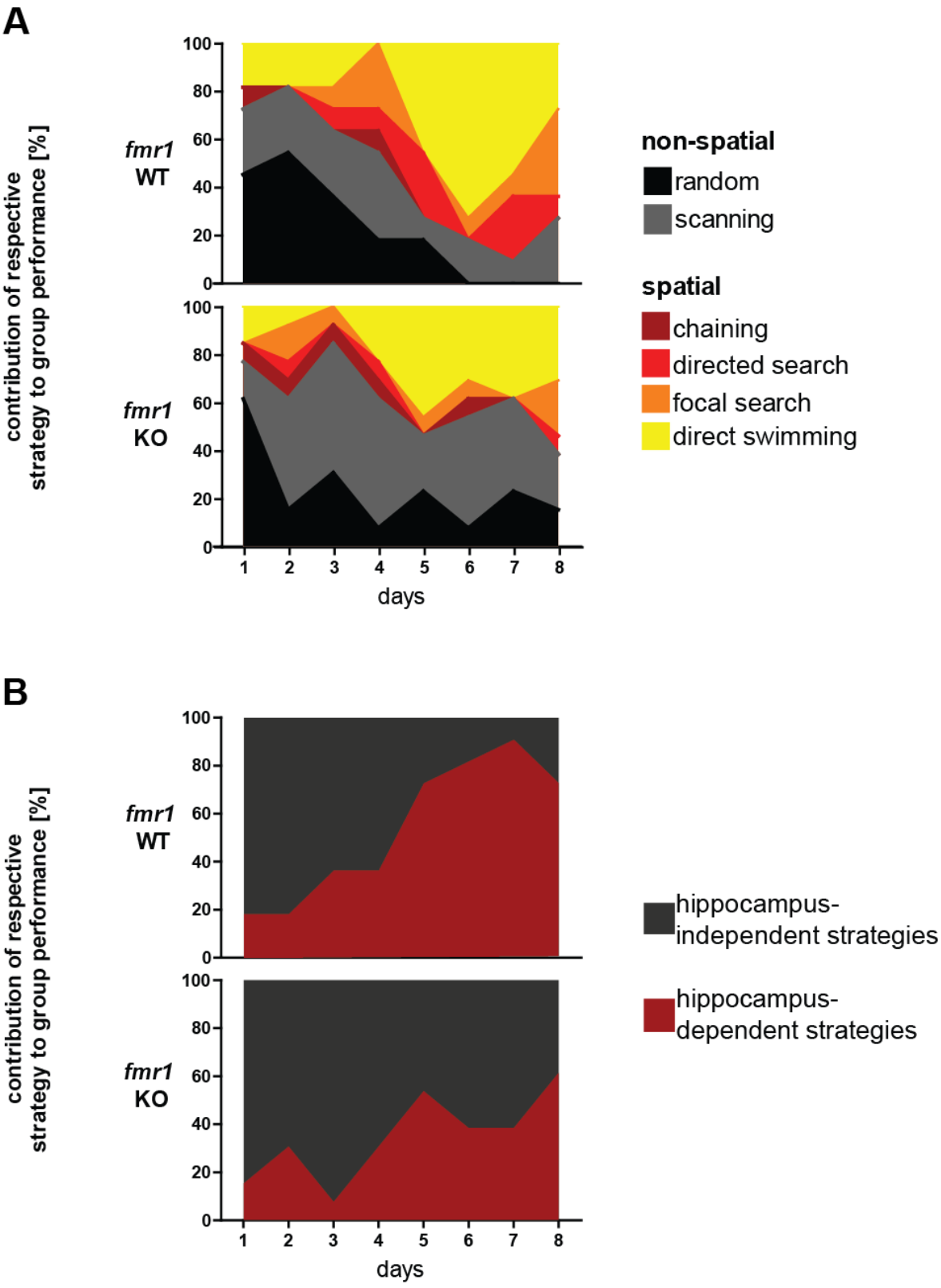

Figure 37 | First trial of training session reinforces differences between WT and *fmr1* KO

(A) *Solely the first trial of each training session was analyzed. Strategies were color-coded. Contribution of non-spatial (random and scanning) and spatial (direct swimming, chaining, directed search, focal search) strategies over training days.* ***(B)*** *Search strategies were categorized into hippocampus-independent (random, scanning and chaining) and hippocampus-dependent (directed search, direct swimming, focal search) strategies.*

Along with repeated trials in the water maze and also with time, egocentric route-based knowledge is gained and combined into an allocentric map, where distal cues provide geometric reference to the mouse's current location. A low allocentric contribution is characterized by a rough guess of the goal's position (e.g. *directed search*) and yields a direct, but not very precise learning strategy. Proceeding training results in growing precision and direct goal approaches from any feasible starting position (e.g. *focal search* and *direct swimming*), as egocentric route-knowledge is integrated more and more into an allocentric representation. While *focal search* points to a directional swim within the goal corridor followed by superimposed loops and turns there, *direct swimming* is even more straightforward including a swimming path with a narrow angle (cp. **Figure 15**).

Straight approaches highly rely on such a cognitive map and while contribution of allocentric knowledge increases, the hippocampus gets progressively involved. Further allocentric knowledge results in increased accuracy with which an animal can find the hidden platform directly (for a review see Garthe & Kempermann 2013). Analysis of learning strategies in *fmr1* WT mice and *fmr1* KO mice revealed a high percentage of random search and scanning in the first days of training (cp. **Figure 36 A**). In general, an efficient progression towards directed navigation aiming at the platform was found in both groups with increasing time, which underlines the fact of memory formation regarding the platform position (*fmr1* WT: random search $F_{(7,70)}$=7.009,p<0.0001; direct search $F_{(7,70)}$=19.29,p<0.0001; *fmr1* KO: random search $F_{(7,84)}$=3.997, p=0.0008; direct search $F_{(7,84)}$=7.443,p<0.0001). While wild-type mice showed a clear progression towards increase of hippocampus-dependent strategies such as *direct swimming* and therefore a fast decrease of the relative amount of random search, knockout animals could not progress as fast to more hippocampus-dependent strategies and thus depicted a higher relative amount of random search patterns even until the last day of training (appr. 20% of group performance). Hence, compared to controls respective strategies contributed differentially to group performance in *fmr1* KO mice. Interestingly, chaining contributed to an almost constant percentage to the overall strategies used on each training day in knockout mice. In contrast, wild-type mice showed fewer chaining trials, especially during later training sessions. In a second step of analysis, the searching strategies were combined by categorization into hippocampus-independent and hippocampus-dependent strategies. Both genotypes were found to rely more on hippocampus-dependent search

strategies with time (cp. **Figure 36 B**). In particular *fmr1* WT mice consistently relied almost entirely on allocentric search patterns with the highest spatial precision to find the hidden platform at the end of the training, thereby showing only few trials with hippocampus-independent strategies like *random, scanning or chaining*.

To directly examine whether WT and KO performances differed during daily trials, exclusively the first trial of each day was analyzed to focus on a 24 h interval (cp. **Figure 37)**. Interestingly, the observation that *fmr1* KO mice were not able to use efficient strategies to the same extent as WT was underlined by the presence of *random search* over the entire training session. In contrast to this, *random search* could not be observed in littermate controls at the last two days of training. However, random search decreased significantly until day 6 in WT ($F_{(7, 70)}$ = 3.675, p=0.0017) as well as in KO ($F_{(7, 84)}$ = 2.42, p=0.0251). Similar to this, scanning search was hardly decreasing over time in knockout animals and revealed a significant difference in the amount of scanning search between groups (genotype, $F_{(1,23)}$=1.583, p=0.0221). According to this, combined hippocampus-independent strategies were significantly more used in KO mice (genotype, day7, $F_{(1,23)}$=5.245, p=0.03) with a total contribution of 61.5% compared to wild-type mice with only 9.1% at day 7. Consequently, the relative proportion of spatial strategies was significantly lower in *fmr1* KO (cp. **Figure 37 B**). Thus, deficits of *fmr1* KO regarding competent use of efficient spatial strategies were further pronounced.

Detailed statistical analysis (ANOVA inter-subject test was used with a non-parametric post-hoc Mann-Whitney in days) of pooled hippocampus-dependent search strategies over training time revealed a significant difference between wild-type and knockout animals at day 6 ($F_{(1,23)}$=20.956, p=0.041) and day 7 ($F_{(1,23)}$=20.956, p=0.002; cp. **Figure 38 B**). No statistically significant differences could be found concerning random search and scanning search ($F_{(1,23)}$=1.583; p=0.221), although *fmr1* KO mice demonstrated a higher percentage of random search close to significance at the last day of training (~19.2% compared to 0%; $F_{(1,23)}$; p=0.055; cp. **Figure 38 A, C**). The time-lapse diagram denotes the delayed progression towards allocentric strategies in knockout mice (cp. **Figure 38 D**).

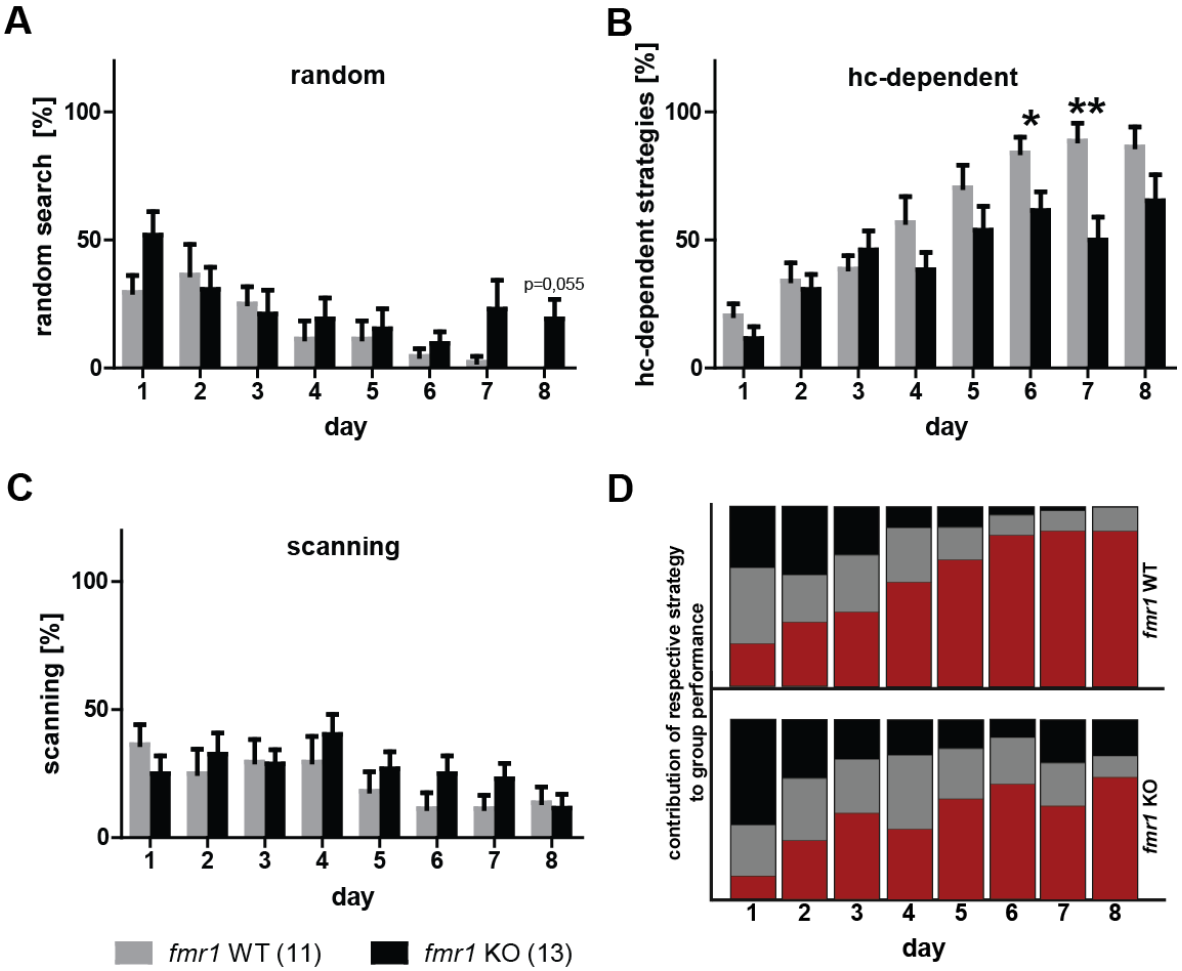

Figure 38 | Contribution of different search strategies over training time

(A) *Random swimming was more pronounced in fmr1 KO mice at the first day of training and close to significance (p=0.055) elevated at the last day of training, whereas it was totally absent in fmr1 WT mice.* ***(B)*** *Hippocampus-dependent search strategies were significantly decreased in fmr1 KO mice at day 6 and day 7 compared to wild-type.* ***(C)*** *Scanning search did not show significant differences between groups.* ***(D)*** *Development of strategy contribution over training session in fmr1 WT and fmr1 KO. Black color: random search; grey color: scanning; red color: direct search. *p<0.05; **p<0.01*

In summary, these results indicate that *fmr1* KO mice exhibit a general deficit in spatial learning and memory formation. Interestingly, differences in performances between *fmr1* KO and WT emerged particularly with respect to precise retrieval of consolidated spatial memory, which is stressed by an impairment in platform-relocalization in knockout animals during the reference memory test. Moreover, this was further strengthened by the fact that *fmr1* knockout mice were not able to use hippocampal-dependent strategies such as direct swimming, directed search or focal search during the acquisition phase to reach the platform to a comparable extent as their *fmr1* WT littermates. Instead, hippocampal-independent strategies which are less precise and consequently less efficient were observed to a higher extent in *fmr1* KO mice even until the end of training.

Since the hippocampal formation has a central role in allocentric, spatial learning and memory formation, this study investigated protein changes in the hippocampi of mice which underwent training in the water maze. Thereby, molecular mechanisms leading to disparities in competent usage of search strategies in KO animals might indeed be revealed by identifying key candidate molecules with altered expression levels in this brain region.

A series of proteins have been linked to spatial memory formation. By analyzing levels of proteins involved in activity-induced actin remodeling such as profilin1, profilin2a and cofilin in hippocampal tissue, changes in gene expression induced by learning could be determined (Ackermann and Matus, 2003; Fukazawa et al., 2003; Neuhoff et al., 2005).

3.7.3 Actin binding protein levels in the hippocampus & mPFC are dysregulated in *fmr1* KO mice

The actin cytoskeleton is believed to be crucial for both functional and activity dependent structural plasticity. Dynamic reorganization of the actin cytoskeleton is therefore most likely of significant importance for processes of learning and memory formation. Importantly, spatial learning can alter expression of genes encoding for proteins involved in activity-induced actin remodeling (Li et al., 2012). Actin regulators like profilin1, profilin2a and cofilin are known to be involved in the cellular processes underlying learning and memory formation and are regulated by activity-dependent neuronal plasticity (Ackermann and Matus, 2003; Fukazawa et al., 2003; Neuhoff et al., 2005). Thus, these three promising candidate proteins were analyzed following the learning paradigm in the MWM. In order to evaluate differences between *fmr1* wild type and *fmr1* KO littermates, relevant brain parts as the hippocampus and the medial prefrontal cortex (mPFC) were removed after the learning task and expression levels of the respective proteins were further studied in detail via western blot.

Immunoblotting verified alterations in protein contents of hippocampus and mPFC between genotypes as well as between the following three groups: firstly, an untrained group of *fmr1* WT and *fmr1* KO mice was used with animals which remained in their home cage, therefore also referred to as “home-cage controls”. Secondly, the yoked control group consisted of *fmr1* WT and *fmr1* KO mice spending the same time in the water maze freely-swimming, but without training (no platform). The purpose of this additional control group was to test for increased protein expression mediated solely by the physical activity in the MWM procedure and the new environment itself. According to this, several studies could show that physical activity up-regulate the transcription of BDNF mRNA in several brain areas of rats (Neeper et al., 1996; Russo-Neustadt et al., 2000) and interestingly, peripheral BDNF concentrations were elevated significantly in response to acute aerobic exercise in humans (reviewed in Huang et al. 2014). Lastly, the learning group of *fmr1* WT and *fmr1* KO mice underwent training in the water maze for 8 days with a hidden platform as described above.

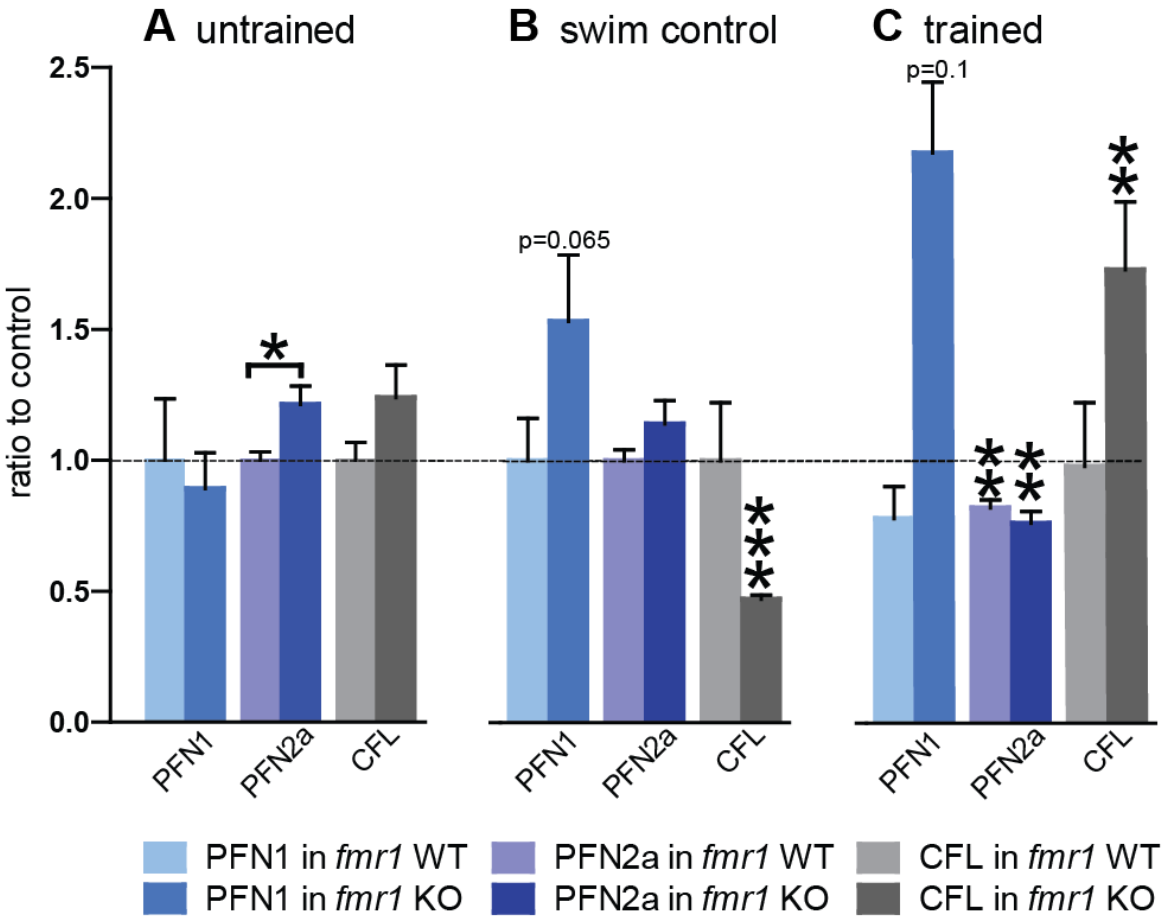

Figure 39 | Hippocampal protein levels of PFN1, PFN2a and CFL differed between *fmr1* WT and *fmr1* KO mice

***(A)** Untrained control mice exhibited a significant alteration in PFN2a amount, as protein level was increased in fmr1 KO by approx. 21%. Significance was tested between genotypes. **(B)** PFN1 level in fmr1 KO swim controls was elevated close to significance (p=0.065). Moreover, swim controls showed a significantly decreased CFL level in case of fmr1 KO by roughly the half. **(C)** Among trained mice the most prominent effects were present, as both CFL amounts were significantly elevated in knockout mice compared to control littermates. PFN2a quantities were significantly lowered in fmr1 WT and KO. Amount of PFN1 was elevated close to statistical significance (p=0.1). Protein levels were normalized to loading control (GAPDH); PFN1 amount: light and dark blue color; PFN2a amount: light and dark violet color; CFL amount: light and dark grey color; statistical analysis of immunoblots was performed with mean, standard deviation and P value from student T test. Unless otherwise indicated the significances were always tested against the swim control *p<0.05, **p<0.01, ***p<0.001*

Protein amounts of hippocampal samples in untrained mice were similar between wild-type and knockout animals regarding PFN1 and CFL, whereas PFN2a expression was significantly elevated by 21.3 ± 7% (cp. **Figure 39 A**) in *fmr1* KO mice. Swim controls, described above as yoked controls, displayed a reduction of cofilin amount in the knockout group (47.1% ± 1.5%) in contrast to control mice with an unaltered cofilin expression level of 100% ± 22.2%. Opposing this, the profilin1 content was higher in *fmr1*

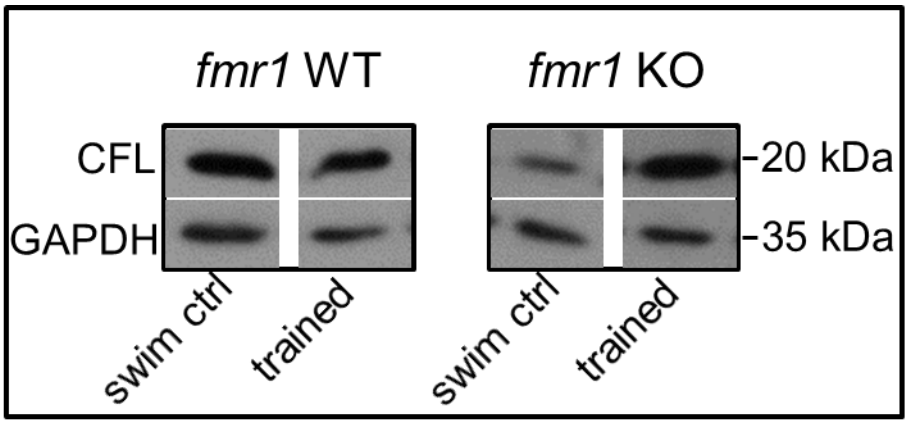

Figure 40 | Cofilin contents in *fmr1* WT and *fmr1* KO hippocampi are regulated differentially.

Representative immunoblots demonstrated unaltered CFL levels of both fmr1 WT swim controls and trained mice (left). In contrast to this, fmr1 KO mice showed a decreased CFL level of swim controls, while CFL was increased in trained mice (right).

KO by trend (100% ± 16% for WT compared to 153% ± 25%). Taken together, protein levels of *fmr1* KO were affected during free-swimming alone, but with entirely different directions. Thus, misregulation of protein expression levels in the KO was already apparent in the home cage situation and appeared to be even more pronounced by physical activity albeit affecting different molecules (profilins versus cofilin). The group of WT yoked controls remained completely unaffected by swimming activity as no changes in PFN1, PFN2a or CFL expression emerged. Remarkably, within the group of learners, protein levels of all three actin-binding proteins were regulated differentially in *fmr1* knockout animals compared to WT control mice. In particular, the hippocampal PFN1 content of knockouts was found to be elevated in comparison to *fmr1* WT, which showed a decreased PFN1 amount upon training in the MWM (78.1% ± 12.3% for *fmr1* WT compared to 218% ± 27.1% for *fmr1* KO). Interestingly, PFN2a level exhibited the same tendency in WT and KO mice, as spatial learning induced in both cases a significant decrease of PFN2a protein amount, which was more pronounced in KO (100% ± 4.3% for *fmr1* WT swim control cp. to 82.3% ± 3.1% for *fmr1* WT trained, p=0.0055; 114% ± 8.9% for *fmr1* KO swim control cp. to 76.4% ± 4.5% for *fmr1* KO trained, p=0.0016).

In comparison to swim controls, trained *fmr1* KO exhibited highly significantly elevated CFL protein level (47.2% ± 1.6% for *fmr1* KO swim control cp. to 173.2% ± 26% for *fmr1* KO trained; p=0.0013; cp. **Figure 40**). These findings are in agreement with a recent study

demonstrating reduced hippocampal PFN2a level upon spatial learning in various mice strains (Li et al., 2012).

Thus, these results emphasized the importance of matched control conditions, since the physical activity induced by free-swimming affects protein level in dependence on the genotype as displayed by altered PFN1 and CFL levels exclusively in the knockout animals.

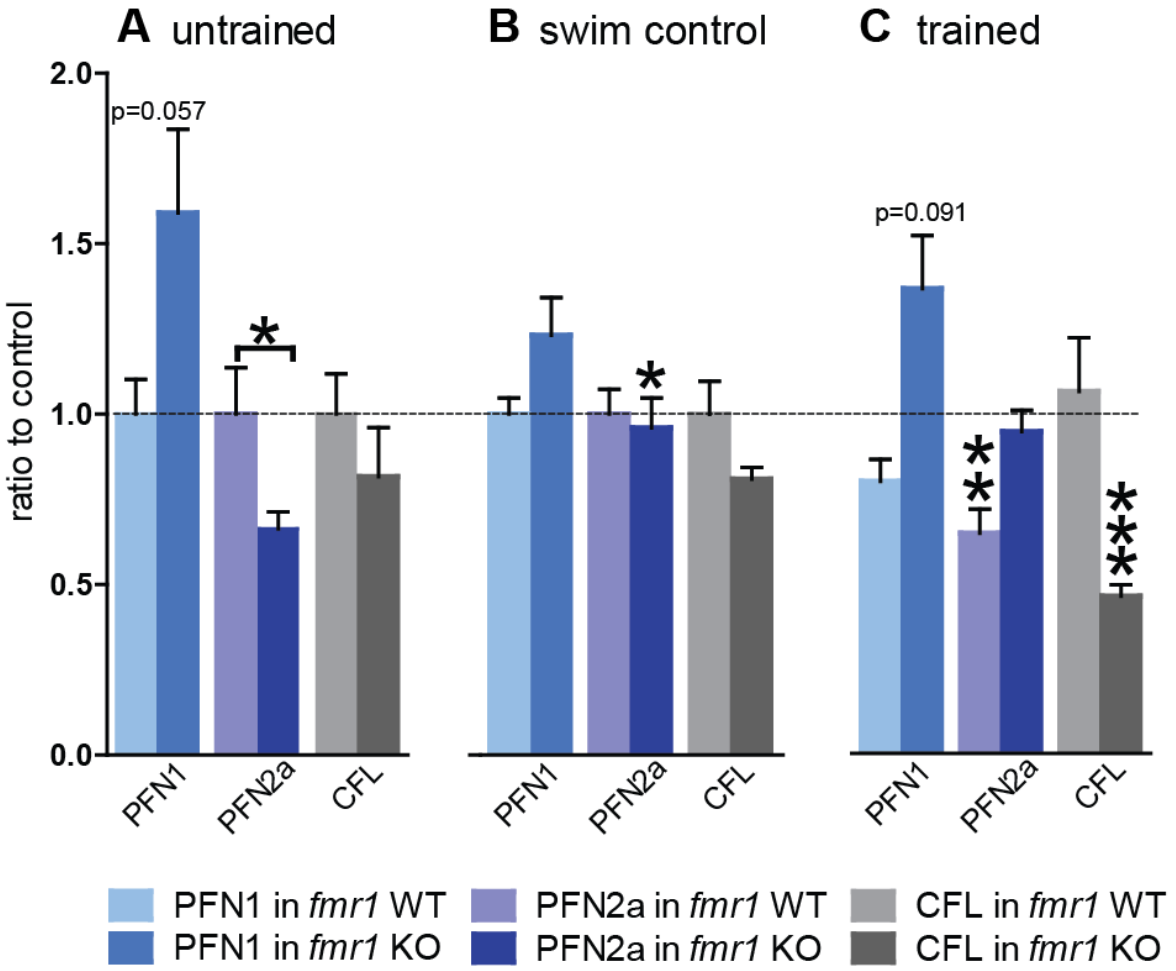

Figure 41 | Cortical (mPFC) protein levels of PFN1, PFN2a and CFL differed between *fmr1* WT and *fmr1* KO mice

***(A)** Untrained control mice showed alterations in protein amounts as PFN1 level was increased in KO mice close to significance. In return, PFN2a level was significantly decreased in fmr1 KO by approx. 35%. Significance was tested between genotypes. **(B)** Swim controls exhibited a significantly decreased CFL level in case of fmr1 KO. **(C)** Among trained mice the most prominent effects were present, as protein amounts of both PFN were reduced in WT mice compared to swim controls. PFN1 level was reduced close to statistical significance while PFN2a quantity was highly significantly lowered in fmr1 WT. In trained mice CFL amount was highly significantly reduced in knockout mice compared to swim controls by approx. 50%). Protein levels were normalized to loading control (GAPDH). Color code cp. **Figure 39**; statistical analysis of immunoblots was performed with mean, standard deviation and P value from student T test between. Unless otherwise indicated the significances were always tested against the swim control. *p<0.05, **p<0.01*

It is important to note that a comparison of trained mice only to cage-controls would lead to a false interpretation of learning induced changes in protein amount.

The medial prefrontal cortex is commonly defined as the cortical area which receives diverse excitatory input from the midline thalamus, contralateral mPFC, basolateral amygdala as well as ventral hippocampus (de Bruin et al., 1994, 1997). In contrast, the mPFC projects back on the hippocampus in an indirect manner via the entorhinal cortex as well as the *nucleus reuniens* of the midline thalamus (Vertes, 2004). Consisting with its purported role in executive functions including strategy switching or behavioral flexibility, accumulating evidence indicates that similar to the hippocampus, the mPFC is involved in both spatial information processing and strategy selection (Shaw et al., 2013).

Given that, it was directly examined whether amounts of proteins believed to be engaged in plasticity processes and memory varied between genotypes in this brain region or were influenced by spatial learning and physical exercise.

In contrast to changes in the hippocampus of untrained *fmr1* KO mice, analysis of mPFCs revealed PFN1 levels being elevated close to significance by approx. 59% ± 25.6% (p=0.0573; cp. **Figure 41 A**) compared to WT animals.

In addition to that, cage-control knockouts showed a significant decrease concerning PFN2a level down to 66.4% ± 11.1% while cofilin levels were comparable between both groups (cp. **Figure 42 A**). Remarkably, levels of the proteins of interest in *fmr1* WT were not affected at all by free-swimming (approx. 100% for PFN1, PFN2a and CFL). Interestingly, protein levels of the swim control group displayed the same trends as they were observed in hippocampal tissue. Indistinguishable from the results obtained from hippocampal tissue, increase in PFN1 could be also observed in the mPFC of *fmr1* KO (cp. **Figure 41 B**).

Moreover, biochemical analysis of mPFC from mice who learned the task bore resemblance with the hippocampal protein contents in case of PFN1. While control mice had lower PFN1 levels (approx. 79% ± 6.4%), knockouts demonstrated the opposing effect with an elevation of PFN1 expression level (136% ± 15.5%; cp. **Figure 41 C**). Similar to the results gained from hippocampal preparations, PFN2a protein amounts were decreased both in *fmr1* WT (64.6% ± 18.76%) and in KO mice (94.46% ± 17.6%), with a significant difference between trained *fmr1* WT and swim controls (p=0.0068). Strikingly, cofilin

protein expression was changed differentially in the mPFC of knockout mice as it was highly significantly lowered by appr. 54% (46.15% ± 9.4%; $p<0.0001$).

These results suggest that learning and physical activity have distinct effects on gene expression both in the hippocampus and mPFC of mice. Analyzed actin-binding proteins (ABPs) were differentially expressed between the untrained, swimming and spatial learning animal groups in knockout mice. Free-swimming itself did not alter investigated protein levels in the WT, but indeed affected the knockouts. Interestingly, analysis of swim controls revealed that physical activity and the new environment led to differentially regulated protein levels in WT and KO animals. Upon training, alterations in protein levels were even more pronounced and differed between certain brain regions. Differential regulation of these proteins, which are known to be involved in synaptic plasticity, may influence memory formation by affecting morphological adaption of neurons or the establishment and maintenance of synaptic connections during learning processes. The data presented here revealed a dysregulation of relevant protein quantities in *fmr1* KO mice in the hippocampus and mPFC, which was already present in the naïve animal and further pronounced during free swimming and the spatial memory formation. Thus, molecular dysfunctions were consistent with behavioral deficits shown in *fmr1* KO mice.

Identified as global factors for spatial memory training, it was further analyzed whether these cytoskeletal proteins were translocated to the nucleus of neurons upon water maze training to address the relationship between hippocampus-dependent memory and protein distribution.

3.7.4 Profilin and cofilin content in hippocampal nuclei of *fmr1* KO mice after MWM

Despite the widely held belief that learning and memory processes are linked to gene transcription, surprisingly little is known concerning the activity-dependent signaling from the cytoplasm to the nucleus. Both profilin isoforms are localized in the soma and within the nucleus of neurons at basal conditions. Interestingly, the functional relevance of the nuclear presence of profilin isoforms remains unclear so far. Recent studies revealed that PFN1 and PFN2a respond differentially to changes in neuronal activity induced by

application of BDNF or stimulation of NMDA receptors and can translocate in a fast and reversible fashion (Birbach et al., 2006; Murk et al., 2012). Thus, activity-dependent accumulation of profilins or cofilin in the nucleus could play an important role in memory formation events.

To investigate if relevant proteins were translocated from cytoplasm to nuclei upon memory formation, nuclear and cytoplasmic fractions of hippocampi of *fmr1* KO and WT mice were extracted as described above (see **2.11.3**). Both profilin isoforms and cofilin quantities were compared between genotypes as well as in trained versus corresponding swimming control mice.

Due to experimental conditions and too little sample size, only results for cytoplasmic fractions of *fmr1* KO swim controls and *fmr1* trained mice are presented here. Upon spatial learning in the water maze, amount of cytosolic CFL was increased in comparison to swim controls. This points to an activity-targeted mechanism of protein transport during memory formation and consolidation.

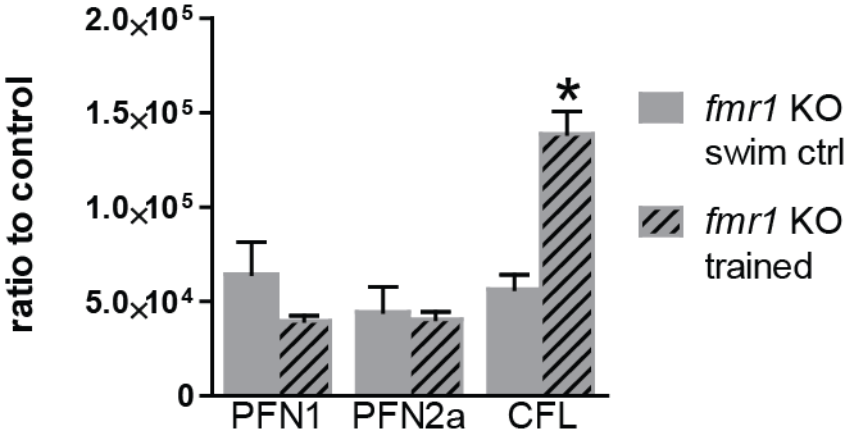

Figure 42 | CFL is enriched in the cytoplasm upon training in the *fmr1* KO.

*Cytoplasmic fractions of fmr1 KO swim controls compared to trained fmr1 KO mice. Hippocampal protein levels of relevant actin-regulators such as PFN1, PFN2a and CFL were analyzed. In trained fmr1 KO mice CFL protein levels were significantly elevated in comparison to swim controls (p=0.0278).*p<0.05*

4 DISCUSSION

The presented data provide new insights into the isoform-specific functions of the two profilins expressed in the mammalian brain. Dendritic architecture of neurons was found to be affected differentially by acute knockdown of PFN1 in comparison to previous data derived from our group concerning the acute knockdown of PFN2a. Thus, recent results emphasize isoform-specific functions of both PFN1 and PFN2a in modulating dendritic as well as spine structure in an age- and subregion-dependent manner. The idea that cellular functions of profilins can be either isoform specific or at least partially overlapping was further supported by the fact that spine numbers were found to be reduced in the absence of PFN1. Indeed, PFN2a knockdown led to a similar reduction of spine number (Michaelsen, 2009). In contrast, comparison of live imaging data obtained in this thesis using the PFN1 KD to previous PFN2a KD data (Remus, 2012) point to a subsidiary role of PFN1 isoform in regulating the motility as well as activity-dependent structural modifications of dendritic spines. In line with that dendritic architecture was also affected differentially by KD of either of both isoforms, which provides further support for the hypothesis that PFN isoforms fulfill specific functions.

Furthermore, I could demonstrate that levels of the important actin regulators PFN1 and cofilin were dysregulated in the brain of *fmr1* KO mice following spatial learning. This also accords with impairments in spatial learning of *fmr1* KO mice revealed by *in vivo* data obtained from the training in the Morris water maze. In cell culture, FMRP deficient neurons of the hippocampus and cortex did not show alterations in spine number, but exhibited alterations in spine morphology as the proportion of the immature spine types was increased. This phenotype was rescued by exogenous expression of both profilin isoforms. Taken together, these results suggest that indeed PFN isoforms play an important role for spine morphology and spine plasticity in health and disease as demonstrated by the mouse model for fragile X syndrome.

4.1 Profilin1-specific functions in neuronal structure

In the mammalian brain, two different isoforms of the actin-regulating protein profilin are expressed. Despite their described role in regulating actin dynamics, the cell-specific role of both profilin isoforms remains largely elusive. Recently, the *in vivo* role in synaptic physiology of PFN2a was addressed by using a PFN2a knockout mouse (Pilo Boyl et al., 2007). While PFN2a was shown to be involved in regulating the presynaptic function of glutamatergic neurons by controlling vesicle exocytosis and presynaptic excitability, dendritic spine morphology and synaptic plasticity in these neurons were described to be unaltered in the conventional knockout mouse (Pilo Boyl et al., 2007). Conventional PFN1 knockout mice are not viable and die at early embryonic stages. Consequently, the impact of PFN1 loss on neuronal morphology in the postnatal brain was difficult to study (Witke et al., 2001).

Profilin1 plays a minor role for dendritic architecture

In order to circumvent embryonic lethality and investigate the contribution of PFN1 to synaptic function, the lab of M. Rust created conditional knockout (cKO) mice through Cre-recombinase under a CamKII promoter (Görlich et al., 2012). Strikingly, the morphology and function of excitatory synapses were preserved in these PFN1 cKO mice. Morphological analysis of hippocampal CA1 *stratum radiatum* neurons revealed normal synapse density, spine morphology, and synapse ultrastructure (Görlich et al., 2012). Additionally, electrophysiological recordings showed that basal synaptic transmission, presynaptic physiology and postsynaptic plasticity were not affected by depletion of PFN1 (Görlich et al., 2012). The absence of a phenotype in these PFN1 cKO mice may be due to the fact that loss of PFN1 is compensated by PFN2a in postsynaptic structures indicating that the mouse model would have some limitations. On these grounds, the importance to perform an acute knockdown of PFN1 was emphasized to analyze if PFN1 is indispensable for actin regulation in postsynaptic structures or activity-dependent morphological changes of dendritic spines in synaptic plasticity processes.

Interestingly, also the conventional PFN2a KO mouse model was described to show no postsynaptic phenotype, as both dendritic spine morphology and synaptic plasticity were preserved in these mice. Instead, a major role for PFN2a in proper presynaptic functioning was demonstrated, as PFN2a-deficient mice exhibited enhanced presynaptic

excitability and neurotransmitter release of glutamatergic synapses (Pilo Boyl et al., 2007). Importantly, in contrast to the KO mouse model, previous studies in our group using an acute shRNA mediated PFN2a knockdown could indeed reveal that PFN2a has a pivotal role for dendritic architecture as well as spine structure, as PFN2a depleted neurons upon RNAi showed a reduced dendritic complexity and a reduced spine density for the mid-apical and basal dendritic compartment (Michaelsen, 2009; Michaelsen et al., 2010). Thus, the work of this thesis was concerned with the issue of whether PFN1 is relevant for modulating neuronal morphology or indispensable for neuronal structure and activity-dependent synaptic plasticity. To address this question, a comprehensive analysis of dendritic morphology taking advantage of an acute vector-based RNAi approach was performed.

In brief, results obtained from organotypic slice cultures revealed only mild effects on dendritic outgrowth and maintenance of neuronal structure in developing as well as in mature neurons. This indicates that reduced amounts of PFN1 protein in neurons do not dramatically alter neuronal morphology, which is in accordance with our previous results demonstrating that PFN1 cannot compensate for the reduction in dendritic complexity upon PFN2a KD (Michaelsen et al., 2010). However, it is reasonable to imagine that the action of PFN1 might depend on neuronal age. PFN1 could act as a positive regulator of dendritic stability at premature stages as the dendritic phenotype was more pronounced in dissociated neurons at earlier stages of development. This may suggest PFN1 as especially important in immature neurons.

Similar to data derived from experiments with OHC, the dendritic structure of dissociated neurons also was in general only mildly affected by PFN1 depletion pointing again to PFN2a as the more important PFN isoform for maintenance of dendritic structures. The study was limited by the lack of information on the specific hippocampal cell type, thus it is likely that in dissociated neurons either CA1 or CA3 cells are affected by PFN1 knockdown while the other cell type is not. Indeed, as shown in this thesis the impact of PFN1 on the morphology of the actin cytoskeleton seems to depend on the cell type or developmental age investigated. It remains to be elucidated if also PFN2a shows an age- and region-dependent effect like this is the case for PFN1. If PFN2a is the main determinant of dendritic architecture, only a mild effect of PFN1 depletion on retraction

or outgrowth of dendrites would be consequential. The results of this study suggest that the role PFN1 might be different during distinct developmental stages, but obviously plays a subsidiary role for maintenance of the dendritic tree in comparison to PFN2a at least in CA1 pyramidal cells at DIV14.

Profilin1 affects spine shape and number in a developmental and region-dependent manner

It is generally accepted that different aspects of synaptic morphology such as the shape of the spine or the endocytosis and exocytosis of postsynaptic receptors may be related to the strength of excitatory synapses and heavily depend on remodeling of the actin cytoskeleton by important regulators such as profilins (Schikorski and Stevens, 1997; Matsuzaki et al., 2001; Michaelsen et al., 2010). Interestingly, acute knockdown of PFN1 has a much stronger impact on spine density and spine shape than on dendrite arborization and dendritic outgrowth, suggesting PFN1 is an important regulator of spine morphogenesis and maintenance of a proper spine number. These findings are in line with published data showing that PFN1, but not PFN2a, can compensate for the $p75^{NTR}$ (p75 neurotrophin receptor) dependent loss of spines in primary hippocampal neurons whereas the dendritic phenotype cannot be compensated by PFN1 (Michaelsen et al., 2010). Besides overlapping functions, accumulating evidence is further supported by this thesis suggesting indeed that each PFN isoform performs particular tasks at the postsynaptic compartment.

Since PFN1 is undoubtedly localized in dendritic spines especially upon activity induction, the clarification of its precise cellular function is crucial for the general understanding of actin organization in the dendritic spine (Neuhoff et al., 2005; Lamprecht et al., 2006; Murk et al., 2012). Recent analysis of Golgi-stained hippocampal pyramidal cells and electron micrographs from the CA1 *stratum radiatum* revealed normal spine morphology in the conditional knockout PFN1 mouse (Görlich et al., 2012). In contrast, the acute knockdown of PFN1 I used in this study led to a globally reduced spine density independent of the developmental age and subregion of the hippocampus, as CA1, CA3 and DG cells were affected to the same extent. Thus, it might be indeed the case that due to the acute approach no compensatory mechanisms occurred, which is likely to be the

case for the cKO mouse model. The absence of any phenotype in the cKO might be explained by the fact that other actin-binding proteins compensate for the lack of PFN1 – the most likely candidate being PFN2a. Interestingly, shPFN2a-expressing CA1 hippocampal neurons showed a significantly decreased spine density not throughout the entire dendritic tree, but restricted to the proximal part, which could be rescued via exogenous expression by PFN1 suggesting that both isoforms can complement one another in spine structures (Michaelsen et al., 2010). The lower spine density observed in the PFN1 or PFN2a depleted neurons could be explained by two different processes: Profilins might be involved either in regulating the formation of new dendritic spines or in controlling their maintenance. Time-lapse imaging of PFN2a-deficient CA1 neurons displayed that increase of spine number over time was delayed compared to control neurons between DIV12 and DIV16 (Remus, 2012). The available evidence suggests a role for PFN2a in promoting the formation of new spines. As data provided by this study was based on fixed tissue, future research should therefore concentrate on live imaging experiments to assess the impact of an acute knockdown of PFN1 on spine formation. More research is required to determine if PFN1 KD results in a retraction of pre-existing spines, thereby leading to synaptic loss, or hinders the emergence of spines during development.

In the current study, however, spine number was influenced in hippocampal subregions CA1 and CA3 equally by PFN1 KD, regardless from the developmental age. In contrast, spine morphology was affected differentially in CA1 versus CA3, as a decreased number of mature mushroom spines was exclusively found in CA3 neurons. A possible explanation for neuronal subtypes being differently affected by the loss of PFN1 could be resulting from altered expression of profilins throughout the hippocampal subregions (cp. **Figure 20**). The data yielded by this study suggest that the protein amount of PFN2a is higher in CA3 neurons than the protein amount of PFN1. PFN amounts were similar in CA1 cells. The issue that cell types were not affected comparably could be further explained by different activity patterns of profilin isoforms caused by various phosphorylation states. Moreover, a plethora of polyproline stretch proteins is known to interact with both PFN isoforms, but with differences in binding affinity (e.g. SMN, Mena/Vasp) (Witke et al., 1998). In addition to that, isoform-specific differences in the interaction between PFN and

the formins mDia1 and mDia2, important actin regulators, were demonstrated (Michaelsen et al., 2010). Thus, differences between PFN1 and PFN2a regarding interaction partners may explain the diverse impacts of altered PFN levels on spine structure in different cell types. Future experiments determining the expression and localization patterns of these proteins might help to further understand profilin isoform specificity.

It is important to note that data obtained from Witke and Rust were obtained *in vivo* whereas the acute knockdown of PFN1 here was performed in the slice culture system and led to a reduction in PFN1 protein by 70%.

PFN1 effects on spine motility depend on the hippocampal cell type and subcellular compartments

Traditionally assumed as relative stable structures, research of the last decades has nicely demonstrated that dendritic spines are motile structures which undergo rapid morphological changes (seconds to minutes) both *in vitro* and *in vivo* (for a review see Bonhoeffer and Yuste, 2002). The high abundance of actin filaments in the spine confirmed by ultrastructural studies represents a specialized cytoskeleton of dynamic actin filaments capable of evoking fast changes in spine morphology. Thus, spine motility might result in parts from the rapid motility of the actin cytoskeleton inside spines (Fifková and Delay, 1982; Matus et al., 1982; Halpain, 2000; Matus, 2000). Importantly, inhibition of actin polymerization via latrunculin as well as volatile anesthetics led to reduced mobility of spines, suggesting that rapid motility might play a crucial role in brain function (Kaech et al., 1999; Korkotian and Segal, 2001). Early in development, spines show a highly dynamic behaviour, which is thought to facilitate the formation of synaptic connections and is most likely the basis for synaptogenesis (for a review see Bonhoeffer & Yuste 2002). Besides the highly motile dendritic filopodia, which might serve a fundamental role in the development of neuronal circuits, the question of whether similar motility can also take place in spines from mature tissue has led to further research. Indeed, dynamic movements of spines can also occur in the adult nervous system, however, with the physiological role of such movements remaining unclear so far. It is important to note that the term “motility” includes different types of morphological changes independent of random Brownian movement, more precisely various

phenomena with different mechanisms and functions (Yuste, 2010). One phenomenon called 'twitching' indicates fast contractions of spines after an action potential, lasting from a few hundreds of a millisecond up to 2 s before the spine relaxes to its original shape (Korkotian and Segal, 2001). Under resting conditions in hippocampal cultures, mature spines continuously undergo morphological changes referred to as 'dancing' or 'morphing', which is different to the protrusive motility of immature dendritic structures (Fischer et al., 1998; Dunaevsky et al., 1999). The elongation of a protrusion and the wiggling/morphing of a spine head has been shown to be regulated by Rac1 and ROCK, as the Rho family does not only affect spine morphogenesis, but also spine motility and stability (Tada and Sheng, 2006). In line with this, Rac1 inhibition decreased spine motility whereas on the other hand blockade of RhoA induced enhanced motility (Tashiro and Yuste, 2004). These data demonstrated that Rac1 and the RhoA/Rho kinase signaling pathways regulate different aspects of spine motility such as head morphing and protrusive motility, stability and maybe also different aspects of synaptic functions. Despite the assumption that changes in spine morphology might mediate synaptic plasticity, the extent of basal spine motility and its regulation and function is not well understood.

However, spine motility is a phenomenon mediated by an actin based cascade and is influenced in an activity-dependent way by synaptic transmission and calcium influx through glutamate receptors (AMPAR and NMDAR), by the Rho family of GTPases, neurotransmitters as well as other molecules such as cadherins, ephrins, neurotrophins, actin-related molecules or PSD proteins (Takeichi, 1990; Luo, 2000; Matus, 2000; Ethell et al., 2001; Hering and Sheng, 2001; Tashiro & Yuste, 2004; for a review see Bonhoeffer and Yuste, 2002). Continued spine motility may serve the purpose to set up and maintain synaptic connections and therefore enables efficient neuronal connectivity, but it remains unclear if spine motility is maybe only the consequence of the dynamic nature of the actin networks. So why is it necessary to constantly spend energy in these structural fluctuations of spines? Volume changes of the spine head modulate synaptic strength, as they directly affect the amplitude and duration of calcium transients (Oertner and Matus, 2005). Thus, spine head dynamics might depict steady-state oscillations of potentiation and depotentiation with possible functional changes of spines (Majewska et al., 2000). Equally important, spine neck geometry is an important determinant of synaptic strength.

The rate of diffusion between the spine and the dendrite depends on the neck length, thereby elongation or retraction of the spine neck during spine motility alters the diffusional coupling between the spine and the dendrite (Majewska et al., 2000). Consequently, the calcium decay kinetics in spines are changed when the spine neck geometry is altered and hence the dendritic excitation is changed (Majewska et al., 2000). Thus, longer necks act as a greater barrier to intercompartmental diffusion. In addition, Richards et al. could elegantly confirm that diffusion is slower in motile spines than in stationary spines (Richards et al., 2004).

The data gathered in this study refer to basal (absence of stimulation) spine motility which was represented by detectable changes in spine shape (spine head diameter and spine length) that occurred between individual image stacks taken with 5 min intervals to determine the extent of these morphological changes. In the present study, spine motility was found to be differently affected between CA1 and CA3 cells upon PFN1 KD. Strikingly, while acute PFN1 KD resulted in a reduced spine motility of apical CA1 neurons, CA3 cells displayed the contrary as spine motility was elevated compared to control cells. Current research in our lab provides evidence for a different rate of actin polymerization in CA1 and CA3 cells, as actin polymerized faster in spines of CA1 cells than in spines of CA3 neurons. These results might explain the bidirectional effects of PFN1 KD in both hippocampal cell types (Michaelsen-Preusse, personal communication). As aforementioned, CA1 cells with a reduced level of PFN1 displayed decreased spine motility restricted to the apical compartment. Interestingly, this is contrary to a previous study regarding PFN2a deficient CA1 cells, which exhibited enhanced dynamics in spine length and spine head (Remus, 2012). Importantly, the increase in spine motility due to a lack of PFN2a could not be compensated by expression of PFN1, suggesting that a proper level of PFN2a is important to stabilize resting dendritic spines in their motility. These data could be explained by the fact that PFN2a is the major isoform in basal dendrites of CA1 neurons, as demonstrated in this study. On these grounds, I would argue that both PFN isoforms play a pivotal role in dendritic spines, but seem to perform distinct functions concerning the tight spatial and temporal regulation of actin polymerization. Indeed, recent FRAP experiments performed in our lab revealed that actin dynamics were drastically slowed down in PFN1 KD cells, whereas actin dynamics were even increased by tendency in PFN2a deficient CA3 neurons indicating faster polymerization (Michaelsen-

Preusse, personal communication). In line with that, FRAP analyses of dissociated astrocytes revealed that solely PFN1 KD and not PFN2a KD impaired actin dynamics in astrocytic processes (Schweinhuber, 2014). These findings lend support to the claim that spines are more stable in PFN1 KD and less stable in PFN2a deficient cells, as the spine phenotype of the respective PFN isoform appeared to be correlated to changes in the actin polymerization rate.

Motility of spine from the basal compartments of CA1/CA3 neurons as well as granule cells were not affected at all, implying that absence of PFN1 is likely to be compensated by PFN2a in particular cell types of the hippocampus or even specific dendritic compartments. Another implication of this finding is that PFN1 is generally of minor importance in those compartments. However, apical spines of CA3 were significantly enhanced in both length and head motility. This increased motility of CA3 neurons lacking PFN1 suggested that spines were less stable upon knockdown. Although so far no data has been gathered on the effect of an acute PFN2a knockdown in the CA3 region, it is tempting to speculate that alterations between different hippocampal subregions can be addressed to altered gene expression of both PFN isoforms as reported in this study. Future experiments are required to explore the various interaction partners of profilins to decipher how both PFN isoforms are regulated differentially in a tight spatiotemporal manner. Moreover, an acute knockdown of both PFN isoforms with simultaneous expression of actin/PLP-binding-deficient or phospho-mimicking-mutants would shed more light into the functional role of profilin isoforms regarding spine motility and the mechanisms involved.

Despite several lines of evidence proposing that synaptic activity affects the motility of dendritic spines, the question if induction of synaptic plasticity itself causes changes in motility is still under debate. In this work the spine motility of PFN1 deficient CA1 neurons after induction of chemical LTP was found to be unaltered. Similar results were obtained in case of control cells, where only a slight but not significant decrease in both head and length motility could be observed. This tendency in decreasing motility might indeed be expected as it could represent a stabilization of spines upon chemical induction of LTP.

PFN1 is dispensable for spine head growth upon activity

Much research has focused on the effects of LTP and LTD on neuronal morphology, as there is close association between activity dependent synaptic plasticity (LTP/LTD) and structural plasticity at individual synapses (Yuste and Bonhoeffer, 2001). Further studies showed that LTP induction causes an increase in spine size (Lang et al., 2004; Matsuzaki et al., 2004a) and formation of new spines (Engert and Bonhoeffer, 1999). A plethora of studies aim at unraveling the relationship between changes in synaptic strength upon LTP induction and the accompanying structural changes such as spine head growth or emerging of new spines (Engert and Bonhoeffer, 1999; Fukazawa et al., 2003; Kopec et al., 2006; Chen and Firestein, 2007). In this study, global long-term potentiation was induced in hippocampal slice cultures by a brief application of glycine. Previous work demonstrated that glycine-induced LTP and theta burst stimulation-induced potentiation share similar cellular processes (Shahi et al., 1993; Musleh et al., 1997).

Live imaging of neurons expressing the control plasmid revealed that induction of cLTP resulted in a robust spine head diameter increase. Larger spines produce large synaptic currents, and have therefore generally a higher efficacy. Interestingly, also PFN1 deficient cells were susceptible to chemical LTP and exhibited a comparable growth of spine heads following the stimulation similar to the control cells. Strikingly, this finding contrasts to that obtained from the previous investigation of PFN2a deficient CA1 cells, which showed a complete impairment in their ability to undergo activity-dependent structural plasticity of spine heads upon cLTP induction. Collectively, these results show that PFN1 depletion in CA1 neurons had no influence on activity-dependent spine head growth, whereas spine head growth was dramatically impaired in PFN2a KD cells as no increase in spine head size could be observed after induction of chemical LTP via glycine (Remus 2012). These results point to the fact that specifically PFN2a is of crucial importance for remodeling the spine cytoskeleton during processes of structural plasticity.

Strikingly, the abolished spine head expansion upon cLTP in PFN2a KD cells could at least be rescued in parts by replacement with exogenous PFN1 or PFN2a (Remus, unpublished data). Thus, it seems that PFN2a plays a pivotal role for activity-induced spine head enlargement under physiological conditions while PFN1 has only a subsidiary role. Nevertheless, PFN1 is able to compensate the loss of PFN2a to a certain extent in activity-dependent structural plasticity. This combination of results provides further support for

the hypothesis that profilins are able to compensate for each other partially as they fulfill overlapping functions. Indeed, compensatory mechanisms could account for the lack of phenotype in LTP in both PFN1 and PFN2a KO mouse models (Pilo Boyl et al., 2007; Görlich et al., 2012).

Remarkably, activity-induced spine targeting was not only shown for PFN2a, but also for PFN1 in case of KCl application, which leads to a global increase of neuronal activity and is therefore less specific and not comparable to LTP induction (Neuhoff et al., 2005; Murk, 2008). Although this cLTP protocol using glycine application caused reliably gradual spine enlargement, it remains unclear if the observed spine head increase remains stable. Since the data reported here focused on spine morphology after 1 h of cLTP induction, there is a possibility that long-term stabilization of an increased spine head might be affected by PFN1 KD. A reasonable approach to address this issue could be to perform further live imaging experiments over a longer period such as 3 h.

The following conclusions can be drawn from the present study: the current findings regarding the role of PFN1 in dendritic architecture suggest that PFN1 plays only a minor role for proper outgrowth of dendrites as well as maintaining the dendritic tree whereas the predominant isoform here is PFN2a. The most important finding was that PFN1 KD caused a global decrease of spine density in all hippocampal cell types at both developmental stages analyzed. It is interesting to note that dependent on the hippocampal subregion also spine morphology was altered upon acute depletion of PFN1. These results regarding spine density match those observed in an earlier study and suggest that PFN1 indeed plays a fundamental role in maintaining spine shape and spine number (Michaelsen et al., 2010). The study presented here confirms that PFN2a and not PFN1 is involved in activity-dependent spine enlargement upon LTP induction. However, the scope of this study was limited as it was restricted to the early phase of structural plasticity. Thus, it is unknown if spines were affected in the long-term stabilization of spine head growth upon PFN1 depletion. Future research should therefore concentrate on the investigation of long-term spine stabilization in PFN1 and PFN2a deficient neurons. A further study could assess the activity-dependent structural plasticity of CA3 cells analogous to CA1 to examine more closely the differences between hippocampal subregions.

Hence, it could conceivably be hypothesized that PFN1 is a factor critical for spine growth during development (DIV 14) as well as spine maintenance in the mature hippocampus (DIV 21). The results of this study do not explain if the formation of new spines is already affected or if existing spines could not be maintained in the absence of PFN1 and thereby retract with time. The motility experiments of this study contribute evidence that suggests a role for PFN1 in actin dynamics under basal conditions as actin polymerization is slowed down in PFN1 deficient cells. Besides, PFN1 might contribute to the stabilization of synaptic structures beyond the initial (early) phase. PFN1 might be important in the late-phase of LTP, which is the more persistent phase. In accordance with aforementioned studies, these findings indicate that both profilins might be involved in regulating spine stability during the basal synaptic activity state. Here, the impact on neuronal morphology might be dependent on the hippocampal subregion as PFN isoforms are differentially expressed in those subfields (shown in this thesis). During processes of neuronal plasticity, specifically PFN2a is of pivotal importance in mediating morphological changes after LTP induction.

In accordance with previous data regarding the role of PFN2a in mediating spine head enlargement upon activity-induced plasticity processes, the results concerning PFN1 from this study can further contribute to a better understanding of profilin function in neurons and point in turn to overlapping as well as isoform-specific functions of profilins in the brain.

4.2 Role of FMRP in neuronal morphology

Cognitive deficits in patients with fragile X syndrome are correlated with structural abnormalities in the brain, but it is still not known how FMRP influences neuronal structure by regulating the synthesis of other proteins.

Much of the current literature on fragile X syndrome pays particular attention to spine density and spine morphology in FXS patients as well as the murine model for FXS that also lacks FMRP, the *fmr1* knockout mouse (Bakker et al., 1994; Irwin et al., 2002). Previous research findings regarding the dendritic spine phenotype in fragile X syndrome have been inconsistent and contradictory. A number of studies have found an unaltered spine number in the cortex and hippocampus of *fmr1* KO mice (Braun and Segal, 2000; Nimchinsky et al., 2001; Grossman et al., 2006; Meredith et al., 2007; de Vrij et al., 2008; Cruz-Martín et al., 2010; Levenga et al., 2011; Su et al., 2011). In contrast to these findings, other studies using *fmr1* KO mice reported that the absence of FMRP results in increased spine density, suggesting a possible failure of synapse elimination. Adult cortical brain regions in humans and mice exhibited a higher spine density, more longer spines with an immature-appearing structure, fewer shorter spines and a concomitant reduction of mature (stubby or mushroom-shaped) spines (Hinton et al., 1991; Irwin et al., 2001). Indeed, a more consistent abnormality of FXS is an elevated proportion of immature-looking spines in various brain regions, as *fmr1* deficient mice display more immature, long and thin spines or an increased proportion of filopodia in the CA1 subfield of the hippocampus, in dissociated neurons of the whole hippocampus or in layer 2/3 and layer 5 pyramidal neurons of the cortex (Comery et al., 1997; Nimchinsky et al., 2001; Irwin et al., 2002; Galvez and Greenough, 2005; McKinney, 2005; Restivo et al., 2005; Grossman et al., 2006; Meredith et al., 2007; Cruz-Martín et al., 2010; Pan et al., 2010; Su et al., 2011). Some authors have speculated that FMRP is important for the formation and maintenance of dendritic spines. Besides that, maturation of spines could be affected, as KO mice displayed a larger pool of transient new spines with a heightened spine turnover. The fact that the lack of FMRP led to more plastic spines in WT implies that this abnormal spine plasticity is might be caused by a failed maturation process. Another likely hypothesis suggests that FMRP is required for the activity-dependent processes of spine shape maturation and pruning, consequently loss of FMRP dendritic spines that would normally either mature or be pruned are maintained in a morphologically immature state

(Churchill et al., 2002; Bagni and Greenough, 2005). Since spine maturation follows a course specific to each brain region, the absence of FMRP will have neuroanatomical consequences that are also specific to each brain region. Although previous studies using Golgi staining did not provide insight into the fate of individual dendritic spines over time, several recent findings support the hypothesis that spines fail to mature properly without FMRP.

In my study spine morphology and dendritic architecture were investigated in an *in vitro* system of primary neurons derived from the hippocampus and cortex of *fmr1* KO mice and WT controls, as in human fetal brain as well as in mice the hippocampus is one of the major sites of *fmr1* gene expression (Abitbol et al., 1993; Hinds et al., 1993). In my comprehensive study dissociated hippocampal and cortical neurons were analyzed at two relevant time points regarding neuronal morphology, in particular spine morphology and dendritic complexity, because most studies focused on primarily spine structure at one single point of time. However, dendritic outgrowth and synapse formation might be interconnected processes regulated by the same molecular signals. The purpose of the current morphological characterization was to determine the impact of different PFN isoforms in a *gain-* and *loss-of-function* approach, as manipulation of expression levels of actin-binding proteins could potentially reverse the pathological phenotype.

In an investigation of the well-characterized *Drosophila* FXS model, Reeve et al. (2005) found a prominent role for dFMRP in regulating the mRNA of profilin/*chickadee* negatively. While overexpression of PFN mimics the phenotype of *dfmr1* mutants on the other hand a decrease of profilin levels suppresses *dfmr1* phenotypes (Reeve et al., 2005). It is important to note that functions of genes in *Drosophila* are often different from corresponding genes in mammals. Additionally, only one PFN isoform is abundant in *Drosophila* while mammals possess five PFN isoforms with two isoforms present in the brain. Nevertheless, a study investigating radial glial cells (RGC) revealed another link between FMRP and PFN, as specific loss of FMRP caused depletion of neocortical RGCs associated with F-actin reorganization. Strikingly, the RGC depletion could be largely rescued by overexpression of PFN1 (Saffary and Xie, 2011).

This misregulation of PFN1 in *Drosophila* also accords with our observations, which showed an altered PFN1 amount in whole brain lysates of *fmr1* KO mice in contrast to WT

littermates. Consequently, in this investigation, the aim was to assess to which extent manipulations of cellular PFN levels control neuronal structures.

Spine number is not altered in dissociated fmr1 KO neurons

Deficits in cognitive function are correlated to abnormal dendritic spines and resulting synaptic dysfunction. Dendritic spines display irregular shapes and abnormal densities in numerous neurodevelopmental disorders characterized by mental retardation such as fragile X syndrome or other neurological diseases including schizophrenia, bipolar diseases and epilepsy (Garey et al., 1998; Glantz and Lewis, 2000; Rosoklija et al., 2000; Nimchinsky et al., 2001). Two-decades of research about the integrity of synapses in the fragile X syndrome and in the well-characterized animal model of this disorder, the *fmr1* knockout mouse, could not determine the exact nature of the spine abnormalities. Since the number of spines is an important determinant of network function, several decades ago spine density was analyzed in neuropsychiatric disorders (Purpura, 1974). The first studies examined dendritic spines in FXS were based on Golgi staining of pyramidal neurons from the neocortex and hippocampus in either autopsy material from adult patients suffering from FXS or in the adult *fmr1* KO mice and revealed a higher proportion of immature spines of Layer 3 and Layer 5 pyramidal cells as well as increased spine density (Hinton et al., 1991; Irwin et al., 2001). Several other groups also found higher spines densities in different layers of the neocortex and in both visual cortex and somatosensory cortices, which strengthened the hypothesis that increased spine numbers resulted from a pruning defect (for a review see He & Portera-Cailliau 2012). In contrast to this, more recent studies investigated *fmr1* KO neurons during early postnatal development with two-photon fluorescence microscopy instead of Golgi staining and failed to display any changes in spine number (Meredith et al., 2007; Harlow et al., 2010; Pan et al., 2010). In summary, *fmr1* KO mice in general show a higher density of spines, as well as a shift from mature to immature morphology, in the first week after birth and throughout adulthood. These studies support the idea that FMRP promotes maturation of the developing cortex, and therefore processes such as spine maturation and pruning are disrupted or delayed in *fmr1* KO mice. More lately, subfields of the hippocampus were also analyzed concerning spine phenotypes. However, spine number was reported to be elevated in CA1 pyramidal neurons, granule cells as well as dissociated neurons (Levenga

et al. 2011; Grossman et al. 2010; Antar et al. 2006). Similar results were obtained for other brain regions than hippocampus such as amygdala or the olfactory bulb (Qin et al., 2011; Scotto-Lomassese et al., 2011). On the other hand, other groups found no alterations in spine density which led to ongoing controversies regarding spine defects in the fragile X syndrome (Grossman et al., 2006; Su et al., 2011).

In light of all this seemingly controversial findings, I analyzed spine density in a dissociated culture system. Primary hippocampal and cortical neurons of E18 WT and *fmr1* KO mice were cultured for 14 and 21 days, a time at which dendritic spines have matured and form synaptic contacts resembling attributes of those seen *in vivo* (Papa et al., 1995). The present study has found that spine number of hippocampal and cortical dissociated neurons transfected with control vector expressing f-GFP was similar between WT and KO cells at immature as well as fully mature developmental stages. However, variation of spine density within the *fmr1* KO group was higher than in WT cells indicating that KO neurons possess different amounts of spines and are therefore more variable. Similar to this, also *fmr1* KO mice demonstrate phenotype variability. An implication of this is the possibility that the population of *fmr1* KO neurons can be further subdivided into different groups according to their spine density phenotype. This finding supports previous research into these brain areas which revealed no gross alterations between WT and KO at all DIVs tested (14 and 20) (Levenga et al., 2011). Importantly, these findings are limited by the use of fixed culture representing only two distinct points of time in the development of hippocampal and cortical neurons. Overall, spine numbers were shown to be unaffected in this study.

Importantly, usage of different methods such as Golgi, DiI or Lucifer Yellow to label neurons in those studies could be responsible for the great diversity of results. Some studies suggest that Golgi staining leads to irregular labeling of cells, thereby labeling only a neuronal subpopulation which might display indeed spine abnormalities (Nimchinsky et al., 2001). Findings like these suggest that FMRP is required for the processes of spine maturation and pruning in multiple brain regions and that the specific pathology and its developmental expression is brain sub-region specific.

In addition to the mere number of spines, synaptic function heavily depends on morphological characteristics of dendritic spines and therefore research focused also on structural aspects of spines in *fmr1* knockout mice. The anatomical landmark of the

disease, both in humans and in the *fmr1* KO mice, is the hyperabundance of immature-looking elongated dendritic spines. According to previous studies, several groups described elevated number of filopodia on dendrites and concomitantly decreased number of mushroom spines in CA1 pyramidal neurons and granule cells of the dentate gyrus (Bilousova et al., 2009; Grossman et al., 2010).

Interestingly, obtained results concerning spine shape demonstrated significant alterations in spine type distribution between WT and KO hippocampal neurons in his work. The proportion of more mature mushroom spines was decreased in the KO, while in turn the proportions of immature thin spines and filopodia were elevated in comparison to WT cells. These results point to a spine morphology defect in young hippocampal cultures in *fmr1* KO mice which is in line with numerous recent findings in dissociated cultures (Antar et al., 2006; de Vrij et al., 2008; Dictenberg et al., 2008; Bilousova et al., 2009; Levenga et al., 2011; Su et al., 2011). Interestingly, analysis of the mature developmental stage could not reveal any defects of spine morphology in *fmr1* KO neurons.

Conclusively, this study could display more immature and less mature spines in the mouse model of fragile X syndrome and points to the fact that spine defects indeed represent a developmental delay in spine maturation. Interestingly, in a next step the FXS phenotype was tried to be restored by exogenous expression of PFN1 or PFN2a to analyze if altered PFN expression can affect the morphology in *fmr1* KO neurons.

Acute expression of exogenous profilin in fmr1 KO neurons rescues spine phenotype

Remarkably, in *Drosophila* mRNA of the PFN homolog *chickadee* was shown to be negatively regulated by dFMRP. Overexpression of PFN mimics the phenotype of *dfmr1* mutants while on the other hand a decrease of profilin levels suppresses *dfmr1* phenotypes (Reeve et al., 2005). Thus, in this study expression of either PFN1 or PFN2a was introduced into WT and KO neurons of distinct developmental ages to detect possibly alterations of the shape and size of spines in the fragile X condition. In immature *fmr1* KO hippocampal neurons, none of the profilin isoforms had an effect on spine density whereas PFN1 overexpressing WT neurons were decreased in spine number. An explanation for these results restricted to WT neurons could be the fact that endogenous

PFN1 levels were decreased in *fmr1* KO mice. By overexpression of PFN1 maybe the physiological protein level was restored with no further impact on spine number. Interestingly, cortical *fmr1* KO neurons demonstrated in contrast to results obtained from hippocampal cells an increased spine number in case of exogenous PFN1 expression indicating different protein compositions in different brain regions.

As a striking result of the overexpression of profilin isoforms the pathological spine type distribution in KO neurons was abolished. Surprisingly, expression of either PFN1 or PFN2a (whose expression level was not altered in the whole brain lysates of KO mice) in *fmr1* KO resulted in an elevated proportion of mushroom spines, which are considered as the mature type, and to a diminished proportion of immature spine types and filopodia comparable to WT neurons. These results imply indeed a role for FMRP in regulating the expression of profilin isoforms during spine maturation, as changes in profilin protein level caused a restoration of the normal spine type distribution in *fmr1* deficient neurons.

In mature neurons of the hippocampus, expression of PFN isoforms had no effects on spine number in both genotypes. Similar to young cortical neurons, also in mature cells derived from the cortex overexpression of PFN1 resulted in a raised spine number in the *fmr1* KO. Opposing to morphological data obtained from young neurons, mature spines were not influenced in their structure by expression of either PFN1 or PFN2a.

Collectively, rescue of the immature spine phenotype by PFN expression was effective in immature hippocampal neurons. Mature neurons of *fmr1* KO mice did not exhibit alterations in spine type distribution and remained unaffected upon PFN overexpression.

FMRP and dendritic structure

Appropriate outgrowth and ramification of dendrites are crucial for functioning of the nervous system, as patterns of dendritic branching determine the nature and amount of innervation that a neuron receives. Published data referring to dendritic architecture in *fmr1* knockout neurons has produced conflicting results. For example, hippocampal neurons derived from *fmr1* KO mice with FVB/NJ 129 background were reported to have shorter dendrites in comparison to WT at both DIV 7 and DIV 21 (Braun and Segal, 2000). Opposing to this data, analysis of layer V pyramidal neurons in the visual cortex of adult *fmr1* WT and KO mice revealed no differences in dendritic complexity. Unfortunately, direct comparisons between published data are difficult, because some studies used

primary dissociated cell culture while other studies were based on intact adult tissue sections. A simple explanation for contradictory results obtained from several studies is the fact that cultured hippocampal neurons differ from neurons *in vivo* in terms of outgrowth or stability which might depend on molecules of the extracellular matrix.

The main findings of this study were a reduced dendritic tree in *fmr1* WT and KO neurons at DIV 14 upon expression of either PFN1 or PFN2a. The diminished dendritic complexity was even more pronounced in the acute knockdown of one of the PFN isoforms indicating that proper profilin levels were needed for maintaining an appropriate dendrite structure. Interestingly, KO neurons of another developmental stage (DIV 21) were totally unaffected alterations in PFN protein levels in contrast to WT, indicating that later stages of development differ in their susceptibility from earlier development and may possess different levels of profilins leading to stability. Since mature WT neurons were affected by changing profilin levels, general integrity of dendrites at this time point can be excluded. However, inappropriately growing dendrites upon modification of profilin level was restricted to the WT condition in mature neurons, maybe due to a missing functional property of FMRP in regulating profilin expression. Strikingly, dendritic complexity decreases with age regardless of the genotype, pointing to the fact that the climax of dendritic arborization has been exceeded at this developmental stage in general.

Immature neurons derived from *fmr1* KO cortices were more complex than corresponding WT, whereas mature KO neurons were found to be less complex. Cortical neurons at both developmental stages were not affected by overexpression of PFN1. Thus, cortical neurons differed significantly from hippocampal neurons as their dendritic architecture remained unaltered. It might be reasonable to think that different brain regions express various levels of profilin isoforms. e.g. the cortex might provide more PFN in comparison to the hippocampus which would lead to a higher tolerance towards changes in protein level. Regarding this issue, studies in *Drosophila melanogaster* were performed, as the nervous system contains the *dFXR* gene, a homolog to the mammalian *fmr1* gene. Interestingly, it could be demonstrated that both outgrowth and branching of neurites were disturbed in the *Drosophila* model for fragile X syndrome. Interestingly, distinct neuronal cell types show different phenotypes, suggesting that *dfxr* differentially regulates diverse targets in the brain of *Drosophila* (Morales et al., 2002).

4.3 *fmr1* KO mice are impaired in spatial learning

Impaired spatial learning is a prominent deficit in fragile X syndrome, although previous studies using *fmr1* KO mice as a model could not report consistent deficits so far. Indeed, often contradicting results were obtained from different groups or even within the same group (Bakker et al., 1994; Kooy et al., 1996; D'Hooge, 1997; Paradee et al., 1999).

Thus, we re-examined spatial learning in the *fmr1* knockout mice using the hippocampus-dependent Morris water maze paradigm. Performances in this study showed that *fmr1* KO mice found the platform with decreasing latency time in the same way like WT mice, as there were no differences concerning escape latencies and path lengths between both genotypes over the course of training time. Reference memory test at the probe trial revealed that *fmr1* KO mice were in general able to retrieve acquired spatial memory as displayed by a preference for the quadrant which contained the platform before. Nevertheless, KO animals spent significantly less time in the target quadrant compared to WT littermates. A detailed analysis of accuracy of spatial memory retrieval during the probe trial via counting the number of "platform" crossings pointed to a reduced precision in case of *fmr1* KO mice. Interestingly, further discrimination between subgroups within *fmr1* KO mice demonstrated that some KO mice had a near-normal performance while others were significantly impaired in spatial learning. Subdivision of knockouts enabled a more precise interpretation of the data and reflects also the wide range of phenotypes in this disorder.

Interestingly, in previous studies it could be demonstrated that *fmr1* KO mice showed mildly impaired spatial learning performances in the Morris water maze as well as trace fear memory tests (Zhao et al. 2005; D'Hooge 1997; Kooy et al. 1996). To investigate the physiological function of the *fmr1* gene regarding its role in spatial learning and resulting memory formation, the well-established Morris water maze test was conducted with *fmr1* KO mice and corresponding *fmr1* WT littermate controls in a few studies, which presents partially controversial results. While some studies using the classic Morris water maze test to assess spatial learning found impairment exclusively in the reversal trial in *fmr1* knockout mice (Bakker et al., 1994; D'Hooge, 1997), other studies could not observe any difference between both genotypes in the learning and the reversal task (Paradee et al., 1999). A possible explanation for the disability in reproducing the relatively slight differences in reversal trials between genotypes could be attributed to different genetic

backgrounds of knockout strains such as C57/Bl6 and FVB-129. Indeed, the effect of strain on transgenic and knockout mice has been reported previously, thereby it is likely that substantial differences in their MWM performances might be due to quantitative trait loci (Owen et al., 1997; Paradee et al., 1999). In line with this, tested FVB-129 KO mice showed a pronounced deficiency in a cross-shaped water maze task in comparison to normal littermates. Contrary, knockout mice with a C57/Bl6 background learned the maze just as well as WT mice while fear conditioning did not reveal any strain-dependent differences. These data indicate that silencing of the *fmr1* gene interfered with learning in FVB-129 mice, but not in C57/Bl6 mice, which may reflect the influence of genetic background in the human condition of fragile X syndrome (Dobkin et al., 2000). More recently, Spencer et al. observed a loss of habituation in *fmr1* KO mice on the B6xFVB/NJ background but not on other background strains, which could be attributed to hyperactivity in the knockouts (Spencer et al., 2011).

Similar to results obtained from reverse trials, near-normal performances of knockout animals were apparent in the probe trial of other studies (Kooy et al. 1996; D'Hooge 1997; Paradee et al. 1999). Those studies failed to detect subtle differences between genotypes as demonstrated in this work.

Importantly, the majority of behavioral studies have used exclusively male mice, so that information is missing regarding the effects of disruption of *fmr1* gene on behavior in females, as fragile X syndrome also occurs in females (Zhao et al., 2005; Bernardet and Crusio, 2006). To illuminate the role gender may play in the phenotype it would be mandatory to evaluate both sexes in further studies.

Recent findings in our lab indicate an impaired reversal learning in aged (19 months old) *fmr1* KO mice compared to WT controls, which could be addressed to a deficit in behavioural flexibility in re-learning tasks (F. Scharkowski, personal communication). Besides common measurements of spatial memory formation, additional information can be gained via the analysis of different searching strategies used by the mice throughout the training. This is the first study so far which has investigated use of different search strategies in the mouse model of fragile X syndrome. In general, an efficient progression towards directed navigation aiming at the platform was found in both groups with increasing time, which underlines the fact of memory formation regarding the platform position. While wild-type mice showed a clear progression towards increase of

hippocampus-dependent strategies such as *direct swimming* and therefore a fast decrease of the relative amount of random search, knockout animals could not progress as fast to more hippocampus-dependent strategies and thus depicted a higher relative amount of random search patterns even until the last day of training. Thus, hippocampal-independent strategies which are less precise and consequently less efficient were observed to a higher extent in *fmr1* KO mice compared to WT.

4.4 *fmr1* KO mice have dysregulated levels of actin-regulating proteins

Spatial memory formation in the Morris water maze is accompanied by protein changes in the hippocampus of trained mice. Importantly, protein levels were different between WT and KO already in the naïve animals leading to the question of how training would affect those protein amounts. To gain more insights into how the protein levels of relevant candidates such as PFN1, PFN2a and CFL were affected upon plasticity processes in the *fmr1* KO mice, analyses of hippocampus and medial prefrontal cortex of trained, untrained and swim controls were performed at the end of training and thereby reflect the long-term effects on protein synthesis. This study stresses the importance of yoked mice (swim control group) in the evaluation of proteins, which is linked to spatial memory in the MWM, as it corrects for swim stress and other confounding factors such as physical activity (John et al., 2009; Sunyer et al., 2008, 2009). In line with this, even swimming alone led to a misregulation of protein levels in the *fmr1* KO in this study. Upon spatial training differential regulations in the hippocampal and mPFC levels of three proteins (PFN1, PFN2a and CFL), which are known to be involved in synaptic plasticity, could be observed. This might affect memory formation by interfering with processes of neuronal plasticity underlying memory consolidation. The data presented here revealed a dysregulation of relevant protein quantities in *fmr1* KO mice in the hippocampus and mPFC, which was already present in the naïve animal and further pronounced during free swimming and again enhanced during spatial memory formation. Thus, molecular dysfunctions were consistent with behavioral deficits shown in *fmr1* KO mice. Unfortunately, this study failed due to technical limitations to further examine if relevant proteins were translocated from the cytoplasm to nuclei upon memory formation.

Therefore, obtained data should be regarded as preliminary and considered as a starting point for further investigation. However, it is known for both PFN isoforms as well as for CFL that these proteins are targeted into spines upon induced activity; thereby at least increased protein amount in the nuclei of *fmr1* WT would be expectable (Ackermann and Matus, 2003; Neuhoff et al., 2005; Murk et al., 2012). Notably, major differences between both PFN isoforms could be observed. Whereas PFN1 was shown to be dysregulated in the *fmr1* KO, PFN2a levels were regulated normally. An additional limitation of this study is given by the fact that whole hippocampi and mPFCs were analyzed. Thus, no subcellular insight into the question where exactly altered protein levels occurred in the distinct subfields of the hippocampus was possible.

Levels of phosphorylated CFL are known to increase in the rat hippocampus during exploration of a novel environment and inhibition of this event also blocks memory formation (Fedulov et al., 2007). As phosphorylation of CFL is downstream of PAK activity, it would be interesting to see whether these cellular processes are disrupted in the hippocampus of *fmr1* KO mice during spatial learning in the water maze to explain impaired precision and less efficient performance.

5 CONCLUSIONS AND OUTLOOK

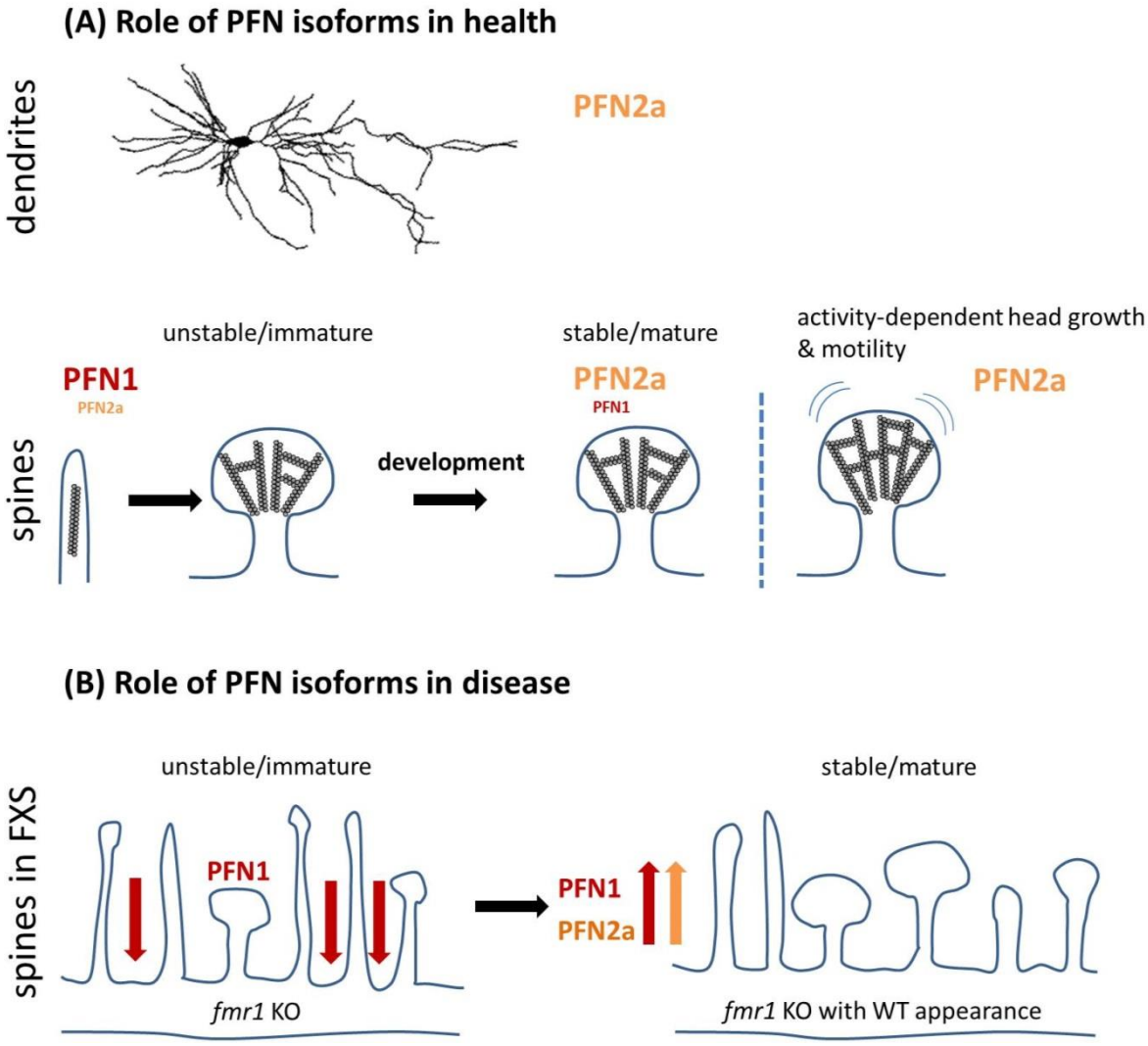

Figure 43 | Proposed model for the role of PFN isoforms in health and disease

(A) *Dendritic architecture of hippocampal neurons is regulated by PFN2a while PFN1 is not important for dendrite stability and outgrowth. In immature spines at early stages of development, PFN1 is crucial for spine number and morphology. In contrast, PFN2a plays a major role in stabilization and maintenance of mature spines. Activity-dependent head growth and basal motility is dependent on PFN2a. PFN1 is dispensable for these processes, but compensates for the loss of PFN2a.*

(B) *In the FXS condition, fmr1 KO hippocampal neurons exhibit an immature spine phenotype as well as misregulated PFN1 levels. By overexpression of either PFN1 or PFN2a, the spine phenotype is rescued in fmr1 KO neurons.*

In the current study, I was able to show that PFN1 plays a subsidiary role in regulating dendritic architecture of hippocampal neurons as well as activity-dependent structural plasticity while it is an important determinant of proper outgrowth and shape of dendritic spines during development. Future experiments concerning the dendritic arbor structure could aim at earlier developmental stages, as affecting the final shape occurs between DIV6-DIV12 when the number of primary dendrites, total dendritic length and branching degree are determined.

Live imaging experiments demonstrated that PFN2a is the major mediator of activity-dependent structural plasticity with PFN1 being dispensable for spine head growth upon LTP. Thus, it could be further underlined that both profilins serve isoform-specific as well as overlapping functions in mature hippocampal neurons as either one of them can compensate for the other. Results from this work indicate that profilin isoforms are expressed differentially within subregions of the hippocampus, as PFN1 and PFN2a showed no differences in the apical compartments of CA1, but in the apical compartment of CA3. In addition, opposing protein amounts in the basal compartments of these regions were found, although it is not understood so far which ratio between profilin isoforms is required for proper maintenance of the actin cytoskeleton in the dendritic spine. The dendrites of a neuron serve a specialized role in regulating neuronal functioning, which is underlined by the fact that a subset of mRNAs are transported to dendrites where local protein translation occurs (for a review see Eberwine et al. 2001). Consequently, in future experiments the profilins' mRNAs could be detected through *in situ* hybridization to further elucidate the local restriction of profilins' actions. In general, phosphorylation provides a fast-time scale modification of profilins activity as the phosphorylation state determines their binding affinity to actin and PLP domains and therefore influences their effects on actin dynamics. Thus, a gene replacement approach of PFN1 or PFN2a phosphorylation-mimicking mutants could be used to determine the differences in activity of profilin isoforms. Additionally, vectors carrying PLP- or actin-binding deficient mutants could be used to reveal how PFN interactions with various interaction molecules are involved in modulating structural plasticity. Experiments aiming at protein-protein-interactions such as crosslinking assays would be helpful here.

In future investigations, stereotaxic injections of recombinant lentiviral particles resulting in silencing of either PFN1 or PFN2a could be performed to provide a high spatiotemporal

control over the genetic manipulations and allow targeting of only a small neuronal population *in vivo* avoiding culture conditions. Thus, only a subpopulation of pyramidal neurons e.g. in the CA1 region at a defined time in the postnatal development would be affected and thereby a possible activation of compensatory mechanisms if the entire brain was altered (what is indeed the case for the KO mouse model) would be circumvented. The use of this method could be a means of analyzing the function of profilin isoforms *in vivo* instead of using cell culture. Subsequent electrophysiological experiments investigating LTP or spatial learning in the water maze are needed to be undertaken. A further study could assess an acute double-KO of both PFN to understand PFN impact on synaptic plasticity. Interaction of PFN1 and PFN2a with isoform-specific ligands should be investigated to answer specific questions. Interestingly, activation of PFN2a is correlated to suppressed actin dynamics and blockade of spine activity. Consequently, acute KD results in elevated basal spine motility whereas PFN1 seems to be of minor importance in this context. It is likely that profilins mediate between the actin cytoskeleton and different surface associated proteins which eventually regulate spine morphology. The motility of dendritic protrusions can be correlated with alterations in network organization and biochemical compartmentalization and was dramatically elevated in PFN2a KD, which could not be rescued by the expression of recombinant PFN1 (Remus, 2012), but the expression of recombinant PFN2a led to a partial rescue of the phenotype, as overexpression of PFN2a increases the stability of dendritic spines (Ackermann and Matus, 2003). A decrease in stability may be the consequence of alterations in cell-cell adhesion by cadherins, as exclusively PFN2 KD alters the balance of cadherin isoforms in epithelial cells (Simpson et al., 2008).

Considerably more work will need to be done to determine how profilins are involved in mediating structural plasticity upon chemical induction of LTP. To further elucidate the time course of action, time-lapse experiments should investigate spine structures directly after LTP induction as well as following longer periods of time to analyze if profilins are involved in different stages of LTP induction and maintenance. In addition to that, a more temporally restricted and local stimulation like two photon glutamate uncaging could be used to discriminate between enlargement and stabilization phase after stimulation. Recently, results obtained from FRAP experiments in our lab also indicate distinct functions of both PFN isoforms, as PFN1 knockdown CA3 cells were impaired in actin

turnover in contrast to PFN2a knockdown cells demonstrating elevated actin dynamics (Michaelsen-Preusse, personal communication). Future experiments in this field should aim at CA1 cells, as indeed cells of different hippocampal subregions exhibit distinct properties.

In the second part of this study, I could show that spatial learning and physical activity influence protein amounts of actin-binding proteins in the mouse model for fragile X syndrome. It is important to note that this study could not reveal if protein synthesis or degradation is affected. To answer this specific question, *in situ* hybridization experiments could clarify if profilins or cofilin are locally synthesized. A further water maze analysis with reversal trials could assess the flexibility in re-learning of FXs mice. *Fmr1* knockout mice have impaired Hebbian-type synaptic plasticity (Huber et al., 2002; Larson et al., 2005), which may contribute to their learning deficits (Mineur et al., 2002; Yan et al., 2004; Koekkoek et al., 2005). Cognitive impairment and low intelligence quotients are characteristic of patients with FXS, but measures of these phenotypes have been difficult to demonstrate in the mouse model (Bernardet and Crusio, 2006). Tests of spatial learning and memory such as the MWM have not shown remarkable effects in KO mice (Bakker et al. 1994; Peier et al. 2000; Yan et al. 2004). In contrast to those studies, we have found impairments of spatial learning in *fmr1* KO mice. The dysregulation of profilin and cofilin in the KO indicates that FMRP may permissively regulate transport and translation of a specific subset of proteins involved in activity-directed pruning or remodeling of synapses, which might account for structural and functional deficits observed in FXS. An issue that was not addressed in this study was whether profilins and cofilin are targeted to the nuclei upon spatial learning. The subcellular localization of profilin isoforms is largely unknown, but KCl treatment resulted in an elevated amount of both profilin isoforms in the nuclei (Murk et al., 2012) and the more specific stimulation via BDNF and thereby activation of the TrkB receptor pathway (for review (Minichiello, 2009) solely led to a redistribution of PFN1 to the neuronal nucleus. The significance of the translocation of PFN1 to the cellular nucleus is not well understood. Profilins are suggested to be involved in the regulation of nuclear processes and might even regulate gene expression. PFN1 also interacts with nuclear actin (Stuven et al., 2003) and colocalizes with several ligands known from the cytoplasm like VASP or mDia1 (Rawe et al., 2006). These results are further supported by the fact that the spine abnormalities

observed in FMRP deficient neurons can be fully restored by introduction of PFN1. It would be also interesting to assess the effect of a cofilin overexpression in dissociated FXS neurons.

Taken together, these findings suggest distinct roles for profilin isoforms as well as overlapping functions regarding spine stability, spine morphology and spatial learning in health and disease as demonstrated in the mouse model for fragile X syndrome.

6 SUPPLEMENT

6.1 Supplementary data

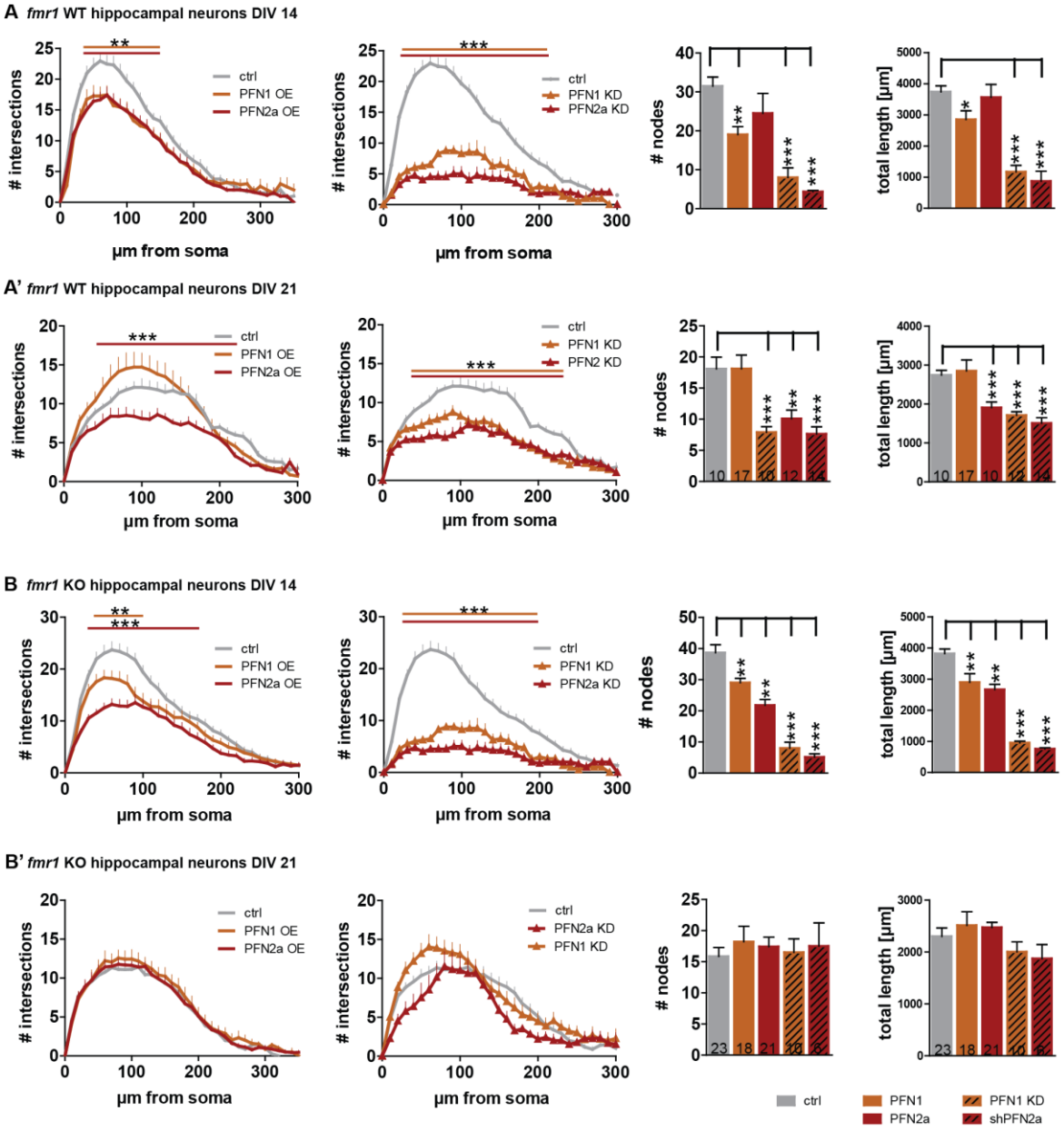

Supplementary figure 1 | Dendritic architecture of *fmr1* WT and KO hippocampal neurons

(A) *fmr1 WT hippocampal neurons at DIV 14 were found to be reduced in dendritic complexity when one of the profilin isoforms was either overexpressed or reduced via RNAi.* ***(A')*** *fmr1 WT hippocampal neurons at DIV 21 were found to be reduced in dendritic complexity in case of knockdown one of the profilin isoforms. Also PFN2a overexpression resulted in reduced dendritic complexity.* ***(B)*** *fmr1 KO hippocampal neurons at DIV 14 were found to be reduced in dendritic complexity when one of the profilin isoforms was either overexpressed or reduced via RNAi.* ***(B')*** *fmr1 KO hippocampal neurons at DIV 21 were unaffected in case of overexpression of one of the profilin isoforms. Also knockdown of PFN1 or PFN2a did not alter dendritic complexity. *p<0.05, **p<0.01, ***p<0.001*

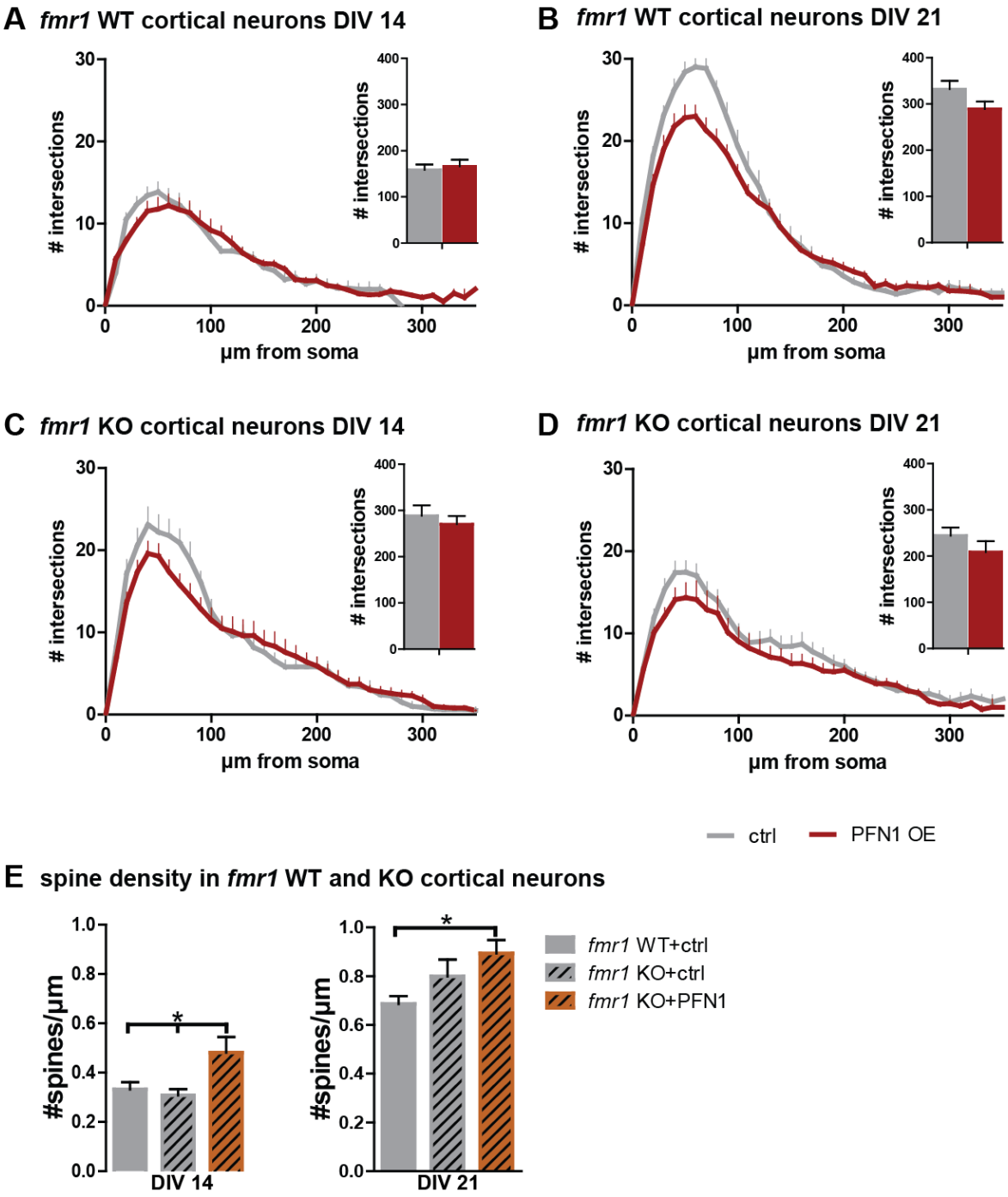

Supplementary figure 2 | Dendritic complexity and spine density in *fmr1* WT and KO dissociated cortical neurons

(A) *fmr1 WT cortical neurons at DIV 14 were not affected due to PFN1 OE.* ***(B)*** *Dendritic complexity was increased at DIV 21 in both control and PFN1 OE condition.* ***(C), (D)*** *fmr1 KO cortical neurons at DIV 14 or 21 were not affected due to PFN1 OE. Dendritic complexity was not increased at DIV 21 in contrast to fmr1 WT.* ***(E)*** *Spine density is elevated in fmr1 KO cortical neurons overexpressing PFN1 at both developmental stages.*

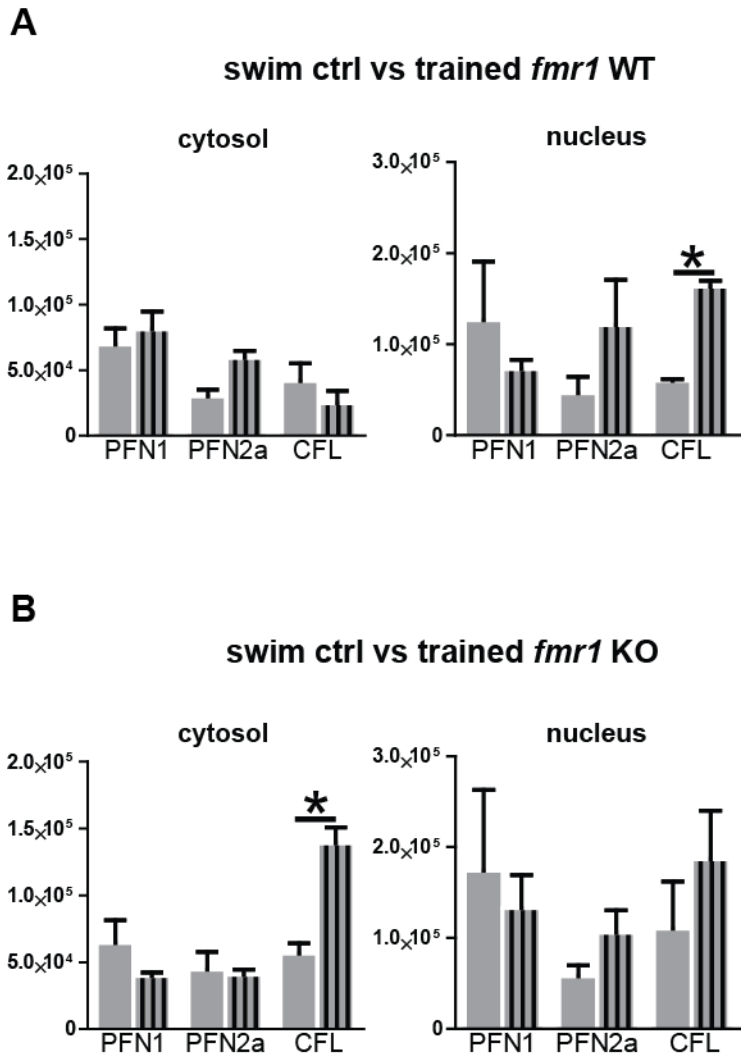

Supplementary figure 3 | Protein levels of *fmr1* WT and *fmr1* KO mice in the cytosolic fraction and nucleus fraction of the hippocampus

(A) *PFN1, PFN2a and CFL levels of fmr1 WT mice in the cytosol (left) and nucleus (right) of hippocampal cells shown as ratios to loading control. Only CFL increases significantly in the nucleus fraction of trained mice. Grey without pattern indicates swim control group, grey with black striped pattern indicates trained group.* ***(B)*** *PFN1, PFN2a and CFL levels of fmr1 KO mice in the cytosol (left) and nucleus (right) of hippocampal cells. Only CFL increases significantly in the cytosolic fraction of trained mice. Grey without pattern indicates swim control group, grey with black striped pattern indicates trained group. n = 3 mice per group.*

Supplementary Table 1 | Spine densities in hippocampal slice cultures

Spine densities presented as mean ± SEM and p-value per µm of dendrite.

	basal	mid-apical	distal-apical	age
CA1 control	1.349 ± 0.09239	1.169 ± 0.06444	0.8791 ± 0.0657	**DIV 14**
CA1 PFN1 KD	0.7759 ± 0.04449	0.7949 ± 0.02244	0.5698 ± 0.03563	
	p = 0.0055	p = 0.0092	p = 0.0227	
CA3 control	1.062 ± 0.08325	1.154 ± 0.06089	0.8053 ± 0.07608	
CA3 PFN1 KD	0.6177 ± 0.06688	0.7736 ± 0.07737	0.5951 ± 0.04314	
	p = 0.0014	p = 0.0015	p = 0.0436	
DG control	1.136 ± 0.1058			
DG PFN1 KD	1.011 ± 0.2165			
	basal	**mid-apical**	**distal-apical**	**DIV 21**
CA1 control	1.212 ± 0.06716	1.150 ± 0.09393	0.8317 ± 0.08319	
CA1 PFN1 KD	0.7293 ± 0.09469	0.8651± 0.06002	0.6011 ± 0.05637	
	p = 0.0007	p = 0.0253	p = 0.041	
CA3 control	1.085 ± 0.09224	1.177 ± 0.07604	0.864 ± 0.04344	
CA3 PFN1 KD	0.768 ± 0.05912	0.9467 ± 0.0693	0.6274 ± 0.06885	
	p = 0.0109	p = 0.043	p = 0.0148	
DG control	1.497 ± 0.04592			
DG PFN1 KD	0.8604 ± 0.15			
	p < 0.0001			

6.2 Abbreviations

appr.	approximately
PT	probe trial
µg	microgram(s)
µl	microliter(s)
µm	micrometer(s)
ABP(s)	actin binding protein(s)
ACSF	artificial cerebrospinal fluid
ADF	actin-depolymerization factor(s)
AMPA(R)	α-amino-3-hydroxyl-5-methyl-4-isoxazole-propionate acid (receptor)
ANOVA	analysis of variance
BSA	bovine serum albumin
CA	cornu ammonis (hippocampal subfields)
Cdc42	Cell division control protein 42 homolog
CFL	cofilin
cLTP	chemical LTP
CMV promoter	human cytomegalovirus immediate-early promoter
cp.	compare(d)
DAPI	4'-6-Diamidino-2-phenylindole
DG	dentate gyrus (hippocampal subfield)
DIV	days in vitro of differentiation
E	east
e.g.	exempli gracia
EC	entorhinal cortex
F-actin	filamentous actin
fEGFP	farnesylated enhanced green fluorescent protein
G-actin	globular actin
GBSS	Gey's balanced salt solution
h	hour(s)
i.e.	id est
KD	knockdown
KO	knockout
LTD	long-term depression
LTP	long-term potentiation
M	Mole
MI	motility index
min	minute(s)
mm	millimole
mPFC	medial prefrontal cortex
MWM	Morris water maze
N	north

n	sample size
NE	north-east
ng	nanogram
nm	nanometer
NMDA(R)	N-methyl-D-aspartate receptor
NW	north-west
OHC	organotypic hippocampal slice
PAGE	polyacrylamide gel electrophoresis
PBS	phosphate buffered saline
PFN 2a	profilin 2a
PFN1	profilin 1
pH	potential of hydrogen
PLP	poly-L-proline
PSD	postsynaptic density
PVDF	polyvinylidene fluoride
RNAi	RNA interference
rpm	revolutions per minute
RT	room temperature
S	south
s	second(s)
SDS	sodium dodecyl sulfate
SE	south-east
SEM	standard error of the mean
shRNA	short hairpin RNA
SW	south-west
vs	versus
W	west
WT	wild-type

7 REFERENCES

Abitbol M, Menini C, Delezoide AL, Rhyner T, Vekemans M, Mallet J (1993) Nucleus basalis magnocellularis and hippocampus are the major sites of FMR-1 expression in the human fetal brain. Nat Genet 4:147–153.

Ackermann M, Matus A (2003) Activity-induced targeting of profilin and stabilization of dendritic spine morphology. Nat Neurosci 6:1194–1200.

Allison DW, Gelfand VI, Spector I, Craig AM (1998) Role of actin in anchoring postsynaptic receptors in cultured hippocampal neurons: differential attachment of NMDA versus AMPA receptors. J Neurosci 18:2423–2436.

Alvarez P, Zola-Morgan S, Squire LR (1994) The animal model of human amnesia: long-term memory impaired and short-term memory intact. Proc Natl Acad Sci U S A 91:5637–5641.

Antar LN, Li C, Zhang H, Carroll RC, Bassell GJ (2006) Local functions for FMRP in axon growth cone motility and activity-dependent regulation of filopodia and spine synapses. Mol Cell Neurosci 32:37–48.

Ascano M, Mukherjee N, Bandaru P, Miller JB, Nusbaum JD, Corcoran DL, Langlois C, Munschauer M, Dewell S, Hafner M, Williams Z, Ohler U, Tuschl T (2012) FMRP targets distinct mRNA sequence elements to regulate protein expression. Nature 492:382–386.

Ashley CT, Wilkinson KD, Reines D, Warren ST (1993) FMR1 protein: conserved RNP family domains and selective RNA binding. Science 262:563–566.

Bagni C, Greenough WT (2005) From mRNP trafficking to spine dysmorphogenesis: the roots of fragile X syndrome. Nat Rev Neurosci 6:376–387.

Bagni C, Oostra B a (2013) Fragile X syndrome: From protein function to therapy. Am J Med Genet A 161A:2809–2821.

Bakker CE, Verheij C, Willemsen R, Helm R Van Der, Oerlemans F, Hoogeveen T, Oostra BA, Vermey M, Bygrave A, Hoogeveen AT (1994) Fmr1 Knockout Mice : A Model to Study Fragile X Mental Retardation. Cell 78:23–33.

Bardoni B, Davidovic L, Bensaid M, Khandjian EW (2006) The fragile X syndrome: exploring its molecular basis and seeking a treatment. Expert Rev Mol Med 8:1–16.

Bardoni B, Mandel JL, Fisch GS (2000) FMR1 gene and fragile X syndrome. Am J Med Genet 97:153–163.

Bear MF, Huber KM, Warren ST (2004) The mGluR theory of fragile X mental retardation. Trends Neurosci 27:370–377.

Bernardet M, Crusio WE (2006) Fmr1 KO mice as a possible model of autistic features. ScientificWorldJournal 6:1164–1176.

Bhakar AL, Dölen G, Bear MF (2012) The Pathophysiology of Fragile X (and What It Teaches Us about Synapses). Annu Rev Neurosci:417–443.

Bilousova T V, Dansie L, Ngo M, Aye J, Charles JR, Ethell DW, Ethell IM (2009) Minocycline promotes dendritic spine maturation and improves behavioural performance in the fragile X mouse model. J Med Genet 46:94–102.

Birbach A (2008) Profilin, a multi-modal regulator of neuronal plasticity. Bioessays 30:994–1002.

Birbach A, Verkuyl JM, Matus A (2006) Reversible, activity-dependent targeting of profilin to neuronal nuclei. Exp Cell Res 312:2279–2287.

Boda B, Mendez P, Boury-Jamot B, Magara F, Muller D (2014) Reversal of activity-mediated spine dynamics and learning impairment in a mouse model of Fragile X syndrome. Eur J Neurosci 39:1130–1137.

Bonacci TM, Hirsch DS, Shen Y, Dokmanovic M, Wu WJ (2012) Small GTPase Rho regulates R-cadherin through Dia1/profilin-1. Cell Signal.

Bonhoeffer T, Yuste R (2002) Spine Motility. Neuron 35:1019–1027.

Bosch M, Castro J, Saneyoshi T, Matsuno H, Sur M, Hayashi Y (2014) Structural and Molecular Remodeling of Dendritic Spine Substructures during Long-Term Potentiation. Neuron 82:444–459.

Bosch M, Hayashi Y (2011) Structural plasticity of dendritic spines. Curr Opin Neurobiol:1–6.

Bourne JN, Harris KM (2008) Balancing structure and function at hippocampal dendritic spines. Annu Rev Neurosci 31:47–67.

Braun K, Segal M (2000) FMRP involvement in formation of synapses among cultured hippocampal neurons. Cereb Cortex 10:1045–1052.

Bresler T, Ramati Y, Zamorano PL, Zhai R, Garner CC, Ziv NE (2001) The dynamics of SAP90/PSD-95 recruitment to new synaptic junctions. Mol Cell Neurosci 18:149–167.

Burnett BG, Andrews J, Ranganathan S, Fischbeck KH, Di Prospero N a (2008) Expression of expanded polyglutamine targets profilin for degradation and alters actin dynamics. Neurobiol Dis 30:365–374.

Burwell RD, Witter MP, Amaral DG (1995) Perirhinal and postrhinal cortices of the rat: a review of the neuroanatomical literature and comparison with findings from the monkey brain. Hippocampus 5:390–408.

Carlisle HJ, Kennedy MB (2005) Spine architecture and synaptic plasticity. Trends Neurosci 28:182–187.

Carlsson L, Nyström LE, Sundkvist I, Markey F, Lindberg U (1977) Actin polymerizability is influenced by profilin, a low molecular weight protein in non-muscle cells. J Mol Biol 115:465–483.

Caroni P, Donato F, Muller D (2012) Structural plasticity upon learning: regulation and functions. Nat Rev Neurosci 13:478–490.

Chen H, Firestein BL (2007) RhoA regulates dendrite branching in hippocampal neurons by decreasing cypin protein levels. J Neurosci 27:8378–8386.

Churchill JD, Beckel-Mitchener A, Weiler IJ, Greenough WT (2002) Effects of Fragile X syndrome and an FMR1 knockout mouse model on forebrain neuronal cell biology. Microsc Res Tech 57:156–158.

Cingolani L a, Goda Y (2008) Actin in action: the interplay between the actin cytoskeleton and synaptic efficacy. Nat Rev Neurosci 9:344–356.

Comery T a, Harris JB, Willems PJ, Oostra B a, Irwin S a, Weiler IJ, Greenough WT (1997) Abnormal dendritic spines in fragile X knockout mice: maturation and pruning deficits. Proc Natl Acad Sci U S A 94:5401–5404.

Cruz-Martín A, Crespo M, Portera-Cailliau C (2010) Delayed stabilization of dendritic spines in fragile X mice. J Neurosci 30:7793–7803.

D'Hooge R (1997) MILDLY IMPAIRED WATER MAZE P E R F O R M A N C E IN. Neuroscience.

D'Hooge R, De Deyn PP (2001) Applications of the Morris water maze in the study of learning and memory.

Da Silva JS, Medina M, Zuliani C, Di Nardo A, Witke W, Dotti CG (2003) RhoA/ROCK regulation of neuritogenesis via profilin IIa-mediated control of actin stability. J Cell Biol 162:1267–1279.

De Bruin JP, Sànchez-Santed F, Heinsbroek RP, Donker a, Postmes P (1994) A behavioural analysis of rats with damage to the medial prefrontal cortex using the Morris water maze: evidence for behavioural flexibility, but not for impaired spatial navigation. Brain Res 652:323–333.

De Bruin JPC, Swinkels W a. M, de Brabander JM (1997) Response learning of rats in a Morris water maze: Involvement of the medial prefrontal cortex. Behav Brain Res 85:47–55.

De Vrij FMS, Levenga J, van der Linde HC, Koekkoek SK, De Zeeuw CI, Nelson DL, Oostra BA, Willemsen R (2008) Rescue of behavioral phenotype and neuronal protrusion morphology in Fmr1 KO mice. Neurobiol Dis 31:127–132.

Dictenberg JB, Swanger SA, Antar LN, Singer RH, Bassell GJ (2008) A direct role for FMRP in activity-dependent dendritic mRNA transport links filopodial-spine morphogenesis to fragile X syndrome. Dev Cell 14:926–939.

Dobkin C, Rabe a, Dumas R, El Idrissi a, Haubenstock H, Brown WT (2000) Fmr1 knockout mouse has a distinctive strain-specific learning impairment. Neuroscience 100:423–429.

Dölen G, Osterweil E, Rao BSS, Smith GB, Auerbach BD, Chattarji S, Bear MF (2007) Correction of fragile X syndrome in mice. Neuron 56:955–962.

Dominguez R (2009) Actin filament nucleation and elongation factors-structure-function relationships. Crit Rev Biochem Mol Biol 44:351–366.

Dos Remedios CG, Chhabra D, Kekic M, Dedova I V, Tsubakihara M, Berry D a, Nosworthy NJ (2003) Actin binding proteins: regulation of cytoskeletal microfilaments. Physiol Rev 83:433–473.

Dudai Y (2004) The neurobiology of consolidations, or, how stable is the engram? Annu Rev Psychol 55:51–86.

Dunaevsky A, Tashiro A, Majewska A, Mason C, Yuste R (1999) Developmental regulation of spine motility in the mammalian central nervous system. Proc Natl Acad Sci U S A 96:13438–13443.

Dutch-belgian T, Helm R Van Der, Oerlemans F, Hoogeveen T, Oostra BA (1994) Fmrl Knockout M ice : A Model to Study Fragile X Mental Retardation. 78:23–33.

Eichenbaum H (2004) Hippocampus: cognitive processes and neural representations that underlie declarative memory. Neuron 44:109–120.

Engert F, Bonhoeffer T (1999) Dendritic spine changes associated with hippocampal long-term synaptic plasticity. Nature 399:66–70.

Ethell IM, Irie F, Kalo MS, Couchman JR, Pasquale EB, Yamaguchi Y (2001) EphB/syndecan-2 signaling in dendritic spine morphogenesis. Neuron 31:1001–1013.

Fähling M, Mrowka R, Steege A, Kirschner KM, Benko E, Förstera B, Persson PB, Thiele BJ, Meier JC, Scholz H (2009) Translational regulation of the human achaete-scute homologue-1 by fragile X mental retardation protein. J Biol Chem 284:4255–4266.

Fedulov V, Rex CS, Simmons DA, Palmer L, Gall CM, Lynch G (2007) Evidence that long-term potentiation occurs within individual hippocampal synapses during learning. J Neurosci 27:8031–8039.

Fifková E, Delay RJ (1982) Cytoplasmic actin in neuronal processes as a possible mediator of synaptic plasticity. J Cell Biol 95:345–350.

Fischer M, Kaech S, Knutti D, Matus a (1998) Rapid actin-based plasticity in dendritic spines. Neuron 20:847–854.

Fischer M, Kaech S, Wagner U, Brinkhaus H, Matus A (2000) Glutamate receptors regulate actin-based plasticity in dendritic spines. Nat Neurosci 3:887–894.

Fortin D a, Srivastava T, Soderling TR (2011) Structural Modulation of Dendritic Spines during Synaptic Plasticity. Neuroscientist.

Frankland PW, Bontempi B (2005) The organization of recent and remote memories. Nat Rev Neurosci 6:119–130.

Fukazawa Y, Saitoh Y, Ozawa F, Ohta Y, Mizuno K, Inokuchi K (2003) Hippocampal LTP is accompanied by enhanced F-actin content within the dendritic spine that is essential for late LTP maintenance in vivo. Neuron 38:447–460.

Gallagher M, Burwell R, Burchinal M (1993) Severity of spatial learning impairment in aging: development of a learning index for performance in the Morris water maze. Behav Neurosci 107:618–626.

Galvez R, Gopal AR, Greenough WT (2003) Somatosensory cortical barrel dendritic abnormalities in a mouse model of the fragile X mental retardation syndrome. Brain Res 971:83–89.

Galvez R, Greenough WT (2005) Sequence of abnormal dendritic spine development in primary somatosensory cortex of a mouse model of the fragile X mental retardation syndrome. Am J Med Genet A 135:155–160.

Garey LJ, Ong WY, Patel TS, Kanani M, Davis A, Mortimer AM, Barnes TR, Hirsch SR (1998) Reduced dendritic spine density on cerebral cortical pyramidal neurons in schizophrenia. J Neurol Neurosurg Psychiatry 65:446–453.

Garthe A, Behr J, Kempermann G (2009) Adult-generated hippocampal neurons allow the flexible use of spatially precise learning strategies. PLoS One 4:e5464.

Garthe A, Kempermann G (2013) An old test for new neurons: refining the Morris water maze to study the functional relevance of adult hippocampal neurogenesis. Front Neurosci 7:63.

Gertler FB, Niebuhr K, Reinhard M, Wehland J, Soriano P (1996) Mena, a relative of VASP and Drosophila Enabled, is implicated in the control of microfilament dynamics. Cell 87:227–239.

Gieselmann R, Kwiatkowski DJ, Janmey PA, Witke W (1995) Distinct biochemical characteristics of the two human profilin isoforms. Eur J Biochem 229:621–628.

Glantz LA, Lewis DA (2000) Decreased dendritic spine density on prefrontal cortical pyramidal neurons in schizophrenia. Arch Gen Psychiatry 57:65–73.

Goehler H et al. (2004) A protein interaction network links GIT1, an enhancer of huntingtin aggregation, to Huntington's disease. Mol Cell 15:853–865.

Goldschmidt-Clermont PJ, Furman MI, Wachsstock D, Safer D, Nachmias VT, Pollard TD (1992) The control of actin nucleotide exchange by thymosin beta 4 and profilin. A potential regulatory mechanism for actin polymerization in cells. Mol Biol Cell 3:1015–1024.

Görlich A, Zimmermann A-M, Schober D, Böttcher RT, Sassoè-Pognetto M, Friauf E, Witke W, Rust MB (2012) Preserved morphology and physiology of excitatory synapses in profilin1-deficient mice. PLoS One 7:e30068.

Govek E-E, Newey SE, Van Aelst L (2005) The role of the Rho GTPases in neuronal development. Genes Dev 19:1–49.

Greenough WT, Volkmar FR (1973) Pattern of dendritic branching in occipital cortex of rats reared in complex environments. Exp Neurol 40:491–504.

Gross C, Bassell GJ (2012) Excess protein synthesis in FXS patient lymphoblastoid cells can be rescued with a p110β-selective inhibitor. Mol Med 18:336–345.

Grossman AW, Aldridge GM, Lee KJ, Zeman MK, Jun CS, Azam HS, Arii T, Imoto K, Greenough WT, Rhyu IJ (2010) Developmental characteristics of dendritic spines in the dentate gyrus of Fmr1 knockout mice. Brain Res 1355:221–227.

Grossman AW, Elisseou NM, McKinney BC, Greenough WT (2006) Hippocampal pyramidal cells in adult Fmr1 knockout mice exhibit an immature-appearing profile of dendritic spines. Brain Res 1084:158–164.

Halpain S (2000) Actin and the agile spine: how and why do dendritic spines dance? Trends Neurosci 23:141–146.

Harlow EG, Till SM, Russell TA, Wijetunge LS, Kind P, Contractor A (2010) Critical period plasticity is disrupted in the barrel cortex of FMR1 knockout mice. Neuron 65:385–398.

Hayashi ML, Rao BSS, Seo J-S, Choi H-S, Dolan BM, Choi S-Y, Chattarji S, Tonegawa S (2007) Inhibition of p21-activated kinase rescues symptoms of fragile X syndrome in mice. Proc Natl Acad Sci U S A 104:11489–11494.

He CX, Portera-Cailliau C (2012) The trouble with spines in fragile X syndrome: density, maturity and plasticity. Neuroscience:1–9.

Hering H, Sheng M (2001) Dendritic spines: structure, dynamics and regulation. Nat Rev Neurosci 2:880–888.

Hinds HL, Ashley CT, Sutcliffe JS, Nelson DL, Warren ST, Housman DE, Schalling M (1993) Tissue specific expression of FMR-1 provides evidence for a functional role in fragile X syndrome. Nat Genet 3:36–43.

Hinton VJ, Brown WT, Wisniewski K, Rudelli RD (1991) Analysis of neocortex in three males with the fragile X syndrome. Am J Med Genet 41:289–294.

Holtmaat A, Svoboda K (2009) Experience-dependent structural synaptic plasticity in the mammalian brain. Nat Rev Neurosci 10:647–658.

Holtmaat A, Wilbrecht L, Knott GW, Welker E, Svoboda K (2006) Experience-dependent and cell-type-specific spine growth in the neocortex. Nature 441:979–983.

Honkura N, Matsuzaki M, Noguchi J, Ellis-Davies GCR, Kasai H (2008) The subspine organization of actin fibers regulates the structure and plasticity of dendritic spines. Neuron 57:719–729.

Honoré B, Madsen P, Andersen AH, Leffers H (1993) Cloning and expression of a novel human profilin variant, profilin II. FEBS Lett 330:151–155.

Hotulainen P, Hoogenraad CC (2010a) Actin in dendritic spines: connecting dynamics to function. J Cell Biol 189:619–629.

Hotulainen P, Hoogenraad CC (2010b) Actin in dendritic spines: connecting dynamics to function. J Cell Biol 189:619–629.

Hotulainen P, Llano O, Smirnov S, Tanhuanpää K, Faix J, Rivera C, Lappalainen P (2009) Defining mechanisms of actin polymerization and depolymerization during dendritic spine morphogenesis. J Cell Biol 185:323–339.

Huang T, Larsen KT, Ried-Larsen M, Møller NC, Andersen LB (2014) The effects of physical activity and exercise on brain-derived neurotrophic factor in healthy humans: a review. Scand J Med Sci Sports 24:1–10.

Huang W, Zhu PJ, Zhang S, Zhou H, Stoica L, Galiano M, Krnjević K, Roman G, Costa-Mattioli M (2013) mTORC2 controls actin polymerization required for consolidation of long-term memory. Nat Neurosci 16:441–448.

Irwin S a, Galvez R, Greenough WT (2000) Dendritic spine structural anomalies in fragile-X mental retardation syndrome. Cereb Cortex 10:1038–1044.

Irwin SA, Idupulapati M, Gilbert ME, Harris JB, Chakravarti AB, Rogers EJ, Crisostomo RA, Larsen BP, Mehta A, Alcantara CJ, Patel B, Swain RA, Weiler IJ, Oostra BA, Greenough WT (2002) Dendritic spine and dendritic field characteristics of layer V pyramidal neurons in the visual cortex of fragile-X knockout mice. Am J Med Genet 111:140–146.

Irwin SA, Patel B, Idupulapati M, Harris JB, Crisostomo RA, Larsen BP, Kooy F, Willems PJ, Cras P, Kozlowski PB, Swain RA, Weiler IJ, Greenough WT (2001) Abnormal dendritic spine characteristics in the temporal and visual cortices of patients with fragile-X syndrome: a quantitative examination. Am J Med Genet 98:161–167.

Izeddin I, Specht CG, Lelek M, Darzacq X, Triller A, Zimmer C, Dahan M (2011) Super-Resolution Dynamic Imaging of Dendritic Spines Using a Low-Affinity Photoconvertible Actin Probe Degtyar VE, ed. PLoS One 6:e15611.

Janke J, Schlüter K, Jandrig B, Theile M, Kölble K, Arnold W, Grinstein E, Schwartz A, Estevéz-Schwarz L, Schlag PM, Jockusch BM, Scherneck S (2000) Suppression of tumorigenicity in breast cancer cells by the microfilament protein profilin 1. J Exp Med 191:1675–1686.

Jockusch BM, Murk K, Rothkegel M (2007) The profile of profilins. Biochem Pharmacol.

Kaech S, Brinkhaus H, Matus A (1999) Volatile anesthetics block actin-based motility in dendritic spines. Proc Natl Acad Sci U S A 96:10433–10437.

Kandel ER, Dudai Y, Mayford MR (2014) The Molecular and Systems Biology of Memory. Cell 157:163–186.

Kao D-I, Aldridge GM, Weiler IJ, Greenough WT (2010) Altered mRNA transport, docking, and protein translation in neurons lacking fragile X mental retardation protein. Proc Natl Acad Sci U S A 107:15601–15606.

Kasai H, Fukuda M, Watanabe S, Hayashi-Takagi A, Noguchi J (2010) Structural dynamics of dendritic spines in memory and cognition. Trends Neurosci 33:121–129.

Kim CH, Lisman JE (1999) A role of actin filament in synaptic transmission and long-term potentiation. J Neurosci 19:4314–4324.

Koekkoek SK, Yamaguchi K, BA O, CI DZ (2005) Deletion of FMR1 in Purkinje cells enhances parallel fiber LTD, enlarges spines, and attentuates cerebellar eyelid conditioning in Fragile x syndrome. Neuron.

Koleske AJ (2013) Molecular mechanisms of dendrite stability. Nat Rev Neurosci 14:536–550.

Koo S, Kim CH, Ahn HC, Kim C (2007) Effects of Long-term Intermittent Oxygen Administration on the Cognitive Function in Rats. Available at: http://synapse.koreamed.org/DOIx.php?id=10.4097/kjae.2007.52.6.687&vmode=PUBREADER [Accessed June 1, 2014].

Kooy RF, D'Hooge R, Reyniers E, Bakker CE, Nagels G, De Boulle K, Storm K, Clincke G, De Deyn PP, Oostra B a, Willems PJ (1996) Transgenic mouse model for the fragile X syndrome. Am J Med Genet 64:241–245.

Kopec CD, Li B, Wei W, Boehm J, Malinow R (2006) Glutamate receptor exocytosis and spine enlargement during chemically induced long-term potentiation. J Neurosci 26:2000–2009.

Korkotian E, Segal M (2001) Regulation of dendritic spine motility in cultured hippocampal neurons. J Neurosci 21:6115–6124.

Korobova F, Svitkina T (2010) Molecular architecture of synaptic actin cytoskeleton in hippocampal neurons reveals a mechanism of dendritic spine morphogenesis. Mol Biol Cell 21:165–176.

Krucker T, Siggins GR, Halpain S (2000) Dynamic actin filaments are required for stable long-term potentiation (LTP) in area CA1 of the hippocampus. Proc Natl Acad Sci U S A 97:6856–6861.

Kullmann J a, Neumeyer a, Wickertsheim I, Böttcher RT, Costell M, Deitmer JW, Witke W, Friauf E, Rust MB (2012) Purkinje cell loss and motor coordination defects in profilin1 mutant mice. Neuroscience 223:355–364.

Kullmann J a, Neumeyer A, Gurniak CB, Friauf E, Witke W, Rust MB (2011) Profilin1 is required for glial cell adhesion and radial migration of cerebellar granule neurons. EMBO Rep 13:75–82.

Kwiatkowski DJ, Bruns GA (1988) Human profilin. Molecular cloning, sequence comparison, and chromosomal analysis. J Biol Chem 263:5910–5915.

Lambrechts A, Braun A, Jonckheere V, Aszodi A, Vandekerckhove L, Lanier LM, Robbens J, Colen IVAN, Ssler RFA, Ampe C (2000) Profilin II Is Alternatively Spliced , Resulting in Profilin Isoforms That Are Differentially Expressed and Have Distinct Biochemical Properties. Society 20:8209–8219.

Lambrechts A, Verschelde JL, Jonckheere V, Goethals M, Vandekerckhove J, Ampe C (1997) The mammalian profilin isoforms display complementary affinities for PIP2 and proline-rich sequences. EMBO J 16:484–494.

Lamprecht R (2014) The actin cytoskeleton in memory formation. Prog Neurobiol.

Lamprecht R, Farb CR, Rodrigues SM, LeDoux JE (2006) Fear conditioning drives profilin into amygdala dendritic spines. Nat Neurosci 9:481–483.

Lamprecht R, LeDoux J (2004) Structural plasticity and memory. Nat Rev Neurosci 5:45–54.

Landis DM, Reese TS (1983) Cytoplasmic organization in cerebellar dendritic spines. J Cell Biol 97:1169–1178.

Lang C, Barco A, Zablow L, Kandel ER, Siegelbaum SA, Zakharenko SS (2004) Transient expansion of synaptically connected dendritic spines upon induction of hippocampal long-term potentiation. Proc Natl Acad Sci U S A 101:16665–16670.

Lauterborn JC, Rex CS, Kramár E, Chen LY, Pandyarajan V, Lynch G, Gall CM (2007) Brain-derived neurotrophic factor rescues synaptic plasticity in a mouse model of fragile X syndrome. J Neurosci 27:10685–10694.

Levenga J, Hayashi S, de Vrij FMS, Koekkoek SK, van der Linde HC, Nieuwenhuizen I, Song C, Buijsen R a M, Pop AS, Gomezmancilla B, Nelson DL, Willemsen R, Gasparini F, Oostra B a (2011) AFQ056, a new mGluR5 antagonist for treatment of fragile X syndrome. Neurobiol Dis 42:311–317.

Li K, Müller I, Patil S, Höger H, Pollak A, Russo-Schlaff N, Lubec G, Li L (2012) Strain-independent global effect of hippocampal proteins in mice trained in the Morris water maze. Amino Acids.

Lightbody AA, Reiss AL (2009) Gene, brain, and behavior relationships in fragile X syndrome: evidence from neuroimaging studies. Dev Disabil Res Rev 15:343–352.

Lin B, Kramár EA, Bi X, Brucher FA, Gall CM, Lynch G (2005) Theta stimulation polymerizes actin in dendritic spines of hippocampus. J Neurosci 25:2062–2069.

Liu Z-H, Chuang D-M, Smith CB (2011) Lithium ameliorates phenotypic deficits in a mouse model of fragile X syndrome. Int J Neuropsychopharmacol 14:618–630.

Luo L (2000) Rho GTPases in neuronal morphogenesis. Nat Rev Neurosci 1:173–180.

Lynch G, Rex CS, Gall CM (2007) LTP consolidation: substrates, explanatory power, and functional significance. Neuropharmacology 52:12–23.

Majewska A, Tashiro A, Yuste R (2000) Regulation of spine calcium dynamics by rapid spine motility. J Neurosci 20:8262–8268.

Malenka RC (1994) Synaptic plasticity in the hippocampus: LTP and LTD. Cell 78:535–538.

Maletic-Savatic M (1999) Rapid Dendritic Morphogenesis in CA1 Hippocampal Dendrites Induced by Synaptic Activity. Science (80-) 283:1923–1927.

Matsuzaki M, Ellis-Davies GC, Nemoto T, Miyashita Y, Iino M, Kasai H (2001) Dendritic spine geometry is critical for AMPA receptor expression in hippocampal CA1 pyramidal neurons. Nat Neurosci 4:1086–1092.

Matsuzaki M, Kaisai H, Honkura E-D (2004a) Structural basis of long-term potentiation in single dendritic spines. Nature.

Matsuzaki M, Kasai H, Ellis-Davies GC, Honkura N (2004b) Structural basis of long-term potentiation in single dendritic spines. 429.

Matus A (2000) Actin-Based Plasticity in Dendritic Spines. Science (80-) 290:754–758.

Matus A, Ackermann M, Pehling G, Byers HR, Fujiwara K (1982) High actin concentrations in brain dendritic spines and postsynaptic densities. Proc Natl Acad Sci U S A 79:7590–7594.

Matus A, Brinkhaus H, Wagner U (2000) Actin dynamics in dendritic spines: a form of regulated plasticity at excitatory synapses. Hippocampus 10:555–560.

McKinney R a (2005) Physiological roles of spine motility: development, plasticity and disorders. Biochem Soc Trans 33:1299–1302.

McNaughton N, Morris RG (1987) Chlordiazepoxide, an anxiolytic benzodiazepine, impairs place navigation in rats. Behav Brain Res 24:39–46.

Medioni C, Ramialison M, Ephrussi A, Besse F (2014) Imp Promotes Axonal Remodeling by Regulating profilin mRNA during Brain Development. Curr Biol 24:793–800.

Meredith RM, Holmgren CD, Weidum M, Burnashev N, Mansvelder HD (2007) Increased threshold for spike-timing-dependent plasticity is caused by unreliable calcium signaling in mice lacking fragile X gene FMR1. Neuron 54:627–638.

Meyer D, Bonhoeffer T, Scheuss V (2014) Balance and Stability of Synaptic Structures during Synaptic Plasticity. Neuron 82:430–443.

Michaelsen K (2009) Molecular mechanisms regulating dendrite architecture of mature pyramidal neurons in the mouse hippocampus.

Michaelsen K, Murk K, Zagrebelsky M, Dreznjak A, Jockusch BM, Rothkegel M, Korte M (2010) Fine-tuning of neuronal architecture requires two profilin isoforms. Proc Natl Acad Sci U S A 107:15780–15785.

Milner B (2005) The medial temporal-lobe amnesic syndrome. Psychiatr Clin North Am 28:599–611, 609.

Miyashiro KY, Beckel-Mitchener A, Purk TP, Becker KG, Barret T, Liu L, Carbonetto S, Weiler IJ, Greenough WT, Eberwine J (2003) RNA cargoes associating with FMRP reveal deficits in cellular functioning in Fmr1 null mice. Neuron 37:417–431.

Montani L, Buerki-Thurnherr T, de Faria JP, Pereira J a, Dias NG, Fernandes R, Gonçalves AF, Braun A, Benninger Y, Böttcher RT, Costell M, Nave K-A, Franklin RJM, Meijer D, Suter U, Relvas JB (2014) Profilin 1 is required for peripheral nervous system myelination. Development 141:1553–1561.

Moon J, Beaudin a E, Verosky S, Driscoll LL, Weiskopf M, Levitsky D a, Crnic LS, Strupp BJ (2006) Attentional dysfunction, impulsivity, and resistance to change in a mouse model of fragile X syndrome. Behav Neurosci 120:1367–1379.

Morales J, Hiesinger PR, Schroeder AJ, Kume K, Verstreken P, Jackson FR, Nelson DL, Hassan BA (2002) Drosophila fragile X protein, DFXR, regulates neuronal morphology and function in the brain. Neuron 34:961–972.

Morris R (1984) Developments of a water-maze procedure for studying spatial learning in the rat. J Neurosci Methods 11:47–60.

Morris RG (1981) Spatial localization does not require the presence of local cues. Learn Motiv.

Morris RG, Anderson E, Lynch GS, Baudry M (1986) Selective impairment of learning and blockade of long-term potentiation by an N-methyl-D-aspartate receptor antagonist, AP5. Nature 319:774–776.

Moscovitch M, Nadel L, Winocur G, Gilboa A, Rosenbaum RS (2006) The cognitive neuroscience of remote episodic, semantic and spatial memory. Curr Opin Neurobiol 16:179–190.

Murakoshi H, Wang H, Yasuda R (2011) Local, persistent activation of Rho GTPases during plasticity of single dendritic spines. Nature 472:100–104.

Murk K (2008) Analyse der funktionellen Diversität der Profilin-Isoformen 1 und 2a.

Murk K, Wittenmayer N, Michaelsen-Preusse K, Dresbach T, Schoenenberger C-A, Korte M, Jockusch BM, Rothkegel M (2012) Neuronal profilin isoforms are addressed by different signalling pathways. PLoS One 7:e34167.

Musleh W, Bi X, Tocco G, Yaghoubi S, Baudry M (1997) Glycine-induced long-term potentiation is associated with structural and functional modifications of alpha-amino-3-hydroxyl-5-methyl-4-isoxazolepropionic acid receptors. Proc Natl Acad Sci U S A 94:9451–9456.

Nägerl UV, Eberhorn N, Cambridge SB, Bonhoeffer T (2004) Bidirectional activity-dependent morphological plasticity in hippocampal neurons. Neuron 44:759–767.

Neeper S a, Gómez-Pinilla F, Choi J, Cotman CW (1996) Physical activity increases mRNA for brain-derived neurotrophic factor and nerve growth factor in rat brain. Brain Res 726:49–56.

Neuhoff H, Sassoè-Pognetto M, Panzanelli P, Maas C, Witke W, Kneussel M (2005) The actin-binding protein profilin I is localized at synaptic sites in an activity-regulated manner. Eur J Neurosci 21:15–25.

Newpher TM, Ehlers MD (2009) Spine microdomains for postsynaptic signaling and plasticity. Trends Cell Biol 19:218–227.

Nimchinsky E a, Oberlander a M, Svoboda K (2001) Abnormal development of dendritic spines in FMR1 knock-out mice. J Neurosci 21:5139–5146.

Nottebohm F (2002) Why are some neurons replaced in adult brain? J Neurosci 22:624–628.

Oertner TG, Matus A (2005) Calcium regulation of actin dynamics in dendritic spines. Cell Calcium 37:477–482.

Oh WC, Hill TC, Zito K (2012) Synapse-specific and size-dependent mechanisms of spine structural plasticity accompanying synaptic weakening. Proc Natl Acad Sci U S A 110:1–8.

Okamoto K-I, Nagai T, Miyawaki A, Hayashi Y (2004) Rapid and persistent modulation of actin dynamics regulates postsynaptic reorganization underlying bidirectional plasticity. Nat Neurosci 7:1104–1112.

Osterweil EK, Chuang S-C, Chubykin AA, Sidorov M, Bianchi R, Wong RKS, Bear MF (2013) Lovastatin corrects excess protein synthesis and prevents epileptogenesis in a mouse model of fragile X syndrome. Neuron 77:243–250.

Owen EH, Logue SF, Rasmussen DL, Wehner JM (1997) Assessment of learning by the Morris water task and fear conditioning in inbred mouse strains and F1 hybrids: implications of genetic background for single gene mutations and quantitative trait loci analyses. Neuroscience 80:1087–1099.

Pan F, Aldridge GM, Greenough WT, Gan W-B (2010) Dendritic spine instability and insensitivity to modulation by sensory experience in a mouse model of fragile X syndrome. Proc Natl Acad Sci U S A 107:17768–17773.

Pantaloni D, Carlier MF (1993) How profilin promotes actin filament assembly in the presence of thymosin beta 4. Cell 75:1007–1014.

Papa M, Bundman MC, Greenberger V, Segal M (1995) Morphological analysis of dendritic spine development in primary cultures of hippocampal neurons. J Neurosci 15:1–11.

Paradee W, Melikian HE, Rasmussen DL, Kenneson a, Conn PJ, Warren ST (1999) Fragile X mouse: strain effects of knockout phenotype and evidence suggesting deficient amygdala function. Neuroscience 94:185–192.

Park M, Salgado JM, Ostroff L, Helton TD, Robinson CG, Harris KM, Ehlers MD (2006) Plasticity-induced growth of dendritic spines by exocytic trafficking from recycling endosomes. Neuron 52:817–830.

Penagarikano O, Mulle JG, Warren ST (2007) The pathophysiology of fragile x syndrome. Annu Rev Genomics Hum Genet 8:109–129.

Pfeiffer BE, Huber KM (2007) Fragile X mental retardation protein induces synapse loss through acute postsynaptic translational regulation. J Neurosci 27:3120–3130.

Pilo Boyl P, Di Nardo A, Mulle C, Sassoè-Pognetto M, Panzanelli P, Mele A, Kneussel M, Costantini V, Perlas E, Massimi M, Vara H, Giustetto M, Witke W (2007) Profilin2 contributes to synaptic vesicle exocytosis, neuronal excitability, and novelty-seeking behavior. EMBO J 26:2991–3002.

Portera-Cailliau C, He CX (2012) The trouble with spines in fragile X syndrome: density, maturity and plasticity. Neuroscience:1–9.

Purpura DP (1974) Dendritic Spine "Dysgenesis" and Mental Retardation. Science (80-) 186:1126–1128.

Qin M, Xia Z, Huang T, Smith CB (2011) Effects of chronic immobilization stress on anxiety-like behavior and basolateral amygdala morphology in Fmr1 knockout mice. Neuroscience 194:282–290.

Ramachandran B, Frey JU (2009) Interfering with the actin network and its effect on long-term potentiation and synaptic tagging in hippocampal CA1 neurons in slices in vitro. J Neurosci 29:12167–12173.

Reeve SP, Bassetto L, Genova GK, Kleyner Y, Leyssen M, Jackson FR, Hassan B a (2005) The Drosophila fragile X mental retardation protein controls actin dynamics by directly regulating profilin in the brain. Curr Biol 15:1156–1163.

Reinhard M, Giehl K, Abel K, Haffner C, Jarchau T, Hoppe V, Jockusch BM, Walter U (1995) The proline-rich focal adhesion and microfilament protein VASP is a ligand for profilins. EMBO J 14:1583–1589.

Remus A (2012) Molecular mechanisms regulating the neuronal architecture in the mouse brain.

Restivo L, Ferrari F, Passino E, Sgobio C, Bock J, Oostra B a, Bagni C, Ammassari-Teule M (2005) Enriched environment promotes behavioral and morphological recovery in a mouse model for the fragile X syndrome. Proc Natl Acad Sci U S A 102:11557–11562.

Rex CS, Lin C-Y, Kramár EA, Chen LY, Gall CM, Lynch G (2007) Brain-derived neurotrophic factor promotes long-term potentiation-related cytoskeletal changes in adult hippocampus. J Neurosci 27:3017–3029.

Richards DA, De Paola V, Caroni P, Gähwiler BH, McKinney RA (2004) AMPA-receptor activation regulates the diffusion of a membrane marker in parallel with dendritic spine motility in the mouse hippocampus. J Physiol 558:503–512.

Rochefort NL, Konnerth A (2012) Dendritic spines: from structure to in vivo function. EMBO Rep 13:699–708.

Rosoklija G, Toomayan G, Ellis SP, Keilp J, Mann JJ, Latov N, Hays AP, Dwork AJ (2000) Structural abnormalities of subicular dendrites in subjects with schizophrenia and mood disorders: preliminary findings. Arch Gen Psychiatry 57:349–356.

Roy P, Jacobson K (2004) Overexpression of profilin reduces the migration of invasive breast cancer cells. Cell Motil Cytoskeleton 57:84–95.

Russo-Neustadt a a, Beard RC, Huang YM, Cotman CW (2000) Physical activity and antidepressant treatment potentiate the expression of specific brain-derived neurotrophic factor transcripts in the rat hippocampus. Neuroscience 101:305–312.

Saffary R, Xie Z (2011) FMRP regulates the transition from radial glial cells to intermediate progenitor cells during neocortical development. J Neurosci 31:1427–1439.

Sajikumar S, Navakkode S, Frey JU (2007) Identification of compartment- and process-specific molecules required for "synaptic tagging" during long-term potentiation and long-term depression in hippocampal CA1. J Neurosci 27:5068–5080.

Saneyoshi T, Fortin DA, Soderling TR (2010) Regulation of spine and synapse formation by activity-dependent intracellular signaling pathways. Curr Opin Neurobiol 20:108–115.

Sanford, J.C., Klein TM (1987) Delivery of substances into cells and tissues using a particle bombardment process. J Part Sci Technol 5:27–37.

Schikorski, Stevens (1997) Quantitative ultrastructural analysis of hippocampal excitatory synapses. J Neurosci.

Schlüter K, Jockusch BM, Rothkegel M (1997) Profilins as regulators of actin dynamics. Biochim Biophys Acta 1359:97–109.

Schweinhuber S (2014) Actin Binding Proteins in the Regulation of the Astrocytic Cytoskeleton.

Scotto-Lomassese S, Nissant A, Mota T, Néant-Féry M, Oostra BA, Greer CA, Lledo P-M, Trembleau A, Caillé I (2011) Fragile X mental retardation protein regulates new neuron differentiation in the adult olfactory bulb. J Neurosci 31:2205–2215.

Scoville WB, Milner B (1957) Loss of recent memory after bilateral hippocampal lesions. 1957. J Neuropsychiatry Clin Neurosci 12:103–113.

Segal M (2005) Dendritic spines and long-term plasticity. Nat Rev Neurosci 6:277–284.

Segal M, Kreher U, Greenberger V, Braun K (2003) Is fragile X mental retardation protein involved in activity-induced plasticity of dendritic spines? Brain Res 972:9–15.

Shahi K, Marvizon JC, Baudry M (1993) High concentrations of glycine induce long-lasting changes in synaptic efficacy in rat hippocampal slices. Neurosci Lett 149:185–188.

Shao J, Diamond MI (2012) Protein phosphatase 1 dephosphorylates profilin-1 at ser-137. PLoS One 7:e32802.

Shao J, Welch WJ, Diprospero N a, Diamond MI (2008) Phosphorylation of profilin by ROCK1 regulates polyglutamine aggregation. Mol Cell Biol 28:5196–5208.

Sharma S, Rakoczy S, Brown-Borg H (2010) Assessment of spatial memory in mice. Life Sci 87:521–536.

Shaw CL, Watson GDR, Hallock HL, Cline KM, Griffin AL (2013) The role of the medial prefrontal cortex in the acquisition, retention, and reversal of a tactile visuospatial conditional discrimination task. Behav Brain Res 236:94–101.

Sheng M, Hoogenraad CC (2007) The postsynaptic architecture of excitatory synapses: a more quantitative view. Annu Rev Biochem 76:823–847.

Spencer CM, Alekseyenko O, Hamilton SM, Thomas AM, Serysheva E, Yuva-Paylor L a, Paylor R (2011) Modifying behavioral phenotypes in Fmr1KO mice: genetic background differences reveal autistic-like responses. Autism Res 4:40–56.

Squire LR, Kandel E (2009) Memory: From Mind to Molecules.

Squire LR, Stark CEL, Clark RE (2004) The medial temporal lobe. Annu Rev Neurosci 27:279–306.

Star EN, Kwiatkowski DJ, Murthy VN (2002) Rapid turnover of actin in dendritic spines and its regulation by activity. Nat Neurosci 5:239–246.

Su T, Fan H-X, Jiang T, Sun W-W, Den W-Y, Gao M-M, Chen S-Q, Zhao Q-H, Yi Y-H (2011) Early continuous inhibition of group 1 mGlu signaling partially rescues dendritic spine abnormalities in the Fmr1 knockout mouse model for fragile X syndrome. Psychopharmacology (Berl) 215:291–300.

Tada T, Sheng M (2006) Molecular mechanisms of dendritic spine morphogenesis. Curr Opin Neurobiol:95–101.

Takeichi M (1990) Cadherins: a molecular family important in selective cell-cell adhesion. Annu Rev Biochem 59:237–252.

Tashiro A, Yuste R (2004) Regulation of dendritic spine motility and stability by Rac1 and Rho kinase: evidence for two forms of spine motility. Mol Cell Neurosci 26:429–440.

Tatavarty V, Kim E-J, Rodionov V, Yu J (2009) Investigating sub-spine actin dynamics in rat hippocampal neurons with super-resolution optical imaging. PLoS One 4:e7724.

Teyler TJ, Rudy JW (2007) The hippocampal indexing theory and episodic memory: updating the index. Hippocampus 17:1158–1169.

Tønnesen J, Katona G, Rózsa B, Nägerl UV (2014) Spine neck plasticity regulates compartmentalization of synapses. Nat Neurosci 17:678–685.

Trachtenberg JT, Chen BE, Knott GW, Feng G, Sanes JR, Welker E, Svoboda K (2002) Long-term in vivo imaging of experience-dependent synaptic plasticity in adult cortex. Nature 420:788–794.

Van Dam D, Errijgers V, Kooy RF, Willemsen R, Mientjes E, Oostra BA, De Deyn PP (2005) Cognitive decline, neuromotor and behavioural disturbances in a mouse model for fragile-X-associated tremor/ataxia syndrome (FXTAS). Behav Brain Res 162:233–239.

Vertes (2004) Differential projections of the infralimbic and prelimbic cortex in the rat. Synapse.

Volkmar FR, Greenough WT (1972) Rearing complexity affects branching of dendrites in the visual cortex of the rat. Science 176:1445–1447.

Wang R, Cleary RA, Wang T, Li J, Tang DD (2014) The Association of Cortactin with Profilin-1 Is Critical for Smooth Muscle Contraction. J Biol Chem.

Witke W (2004) The role of profilin complexes in cell motility and other cellular processes. Trends Cell Biol 14:461–469.

Witke W, Podtelejnikov a V, Di Nardo a, Sutherland JD, Gurniak CB, Dotti C, Mann M (1998) In mouse brain profilin I and profilin II associate with regulators of the endocytic pathway and actin assembly. EMBO J 17:967–976.

Witke W, Sutherland JD, Sharpe a, Arai M, Kwiatkowski DJ (2001) Profilin I is essential for cell survival and cell division in early mouse development. Proc Natl Acad Sci U S A 98:3832–3836.

Wittenmayer N, Jandrig B, Rothkegel M, Arnold W, Haensch W, Scherneck S, Jockusch BM, Ro R (2004) Tumor Suppressor Activity of Profilin Requires a Functional Actin Binding Site. 15:1600–1608.

Wolfer DP, Stagljar-Bozicevic M, Errington ML, Lipp H-P (1998) Spatial Memory and Learning in Transgenic Mice: Fact or Artifact? News Physiol Sci 13:118–123.

Yarmola EG, Bubb MR (2009) How depolymerization can promote polymerization: the case of actin and profilin. Bioessays 31:1150–1160.

Yuste R (2010) Dendritic Spines.

Yuste R, Bonhoeffer T (2001) Morphological changes in dendritic spines associated with long-term synaptic plasticity. Annu Rev Neurosci 24:1071–1089.

Yuste R, Bonhoeffer T (2004) Genesis of dendritic spines: insights from ultrastructural and imaging studies. Nat Rev Neurosci 5:24–34.

Zagrebelsky M, Holz A, Dechant G, Barde Y-A, Bonhoeffer T, Korte M (2005) The p75 neurotrophin receptor negatively modulates dendrite complexity and spine density in hippocampal neurons. J Neurosci 25:9989–9999.

Zhao M-G, Toyoda H, Ko SW, Ding H-K, Wu L-J, Zhuo M (2005) Deficits in trace fear memory and long-term potentiation in a mouse model for fragile X syndrome. J Neurosci 25:7385–7392.

Zhou Q, Homma KJ, Poo M (2004) Shrinkage of dendritic spines associated with long-term depression of hippocampal synapses. Neuron 44:749–757.